

Association Behavior of Hydrophobically Modified Copolymers in Aqueous Medium

Dissertation

Zur Erlangung des Doktorgrades
der Naturwissenschaften
(Dr. rer. nat.)

Technische Universität Dortmund

Fakultät für Chemie und Chemische Biologie

Arbeitsgruppe Polymer Hybridsystem

vorgelegt von

Sotoodeh Mohammadi

aus dem Iran

Dortmund 2019

Statement of Contributions and Collaborators

I hereby declare that I am the sole author of this dissertation. I have done all the experimental parts, performed analytical studies and wrote all the parts in this research.

My supervisor, Prof. Dr. Ralf Weberskirch, provided me a constant support, availability, constructive suggestions and editorial comments for all of my written work. The quality of this dissertation has been tremendously improved through his guidance.

Sotoodeh Mohammadi

Faculty of Chemistry and Chemical Biology
Technical University of Dortmund
Germany

Acknowledgment

First and foremost, I would like to express my deepest gratitude and sincere thanks to my supervisor, Prof. Dr. Ralf Weberskirch, for providing me the opportunity to work on this interesting project. The enthusiasm and joy he has for his research was contagious and motivational for me, even during tough times in my Ph.D. study. Without his guidance and constant feedback this doctoral study would not have been achievable.

Besides my supervisor, I am also deeply grateful to Prof. Dr. Jörg C. Tiller for kindly agreeing to be the second evaluator of my Ph.D. defense. I am also grateful to him for giving me the opportunity to use his analytical equipment.

My sincere thanks goes to Katja Weber for providing all the lab requirement and equipment, as well as Andrea Bokelmann for her help in analytical questions. Silvia Lessing has always done her best to render whatever help she could and thank her for that. Also thank you to Andreas Hammer and Heidi Auer for all their assistance with any organization issues.

I would like to thank all my colleagues present and past: Dr. Golnaz Bissadi, Dr. Patrick Bolduan, Omar Sallouh, Christian Gramse, Hanne Petersen, Irene Pretzer and Dr. Andrea Ernst for all of their helps.

Last but not the least I would like to thank my wonderful parents for their continuous encouragement, patience and love. Special thanks to my brother for his unbelievable support. I cannot thank my family enough for their gratitude and love.

Abstract

In the past years stem cells have been recognized as a promising source to treat a wide spectrum of human diseases. Stem cell fate of adult stem cells is mainly controlled by the stem cell microenvironment which is also called a stem cell niche. The stem cell niche is composed of the extracellular matrix (ECM), other small molecules and other cells. The extracellular matrix provides the scaffold for cell adhesion and therefore biochemical and biophysical aspects of the ECM have a huge influence on stem cell fate.

Five types of hydrophobically modified (HM) copolymers have been investigated in this work that are able to form physical hydrogel networks with tunable stiffness to mimic the natural extracellular matrix of adult stem cells. The first group was composed of *N,N'*-dimethylacrylamide (DMAM) and lauryl methacrylate (LMA) (1.25 to 10 mol %) or stearyl methacrylate (SMA) (1.25 to 2.5 mol %). These copolymers served as water-soluble, neutral reference copolymers. The second copolymer group contained an additional cationic monomer, the third group an additional zwitterionic monomer, the fourth group a RGD-peptide-functionalized monomer and the last group mono and polyunsaturated fatty acids. These copolymers were synthesized by free radical polymerization and the solution and gel-like properties investigated and compared by rheology measurements.

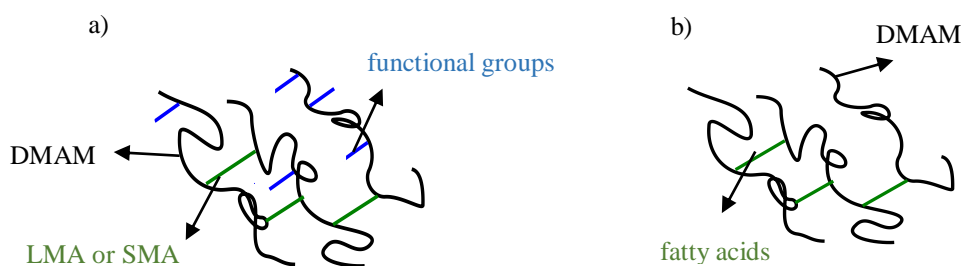


Figure 1. Schematic diagram for HM copolymer containing a) functional groups and b) fatty acids.

Kurzfassung

In den vergangenen Jahren wurden Stammzellen als vielversprechende Quelle für die Behandlung eines breiten Spektrums menschlicher Erkrankungen angesehen. Das Schicksal von adulten Stammzellen wird hauptsächlich durch die Mikroumgebung der Stammzelle gesteuert, die auch Stammzellennische genannt wird. Die Stammzellennische besteht aus der extrazellulären Matrix (EZM), anderen kleinen Molekülen und weiteren Zellen. Die extrazelluläre Matrix ist das Gerüst für die Zelladhäsion. Daher haben biochemische und biophysikalische Aspekte des EZM einen großen Einfluss auf das Schicksal der Stammzellen.

In dieser Arbeit wurden fünf Arten von hydrophob modifizierten (HM)-Copolymeren untersucht, die in der Lage sind, physikalische Hydrogelnetzwerke mit einstellbarer Festigkeit zu bilden, um die natürliche, extrazelluläre Matrix von adulten Stammzellen nachzuahmen. Die erste Gruppe bestand aus *N,N'*-Dimethylacrylamid (DMAM) und Laurylmethacrylat (LMA) (1,25 bis 10 Mol-%) oder Stearylmethacrylat (SMA) (1,25 bis 2,5 Mol-%). Diese Copolymere dienten als wasserlösliche, neutrale Referenzcopolymere. Die zweite Copolymergruppe enthielt ein zusätzliches kationisches Monomer, die dritte Gruppe ein zusätzliches zwitterionisches Monomer, die vierte Gruppe ein RGD-Peptid-funktionalisiertes Monomer und die letzte Gruppe einfach und mehrfach ungesättigte Fettsäuren. Diese Copolymere wurden durch radikalische Polymerisation synthetisiert und die Eigenschaften in Lösung bzw. im Gel durch Rheologiemessungen untersucht und miteinander verglichen.



Abb. 1. Schematische Abbildung für hydrophob-modifizierte Copolymere mit a) funktionellen Gruppen und b) Fettsäuren.

Table of Contents

Chapter 1. Introduction	1
Chapter 2. Literature Review	4
2.1. Introduction to stem cells	4
2.2 Hydrogels.....	5
2.2.1 Hydrogels classification.....	5
2.2.2 Hydrogel applications	6
2.3 Hydrophobically modified polymers.....	9
2.4 Polyelectrolyte	15
2.4.1 Cationic polymers	16
2.4.1.1 Natural cationic polymers	16
2.4.1.2 Synthetic cationic polymers	18
2.4.2 Zwitterionic polymers	21
2.4.3 Peptide based polymers.....	24
2.4.3.1 Chemical methods for synthesis of peptide.....	25
2.4.3.2 RGD interaction with cell surface integrins	26
2.5 Polymeric Materials for Cell Culturing Applications	27
Chapter 3. Objective of the Thesis	36
Chapter 4. Synthesis and Rheological Studies of Functionalized, Hydrophobically Modified Cationic Polymers	37
4.1 Introduction	37
4.2 Results and Discussions.....	38
4.2.1 Cationic copolymers preparation	38
4.2.2 Solubility of the copolymers	43
4.2.3 Rheological Studies	45
4.2.3.1 Steady Shear Flow Measurements	46
4.2.3.2 Effect of copolymers concentration on viscosity	48
4.2.3.2 Complex modulus	51
4.2.3.3 Modulus as a function of time.....	54
4.2.3.4 The impact of temperature on the modulus.....	56
4.2.4 Fluorescence measurements of the hydrophobic domains.....	58
4.3 Conclusions	58

4.4 Experimental.....	59
4.4.1 Synthesis of cationic copolymers.....	59
Chapter 5. Synthesis and Rheological Study of Functionalized Hydrophobically Modified zwitterionic Polymer	62
5.1 Introduction	62
5.2 Results and Discussions.....	64
5.2.1 The rheological behavior of P2.....	66
5.2.1.1 Viscosity as a function of shear rate.....	67
5.2.1.2 Viscosity as a function of concentration	69
5.2.1.3 Complex modulus	70
5.2.1.4 Complex modulus as a function of time.....	71
5.3.1 Effect of salt.....	73
5.3.1.1 Viscosity as a function of shear rate.....	73
5.3.1.2 Modulus as a function of time.....	74
5.4 Conclusion	76
5.5 Experimental.....	76
5.5.1 Synthesis of zwitterionic copolymer.....	76
Chapter 6. Synthesis and Rheological Characterization of Cationic, Hydrophobically Modified Copolymers containing Peptide moieties in the side chain.....	79
6.1 Introduction	79
6.2 Results and discussion	80
6.2.1. Copolymer containing peptide and cationic functional groups (P3).....	83
6.2.2 Rheological Study.....	84
6.2.2.1 Viscosity as a function of shear rate.....	84
6.2.2.2 Complex modulus	85
6.3 Conclusion	87
6.7 Experimental.....	87
6.7.1 Peptide monomer synthesis.....	87
6.7.2 Copolymer containing peptide.....	88
6.7.3 Cationic copolymer containing peptide	89
Chapter 7. Synthesis and Characterization of Hydrophobically Modified Polymers Based on Fatty Acid monomers	91
7.1 Introduction	91
7.2 Results and Discussion	92
7.2.1 Synthesis of oleyl acrylamide copolymer (POA)	92

7.2.2 Rheological Study	95
7.2.2.1 Viscosity Measurements	95
7.2.2.2 Modulus as a function of frequency	97
7.2.2.3 Modulus as a function of time	99
7.2.3 Synthesis of copolymer containing oleyl acrylamide and cationic monomer (PCOA1.25)	100
7.2.4 Synthesis of linoleyl methacrylate copolymer (PLM)	101
7.2.5 Viscosity as a function of shear rate	103
7.2.3 Photo-dimerization of unsaturated double bonds	104
7.4 Conclusion	106
7.5 Experimental.....	106
7.5.1 Synthesis of Oleylacrylamide	106
7.5.2 Monomer synthesis based on linoleic acid	107
7.5.3 Synthesis of POA	109
7.5.4 Synthesis of copolymer containing oleyl acrylamide and cationic monomer	110
7.5.5 Synthesis of PLM.....	110
Chapter 8. Characterization techniques.....	112
8.1 Nuclear magnetic resonance spectroscopy	112
8.2 Size exclusion chromatography	112
8.3 Ubbelohde viscometer	112
8.4 Rheology.....	112
8.5 Fluorescence spectroscopy	113
8.6 High-performance liquid chromatography	113
8.7 Ultraviolet- visible spectroscopy	113
8.8 Mass Spectrometry	113
Chapter 9. Conclusions and Recommendations	115
Chapter 10. References.....	119
Chapter 11. Appendix	138
11.1 List of Figures.....	138
11.2 List of Tables	142
11.3 Nomenclature.....	143
11.3.1 Abbreviations.....	143
11.3.2 Symbols.....	147
11.4 ¹ H NMR and mass spectrometry of peptide monomer.....	148

11.5 Modulus as a function of frequency for Pref and P1 at different concentration..... 149

Chapter 1. Introduction

The reciprocal interactions between cells and their microenvironment play a fundamental role in multiple cellular processes which are essential for regeneration, homeostasis and tissue development. Growth factors, cytokines and the extracellular matrix (ECM) are the microenvironment key players. ECM is composed of polysaccharides, proteins and soluble factors which surround cells and regulate stem cell fate within the niche. Recently, polymeric biomaterials have attracted much attention to understand the contribution of extracellular matrix properties on the cell behavior. Among the various forms of polymeric biomaterials, hydrogels have been extensively utilized as artificial extracellular microenvironment because of their biophysical similarity to the natural ECM. By developing artificial ECMs, much progress has been achieved in regenerative medicine and tissue engineering [1,2].

Hydrogels are three-dimensional (3D) crosslinked hydrophilic polymer networks with the potential to absorb large amounts of water. The crosslinks can be made by physical or chemical interactions. Physical hydrogels are formed by non-covalent associations through molecular entanglement and crystallization and/or secondary forces such as H-bonding, ionic or hydrophobic interactions. Chemically crosslinked hydrogels can be prepared either by copolymerization of mono-functional and multi-functional monomers or by the reaction of precursor polymers with complementary functional groups e.g. via click chemistry, Michael-type addition, photo-crosslinking, Schiff-base crosslinking, enzyme-mediated chemistry or disulfide crosslinking [3,4]. Hydrogels have been applied to support both two-dimensional (2D) and three-dimensional (3D) cell culture model [5].

Tissues in the human body have different mechanical properties, with a stiffness ranging from soft tissues like that of the brain to hard tissues like collagenous bones. Therefore, the study of the mechanical properties of the matrix is essential to understand tissue and cell functions. The hydrogel stiffness can be controlled by the crosslink density [1,6]. Additionally, the matrix stiffness has been shown to have a direct influence on different cell functions like adhesion, proliferation and differentiation [6,7].

Hydrophobically modified (HM) polymers composed of a hydrophilic polymer backbone with a small amount of hydrophobic associative (stickers) moieties have attracted considerable attention over the past few decades. These polymers can self-organize in aqueous solution and form a transient network above a critical concentration. Thus they show unique rheological behavior that make them very valuable rheology modifiers in coating and cosmetics, drug carriers, pharmaceutical formulations, injectable hydrogels and other water-

based applications [8,9]. The thickening ability of HM polymers can be controlled by the chemical structure of the hydrophilic groups, varying the molecular weight, the content and the nature of the hydrophobic moieties, or/and the distribution of hydrophobic groups along the backbone [10].

The incorporation of charged groups to hydrophobically modified polymers have some advantages. The presence of both non-polar hydrophobic and charged groups in the chain make hydrophobically modified polyelectrolytes good candidates to study the role of the hydrophobic and electrostatic interactions in the polymer solutions and have shown to be promising materials in medical, pharmaceutical and biological research [11,12]. For example, cationic copolymers are used as agents to increase the delivery of RNA or DNA into cells [13] or polyzwitterions are recognized as effective anti-fouling materials and implanted zwitterionic hydrogels resist a foreign-body reaction. Decreasing the foreign-body reaction to implanted compounds increases their *in vivo* application in tissue engineering [14]. In this study hydrophobically modified copolymers with various functional groups were prepared by free radical polymerization using *N,N'*-dimethylacrylamide (DMAM) as hydrophilic monomer and their rheological properties in aqueous medium were studied.

Chapter 2. Literature Review

2.1. Introduction to stem cells

The increasing number of patients suffering from organ function failure because of disease, aging or injury leads to enhancement of financial burdens worldwide and also have remarkable impact on the quality of life of patients. For example, spinal cord injury (SCI) is a disability that results in a loss of function like feeling or mobility and it costs \$9.7 billion each year only in the United States [15,16]. Therefore, the demand for methods to fabricate synthetic tissues outside the body has steadily increased [17]. Tissue engineering is a new potential approach in the biomedical field, which combines materials and life sciences for the purpose of repairing, replacing or regenerating diseased or damaged tissue [18]. To achieve the particular purpose in tissue engineering, stem cells and polymeric materials have been shown to be the best choices because of their unique properties [17]. Stem cells are cells with the ability to self-renew (make copies of themselves) and differentiate into specialized cell types in the body during early life and growth [19,20]. Stem cells can commit to particular cell lineage under proper stimuli, resulting in great regenerative potential of the final tissue. According to the stem cells differentiation potential in the area of tissue engineering, they are classified in two categories, (i) pluripotent stem cells and (ii) multipotent stem cells [15]. Embryonic stem cells (ESC) and induced pluripotent stem cells (iPSC) belong to the pluripotent stem cells category [21]. ESC are obtained from the inner cell mass of embryos and the isolation is carried out during embryological development. Therefore their application in tissue engineering is more limited due to ethical reasons. More recently, much attention has been paid to iPSCs because they can be obtained from reprogrammed somatic cells [22]. In general, pluripotent cells can self-renew indefinitely in comparison to multipotent stem cells such as adult stem cells. Adult stem cells are detected in various adult tissue such as peripheral blood, nervous tissue, muscles, bone marrow, dermis, adipose tissue and others. They show limited capacity to differentiate anymore in specialized cells and the concentration in the tissue is rather small with exception of the bone marrow. For any therapeutic application they need to be expanded *in vitro* before they can be applied [23,24].

Polymers have attracted increased attention in the wide field of biomaterials because they can be biodegradable and biocompatible with wide range of mechanical properties. Therefore, they are perfectly suited to fabricate well-defined three-dimensional scaffolds to control cell adhesion and proliferation [15,17].

In vivo stem cell fate is regulated by signals from the surrounding microenvironment, the stem cell niche. The extracellular matrix (ECM) is the scaffold material that provides mechanical stiffness and biological cues and is the main component where the cells reside. The ECM is a 3D network composed of proteoglycans, glycosaminoglycans and fibrillar proteins. The control of stem cell behavior in a reproducible way outside the body is a major challenge in the tissue engineering field. Therefore, the design of a novel synthetic microenvironment to regulate stem cells fate is important and researchers have devoted much effort to mimic the natural stem cell ECM. One of the most interesting class of materials to achieve this goal are hydrogels [25,26].

2.2 Hydrogels

A hydrogel is a network of polymer chains, which can retain large quantities of biological fluids or water. In most cases, the network is made from water-soluble macromolecular chains (gelators) that are crosslinked. These crosslinks can be permanent covalent bonds (= chemical hydrogels) or temporary junctions (= physical hydrogels). Hydrogels have unique properties that make them attractive in the biomedical fields. First of all, they are biocompatible due to their high water content. Moreover, due to their physiochemical similarity to the native extracellular matrix they can imitate the biophysical nature of soft tissue in the body. Mechanical stress and damage to surrounding tissue is limited by the soft and pliable nature of hydrogels. Finally, they exhibit good permeability for nutrients and metabolites which makes hydrogels excellent candidates to support the survival and growth of encapsulated cells [3,9,27,28,29,34].

2.2.1 Hydrogels classification

Hydrogels can be classified according to their synthesis route, type of ionic charges and crosslinking, physical structure, sources and physical appearance [30].

- **Route of their synthesis**

- Homopolymeric hydrogels, crosslinked network with only one type of hydrophilic monomer, such as polyvinyl alcohol (PVA) [31] and polyacrylic acid (PAA).

- Copolymeric hydrogels, prepared by copolymerization of two or more monomers with at least one hydrophilic unity. They can be formed in a random or blocky structure, such as three block ABA poly(L-lactic acid)-block-poly(ethylene oxide)-block-poly(L-lactic acid) triblock copolymers [32].

- Semi interpenetrating network (Semi-IPN), where a linear polymer can penetrate a polymer network without any chemical bonding like starch-g-poly(acrylic acid-co-acrylamide)/PVA semi-IPN hydrogels [33].

- Interpenetrating networks (IPN), that can be formed by a combination of two or more polymers with at least one system being prepared in the presence of another network like poly(*N*-isopropylacrylamide) (PNIPA) and chitosan [34].

- **Type of ionic charges**

- Nonionic hydrogels (neutral) [35]

- Ionic hydrogels (containing anionic or cationic charges)

- Amphoteric electrolyte (ampholytic) composed of both acidic and basic groups

- Zwitterionic hydrogels (polybetaines) contain positive and negative charges in the same repeating unit

- **Hydrogels source**

- Natural

- Synthetic

- **Physical structure**

- Amorphous, with randomly arranged chains

- Semicrystalline, dense regions of ordered network

- Crystalline, exist as hydrogen-bonded hydrogel or hydrocolloidal aggregates

- **Type of crosslinking**

- Chemically crosslinked hydrogels, covalently bonded hydrogels with permanent junction.

- Physically crosslinked hydrogels, with transient networks which are held together by physical interaction like hydrogen bonds, ionic and hydrophobic interactions.

- **Physical appearance**

With respect to the polymerization technique, hydrogels can be applied as matrix, film or microsphere.

2.2.2 Hydrogel applications

After the establishment of the first synthetic hydrogels by *Whichterle and Lim* in 1954, it is more than half a century that they have been widely applied for diverse biological and industrial applications [36]. Some of the applications are shown in Figure 2.1. As it is obvious for hydrogel applications, they are mainly used in biomedical research, due to a number of reasons: (i) A proper semi-wet, three dimensional environment can be prepared by hydrogels for well-defined biological interactions. (ii) Some hydrogels show antifouling properties, which

prevents non-specific protein adsorption due to their inert surfaces. (iii) With well-established chemistries, biologically-active molecules can be covalently attached to hydrogel networks. (IV) Hydrogels can be designed with tunable physical and mechanical properties. (V) Hydrogels can be prepared to undergo property changes such as swelling/collapse or solution-to-gel transition, which may occur in response to different physical stimuli like temperature, electric/magnetic field, light, pressure and sound or chemical stimuli like pH, solvent, small (bio) molecules and ionic strength [37].

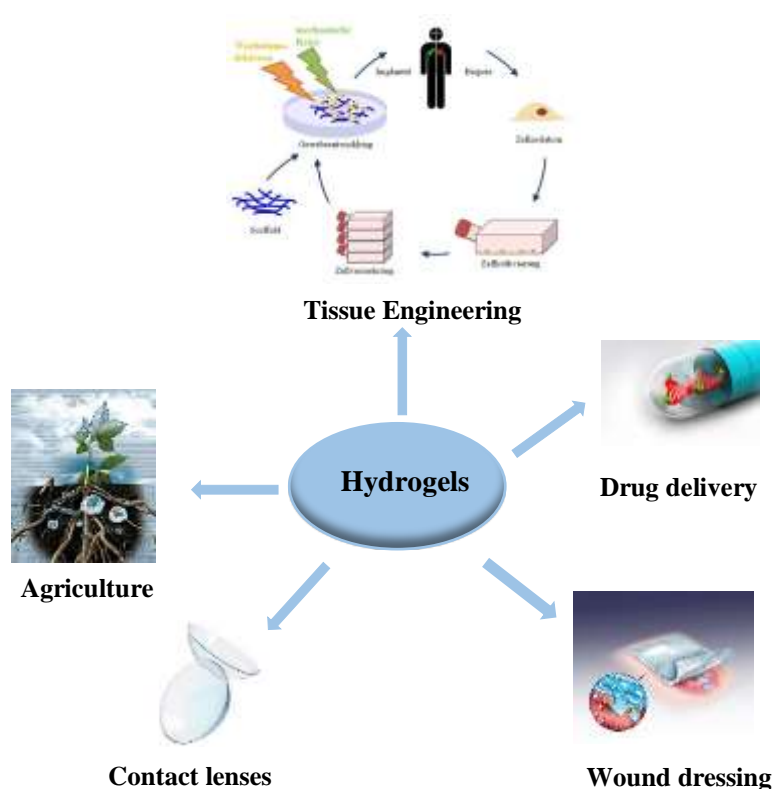


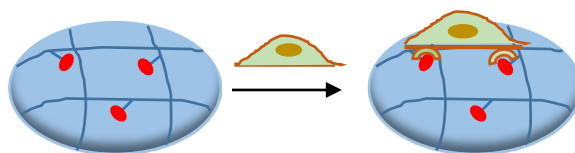
Figure 2.1. Applications of hydrogels.

With respect to the hydrogel composition, it is possible to define natural and synthetic hydrogels. Collagen, chitosan, alginate, hyaluronic acid (HA) are natural hydrogels. The advantages of the natural hydrogels are the biodegradability and intrinsic cell interactions. High water content, mechanical properties and inherent chain flexibility make them ideal candidates to mimic the natural ECM. Additionally, in the cellular microenvironment, natural polymers have the potential to degrade by occurring cell-secreted enzymes which helps to mimic the dynamic nature of ECM [38]. Although hydrogels derived from natural biomacromolecules display excellent biocompatibility, they show very often only low mechanical strength and may

change in their composition due to batch-to-batch variation [39]. To overcome these problems well-defined synthetic polymers have been developed over the past decades for different medical applications. However, synthetic materials need further functional groups to show biocompatibility and only selected polymers are biodegradable. To address these drawbacks, many studies have been conducted especially in tissue engineering to create biomimetic hydrogels that mimic the biological properties and physiochemical of natural materials [40]. Biomaterials play an essential role in the success of tissue engineering, they may be synthesized to control cell behavior with incorporating bioactive ligands. Among the functional bioactive moieties, the Arg-Gly-Asp (RGD) peptide sequence derived from fibronectin (a protein of the ECM) is the most well-known example. Cells attach to hydrogels functionalized with RGD by special interactions between the RGD-peptide and integrin receptors located on the cell membrane (Figure 2.2 i) [41,42].

One emerging concept is the incorporation of biology-to-material interactions into synthetic hydrogels, whereby cells or biomolecules trigger a macroscopic response, like swelling/collapse or sol-gel transition. However, the presence of receptors for biomolecules in these bioresponsive networks can lead to localized or bulk changes when they are exposed to stimulation [42,43]. Specially, these materials can be used to discover disease signs and reply to them to repair the diseased region. *Ulijn et al.* [42] have published a review on bioresponsive hydrogels that respond to three types of stimuli. (Figure 2.2 ii) A) Hydrogels can be modified to bear small biomolecules which are able to selectively attach to biomacromolecules, containing antibodies or protein receptors. This attachment leads to a macroscopic transition in hydrogels. B) In this fashion, hydrogels are improved with enzyme sensitive substrates, for example short peptides. Chemical change occurs with a molecular recognition event which includes making or breaking of substrate-molecules bonds. C) In the last category, biomacromolecules are incorporated into the hydrogel network. Biomacromolecules such as enzymes have the potential to identify small biomolecules and turn them into a system with variety of physical properties such as different acidity and so on. The resulting response can generate swelling or collapse of the hydrogels, and the signals can be used for biosensing goals.

(i) Bioactive



(ii) Bioresponsive

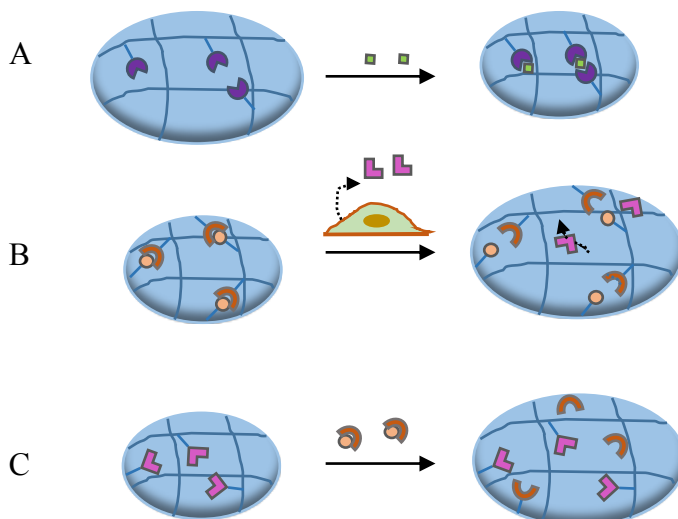


Figure 2.2. (i) Bioactive hydrogel, (ii) bioresponsive hydrogel in three different types with varying the properties in response to A) small molecules through receptor or ligand interactions, B) enzymes by cleavable linkers, C) small molecules that are changed by immobilized enzymes. The macroscopic transition like swelling or collapse of the hydrogels are illustrated. (adapted from [42])

2.3 Hydrophobically modified polymers

Over the last decades, considerable attention has been paid to the development of polymers for use as associative thickeners. Associative thickeners are copolymers composed of a hydrophilic monomer and a hydrophobic comonomer with a long alkyl side chain. Areas of application include coating fluids, cosmetics, water-borne paints and personal care goods, drug delivery systems and water treatment. However, they also have attracted significant interest because of their relevance to biological macromolecular systems [44-52]. With attention to the synthesis method or hydrophobic comonomer distribution, associative polymers are divided in two groups: (i) the simplest classes are telechelic polymers which have comonomers only at their α, ω -ends, (ii) multisticker polymers, with stickers anchored onto the polymer backbone in a blocky or random way depending on the method of synthesis. These hydrophobically modified polymers (HM) show unusual behavior in aqueous solution due to hydrophobic interactions that minimize water-hydrophobe contact [45] (Figure 2.3).

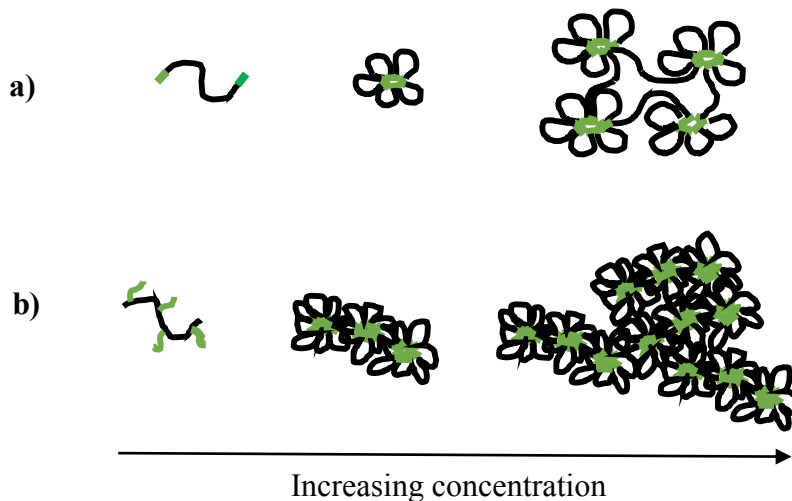


Figure 2.3. Schematic drawing of associating copolymers, a) telechelic and b) multisticker polymers with the hydrophobic units (in green) and the solvophilic blocks (in black). (adapted from [46]).

The presence of hydrophobic moieties leads to intramolecular and intermolecular association of these polymers in aqueous medium. In aqueous solution, above a certain concentration hydrophobic moieties form intermolecular association and create a transitory three-dimensional network which is accompanied by the change of important parameter such as the increase of viscosity, elasticity and gelation behavior. Therefore, most applications of HM mentioned before arise from their unique solution properties [47]. To define the viscoelastic behavior of associative polymers solution, three different concentration regimes can be distinguished (Figure 2.4).

(i) Dilute regime ($c < c^*$): In this regime hydrophobic chains have little chance to interact with each other because small aggregates with small hydrodynamic volume are formed in solution. In this low polymer concentration regime intramolecular association are dominant over intermolecular one, consequently, chain contraction occurs due to intramolecular association. Hence, solution viscosity would be expected to be similar or even lower compared to unmodified polymer analogs [48,49].

(ii) Semi-dilute unentangled regime ($c^* < c < c^{}$):** In this regime the reptation model can be used to analyze the dynamic properties of pairwise associating polymers. *Rubinstein* and *Semenov* [50] predicted a dependence of the viscosity as a function of polymer concentration when the possibility of intermolecular interactions enhance at the expenses of the intramolecular one. Three different scaling regimes can be expected when studying the viscosity of the polymer solution as a function of polymer concentration. According to the

Rubinstein and Semenov model in the semi-dilute unentangled regime: (1) The exchange from intra- to intermolecular association, shows a concentration dependence ($\eta \sim c^{4.2}$), (2) increasing the viscosity by a factor of $c^{5.9}$, owing to a high conversion of intra- to intermolecular association, whereas a lifetime normalization of the associations is required due to the probability enhancement that two hydrophobic side chains associate and disassociate many times before finding new partners, (3) according to the situation that most of the pairwise aggregations are interchain, with a power law: $\eta \sim c^{1.1}$.

(iii) Semi-dilute entangled regime ($c > c^{}$):** The reptation model in this regime still holds, but the scaling behavior is different. With attention to renormalized bond lifetime in a good solvent, the power law viscosity dependence on concentration possesses two exponents. If the network strands between stickers are entangled, the power law exponent is predicted to be 4.72, but when the stickers are overlapping the power law exponent theoretically decreases to 3.75.

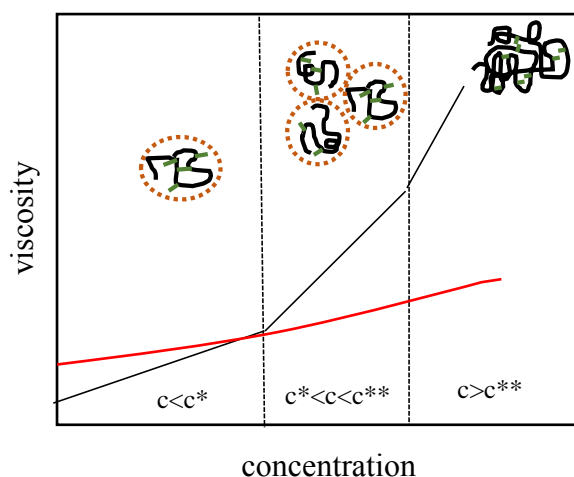


Figure 2.4. Schematic illustration of hydrophobically modified polymer solution viscosity as a function of concentration in three different regimes (black line), unmodified polymer (red line).

In addition to the viscosity, viscoelastic behavior is another important parameter which can be influenced by the hydrophobically modified polymers. G'' (loss modulus) and G' (storage modulus) indicate the viscosity and elasticity of polymer solutions under dynamic oscillatory measurements. In oscillatory frequency sweep measurements, the moduli are determined as a function of frequency at constant strain. Many researchers have studied [49-51] the frequency dependence of the elastic and viscous modulus and obtained similar behavior for associative polymers in semi-dilute unentangled and entangled regimes (Figure 2.5A). Both moduli

enhance with increasing the frequency, at lower frequencies G'' is higher than G' and after a certain frequency (ω_{cross}) the elastic modulus (G') becomes larger than the loss modulus (G''). After the crossing point these copolymer solutions display an elastic character and behave like a weak viscoelastic gel. *Volpert and coworkers* [52] compared viscoelastic properties of hydrophobically modified (HM) copolymers with unmodified polymers. They found that HM polymers have higher elastic and viscous modulus in the same frequency range whereas unmodified polymers show a higher G'' over the entire frequency area (Figure 2.5B). The dynamic storage and loss modulus show a totally different behavior when copolymers form a chemically cross-linked hydrogel (Figure 2.5C) because the elastic modulus (G') is larger than the viscous modulus (G'') in the entire frequency range. This behavior is consistent with the elastic nature of the hydrogels. *Hao and coworker* [53] prepared hydrogels from *N,N'*-dimethylacrylamide (DMAM) and 2-(*N*-ethylperfluorooctane sulfonamido) ethyl acrylate (FOSA) with different amount of FOSA. They observed in all hydrogels that G' is larger than G'' at room temperature over the whole frequency range.

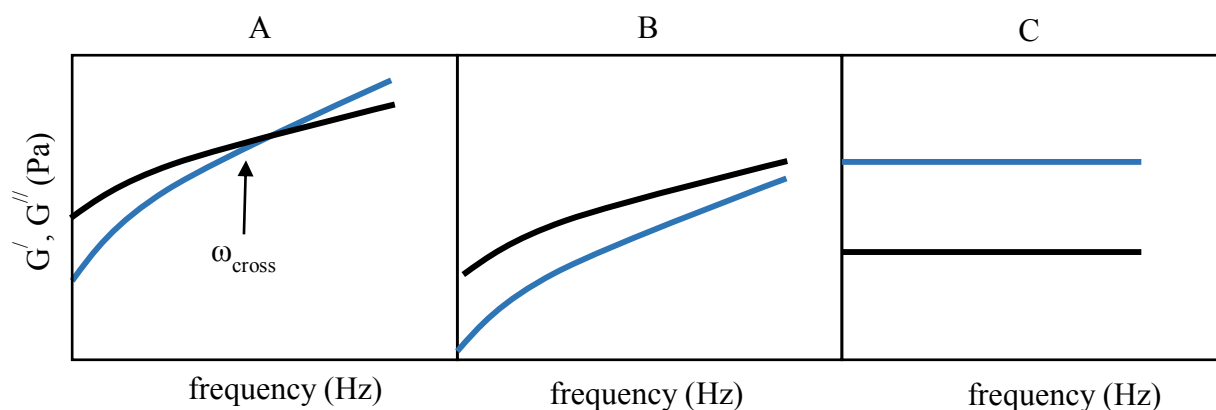


Figure 2.5. Schematic diagrams of storage (G') (blue line) and loss (G'') (black line) modulus as a function of frequency for A) hydrophobically modified polymers, B) unmodified polymers, C) hydrogels, at the same frequency range.

Strauss and Jackson synthesized the first HM copolymers as model to mimic conformational behavior of proteins [54]. *Strauss and coworkers* also developed polysoaps which are the original HM water-soluble polymers by utilizing hydrophobic moieties such as n-dodecyl bromide and decyl vinyl ether [55-57]. *McCormick et al.* [58], *Winnik et al.* [59] and *Morishima et al.* [60] have done much research on such polymers to investigate the rheological properties. Although many monomers have been used to design associating polymers, acrylamide is the most commonly used hydrophilic monomer [61]. Up to now, most of HM polyacrylamides and

other associative polymers have been prepared by a free radical micellar polymerization technique. In this method, a surfactant like sodium dodecyl sulfate (SDS) is used in aqueous solution to solubilize the hydrophobic monomer. The hydrophobic monomer in this procedure is distributed along the backbone in a blocky fashion. Therefore, the rheological properties of the polymer solution can be controlled by varying the amount of hydrophobic monomer to surfactant. The results illustrate that longer hydrophobic blocks lead to higher viscosity of the solution [62]. *Regalado and coworkers* [63] synthesized hydrophobically modified polyacrylamides with *N,N*-dihexylacrylamide (DiHexAM) as a hydrophobic monomer which can be dissolved in aqueous medium by sodium dodecyl sulfate (SDS). They calculated the number of hydrophobes per micelle (N_H) by the following equation:

$$N_H = \frac{([H] N_{agg})}{[SDS] - cmc_{SDS}} \quad \text{eq. [2.1]}$$

[H] is the hydrophobic content which is equal to the monomer feed in the reaction, N_{agg} is the aggregation number, [SDS] is molar surfactant concentration and cmc its critical micelle concentration. The prepared multiblock copolymers have variable viscoelastic properties with three characteristic parameters: First, molecular weight ($M_w \sim 4.2 \times 10^4 - 2.7 \times 10^6$ g/mol), secondly, hydrophobe content ([H] = 0.5-2 mol%) and thirdly, hydrophobic block lengths ($N_H = 1-7$ units for each block). The effect of one parameter was examined while two other parameters were kept constant. The zero-shear viscosity was studied as a function of concentration. For all systems the same behavior was observed: Above a certain concentration (C^*) the viscosity increased sharply, but C^* is independent of N_H and H whereas M_w has a strong effect on C^* . The concentration (C^*) decreases with increasing M_w . *Hill et al.* [64] synthesized acrylamide-based copolymers with *N*-4-ethylphenylacrylamide (e ϕ AM) as a hydrophobic monomer. The hydrophobicity of e ϕ AM is not too high so they could study different preparation methods, with or without surfactant. The methods are divided into three techniques: (1) Micellar polymerization with surfactant, allows to dissolve the hydrophobic monomer, (2) a ‘‘homogeneous’’ technique with a miscible co-solvent, (3) a ‘‘heterogeneous’’ method where the hydrophobic monomer is being dispersed in the aqueous medium due to the absence of additives. Their study demonstrated that different methods have a significant influence on the final copolymer solution properties. The copolymers obtained by the second and third approach without surfactant do not form hydrophobic associations, hence, these copolymers act like polyacrylamide homopolymer. The micellar process with a rather blocky structure (Figure 2.6)

promotes the intermolecular hydrophobic aggregation and leads to the thickening properties of the aqueous polymer solution. Consequently, the rheological properties can be controlled by the degree of association that resulted from the hydrophobic moieties per micelle, which were calculated from the surfactant-monomer composition.

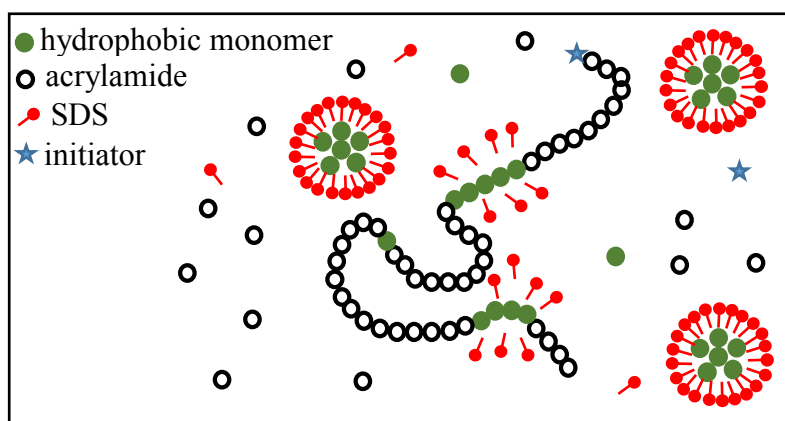


Figure 2.6. Scheme of the micellar copolymerization reaction medium. (adapted from [65]).

The micellar polymerization is the most applied method for fabricating HM polymers, due to the excellent thickening ability of the blocky structure of the hydrophobic monomer. However, the main disadvantages of this method are the rather low initial concentrations of the reaction medium due to the gel effect as conversion increases. Moreover, due to the low water solubility of the final HM polymer, it is difficult to employ them for practical applications [66]. These disadvantages can be solved with the use of inverse emulsion and inverse microemulsion polymerization, however, these techniques require a large amount of surfactant which limits their applications [67]. *Gong and coworker* [66] used inverse miniemulsion polymerization (IMEP) to synthesize water-soluble HM copolymers. This method can be carried out with a rather low surfactant content. They investigated the inverse miniemulsion of acrylamide with the cationic monomer dimethyloctane (2-acrylamidopropyl) ammoniumbromide (DOAB) which is also used as a hydrophobic moiety and polyacrylic acid (PAA) as a template. The robust interaction between opposite charged DOAB and PAA leads to the formation of tight complexes. In addition to inverse miniemulsion (IME)/oil interface droplets, the complexes were present in the IME interior droplets. The viscosity study of the obtained polymer demonstrated excellent thickening ability.

Although different techniques containing surfactant have been reported to prepare HM acrylamide copolymers, *Cram et al.* [68] employed an easier process to design associative polymers without the use of surfactant with interesting rheological behavior. They used *N,N'*-dimethylacrylamide (DMAM) instead of acrylamide because of the higher solubility in organic solvents, hence, the hydrophobic moieties can be incorporated into DMAM in a homogenous reaction medium. Dodecyl acrylate (DA) and octadecyl acrylate (ODA) were used as hydrophobic moieties with 12 and 18 carbons in the side chain, respectively, to examine the effect of chain length on the copolymers properties Figure 2.7.

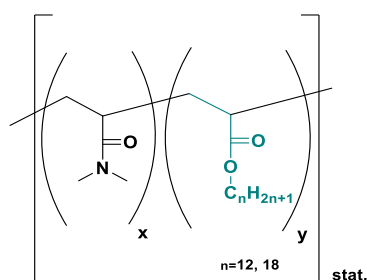


Figure 2.7. DMAM associative copolymer containing dodecyl acrylate (DA) or octadecyl acrylate (ODA).

The copolymers were prepared via free radical polymerization with AIBN as an initiator in homogenous solution of toluene. The copolymers in this case have a random structure which exhibit lower thickening ability in comparison to the HM polymers with microblock structure. Apart from the simplicity of the method, the copolymerization can be carried out without surfactant, therefore, the final product shows high purity. Furthermore, the viscoelastic properties can be easily changed with varying the hydrophobic content and the chain length. Due to these advantages this copolymer was chosen as reference system in this study.

2.4 Polyelectrolyte

Polyelectrolytes are water-soluble polymers that are categorized into three main types according to their charges: cationic, anionic and amphoteric which are carrying positive, negative and equal numbers of positive and a negative charges, respectively. These charges can be located on the side chain or distributed along the backbone [69].

The great advantage of polyelectrolyte based gels is the special response to environmental stimuli like electrically-induced chemomechanical contraction resembling a biological response. Moreover, biological tissues include polyelectrolytes that show properties originating

from their polyelectrolyte nature. Consequently, polyelectrolyte based hydrogels have significant potential as scaffold for cellular adhesion, differentiation and proliferation and can be utilized as artificial tissues for replacement of injured ones [70]. In the following section the polyelectrolytes are described which have been used in this research.

2.4.1 Cationic polymers

Macromolecules with positive charges are classified as cationic polymers. They have been widely studied for different therapeutic applications [71]. Polymeric chain flexibility, hydrophobic interactions, pK_a -value, electrostatic forces, H-bond formation, amine group and its neighboring functionality in addition to the nucleophilic character are the factors which determine the properties of cationic polymers [71]. According to their origin they are classified into two categories: natural and synthetic (Figure 2.8).

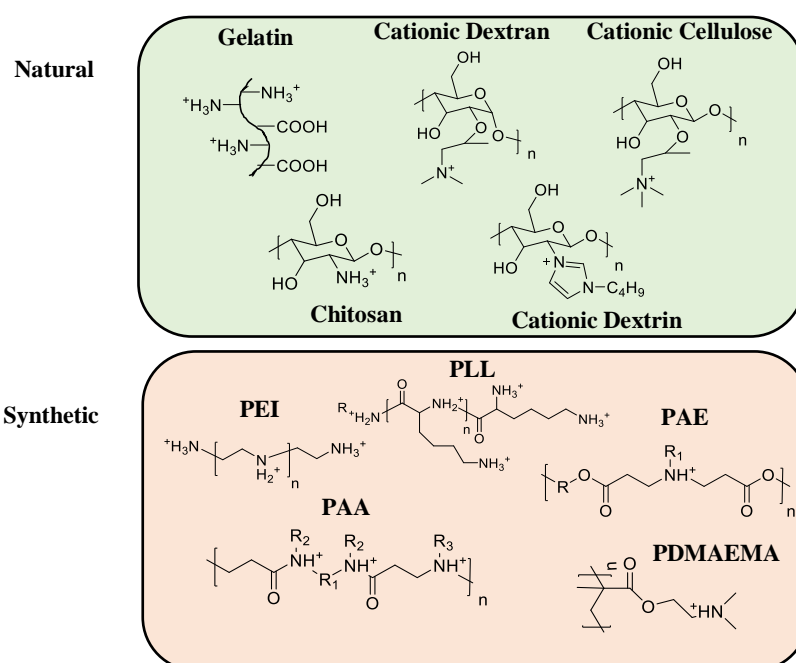


Figure 2.8. Classification of cationic polymers.

2.4.1.1 Natural cationic polymers

Natural cationic polymers are obtained from renewable resources, they are biodegradable and biocompatible with mostly low immunogenicity and low toxicity. Additionally, they have reactive sites which can be functionalized to improve their physiochemical properties [71,72].

Gelatin

Gelatin is a natural polymer extracted from porcine or bovine bone, its excellent biodegradability makes it a good candidate for pharmaceutical and medical applications [73]. *Tseng and coworkers* [74] found that cationic gelatin nanoparticles (GPs) can be a promising new medical material for ocular disease due to the ability to encapsulate dye/drug/gene. Research shows that GPs with less than 200 nm lead to high cellular uptake in tumor cells, which can result in greater drug accumulation in tumor tissue and induce a stronger therapeutic effect [75]. *Chou and coworkers* [76] created cationic polyethyleneimine (PEI)-modified GPs with approximately 135 nm particle size. Their study proved that the particles were stable under different pH and temperature conditions with high protein loading efficiency. Additionally, the promising cell results make PEI-modified GPs systems a good candidate for use in regenerative medicine and cancer therapy.

Chitosan

Randomly distributed *N*-acetyl-D-glucosamine and D-glucosamine are the main components of the natural cationic polymer chitosan. Chitosan has attracted increasing interest due to its very good biodegradability, low allergenicity, biocompatibility and non-toxicity [77]. Furthermore, antimicrobial [78], antioxidant [79] and antitumor [80] activities have been associated with chitosan in different applications. Chitosan has been also studied in stem cell research especially in the field of nerve repair [81,82]. *Yang and coworkers* [83] studied the effect of three types of biomaterials on rat neural stem cells, (i) a collagen gel membrane, (ii) a chitosan membrane and (iii) a chitosan-collagen membrane. All three materials revealed low cytotoxicity with the potential to promote adhesion, migration, differentiation and proliferation of neural stem cells. But the results showed also that the neurospheres are able to attach more onto the chitosan-collagen membrane which led to a higher degree of differentiation.

Cationic Cyclodextrin

Cyclodextrins (CDs) are obtained by enzymatic degradation of starch, they are essentially sugar derivatives that include 6-8 α -1,4-connected glucose unit. These cyclic molecules are divided into α , β and γ groups according to their glucose unit amount. Every cyclodextrin unit with hydrophobic cavity can behave as a host for small hydrophobic molecules. The great biocompatibility, low immunogenicity and low toxicity of cyclodextrin in addition to its excellent functionalization capacity due to a high amount of hydroxyl groups make CDs an

excellent candidate for medical applications [84,85]. Many CD-polymer conjugates were designed by chemical modification of CDs. Polycationic amphiphilic CDs have been reported [86] as efficient gene delivery system. They can be modulated to alter the cationic charge density and introduction or removing of hydrogen bonding functionalities can change the polymer chain flexibility.

Functionalized cationic dextran derivatives

Dextran is the homopolysaccharide of glucose units which becomes cationic after appropriate functionalization and is utilized in gene delivery and tissue engineering. Dextran emerges to apply for polymeric carrier because it is biodegradable, broadly available and can be easily modified. *Cohen and coworkers* [87] reported a new delivery vehicle made of spermine modified acetalated-dextran (Spermine-Ac-DEX) that is able to deliver siRNA to cancer cells. *Mai et al.* [88] developed a novel dextran-based system with efficient gene delivery abilities. The system was designed by poly(amidoamine) dendrons conjugation onto dextran to deliver plasmid DNA successfully to human embryonic kidney cells (HEK293).

Functionalized cationic cellulose

Cationic cellulose is the most abundant biopolymer which possesses a polysaccharide structure. Renewable cationic cellulose-based materials with outstanding characteristics including biodegradability, hydrophilicity and antibacterial properties have been used in therapeutic fields. The cellulose hydroxyl units can be further functionalized that resulted in an expanded set of applications [89]. The functionalization is usually done by cellulose esterification utilizing glycidyl ammonium salts or epoxidation reactions [90]. Properties such as antibacterial activity or hydrophobicity can be achieved with these modifications. *Littunen et al.* [91] and *Chaker and coworkers* [92] prepared cationic nanofibrillated cellulose with quaternary ammonium groups which presented antibacterial activity. In another study [93], quaternized cellulose (QC) nanocomposite hydrogels containing cationic cellulose nanocrystals (CCNCs) and β -glycerophosphate (β -GP) as a crosslinking agent was synthesized. This injectable hydrogel (QC/CCNC/ β -GP) system showed mild inflammatory reactions with no obvious cytotoxicity.

2.4.1.2 Synthetic cationic polymers

Synthetic cationic polymers as well as natural groups have been studied for therapeutic applications. The important drawback of natural polymers is batch-to-batch variation which can

be solved by synthetic polymers. The disadvantage of the synthetic polymers is that a high cationic charge density leads to increased cytotoxicity. However, this can be overcome by the incorporation of bioactive functionalities and biodegradable linkers [71,72]. In Figure 2.9 the most commonly used synthetic cationic polymers structures are shown but in the upcoming paragraphs only PDMAEMA is investigated.

Quaternary ammonium groups of cationic polyelectrolyte are divided into two categories, according to the synthetic routes: (i) appropriate monomers are polymerized through step or chain polymerization (Figure 2.9 i) or (ii) reactive precursor polymers are functionalized [94] (Figure 2.9 ii).

The obtained polymers of method (i) have 100% functionality but it is difficult to characterize the polycations because of their conformational sensitivity in aqueous solution towards ionic strength and because of interactions with other materials like chromatography column material that disturb efficient separation [95]. The advantage of using method (ii) is that the precursor monomers can be easily polymerized and the resulting polymers can be characterized by conventional methods. The quaternization reaction is then carried out in a polymer-analogous fashion with high conversions.

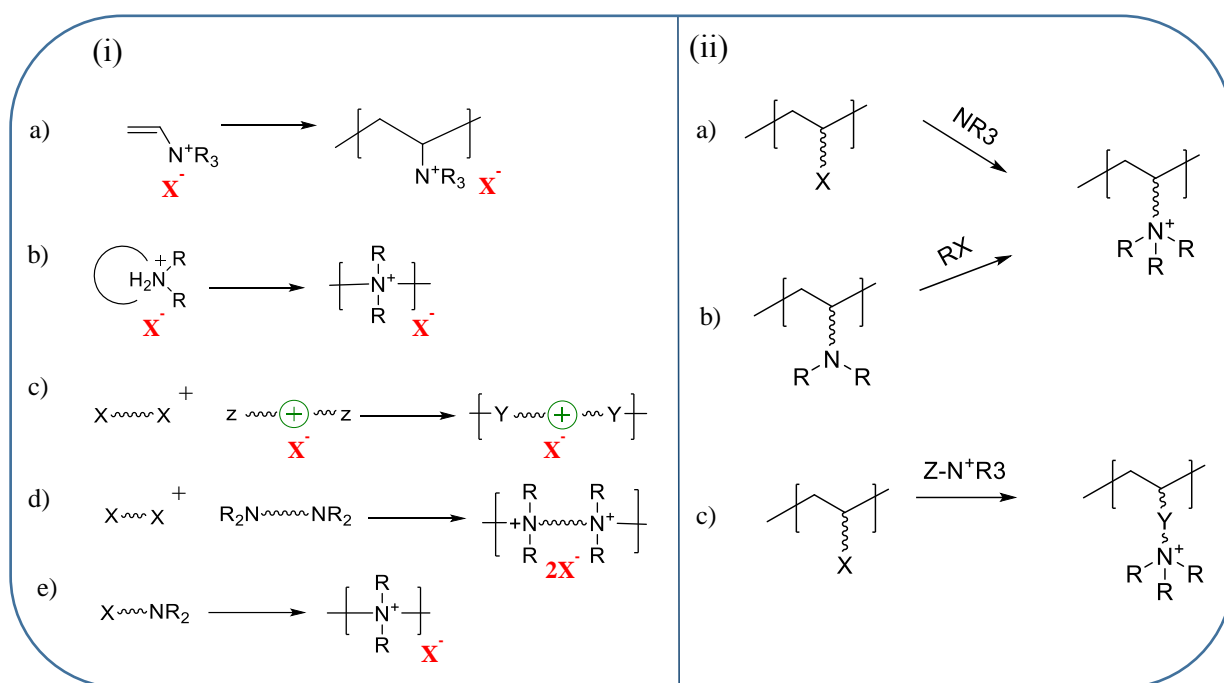


Figure 2.9. (i) Typical polymerization methods to form polycations, (ii) reactive precursor polymers and their quaternization. (adapted from [94]).

Chain polymerization of cationic vinyl monomers results in most cases in polyelectrolytes with the cationic charge located in the side chain (Figure 2.9 i-a). Step polymerization usually creates

cationic polymers with the positive charge in the polymer backbone (Figure 2.9 i- b-e). Cationic polymers through ring-opening polymerization have only be obtained in very few cases (Figure 2.9 i-b).

When the cationic charge is a quaternary ammonium group it can be synthesized by utilizing a quaternization reaction (Figure 2.9 ii). This can be accomplished via (i) addition of tertiary amine to a polymer containing alkyl halogens, (ii) the quaternization of the polymer including tertiary amine groups using aryl or alkyl halides, (iii) quaternization based on the Mannich reaction which is followed by modification of polymeric amides with a secondary amine and aldehyde and (iv) polymers including OH-groups can be quaternized with agents such as 2,3-epoxypropyltrimethylammonium chloride.

Poly[2-(*N,N*-dimethylamino)ethyl methacrylate] (PDMAEMA)

Aqueous solutions of PDMAEMA have been widely studied because of their sensitivity to variation in pH or temperature. PDMAEMA has tertiary amine groups which may be protonated at physiological pH. Therefore, the charge density of this weak polyelectrolyte can be changed by varying the pH. The amine groups of the polymer has a pK_a value of around 7.0. Hence, at $pH < 7$ the tertiary amine groups are protonated and PDMAEMA behaves like a polycation. The quaternized nitrogens can interact with enzymes or pure polyanion such as DNA by electrostatic attraction [96,97].

pH-responsive polymers are useful to exploit the various pH gradients that exist in the body, for example between cell compartments and extracellular tissue or between normal tissue and tumor tissue [98,99]. *Car and coworkers* [98] synthesized a series of block copolymers of the type PDMS-block-PDMAEMA through atom transfer radical polymerization (ATRP). Self-assembly of these block copolymers created micelles between 80-300 nm in size, which are able to encapsulate doxorubicin (DOX). Their cell experiment results showed that the PDMAEMA block lengths have a direct effect on cell viability. Micelles based on block copolymers with 5 units PDMAEMA resulted in excellent cell viability whereas block copolymers with 13 and 22 units of PDMAEMA showed increasing cytotoxicity. Interestingly, the release of DOX is controlled by the pH-value of the surrounding solution. At pH 7.4, the DOX loaded micelles kept 80 wt% of the drug for 72 h, while at pH 5.5 more than 80 wt% of the encapsulated DOX was released within 48 h.

2.4.2 Zwitterionic polymers

By definition, polyzwitterions or polybetains possess equal numbers of anionic and cationic groups along the same polymer chains [100]. The combination of oppositely charged moieties is responsible for the ultra-hydrophilicity of the polymer, while at the same time retaining an overall neutral state. Figure 2.10 shows the several possibilities to introduce ion pairs within a polymer to prepare zwitterionic polymers.

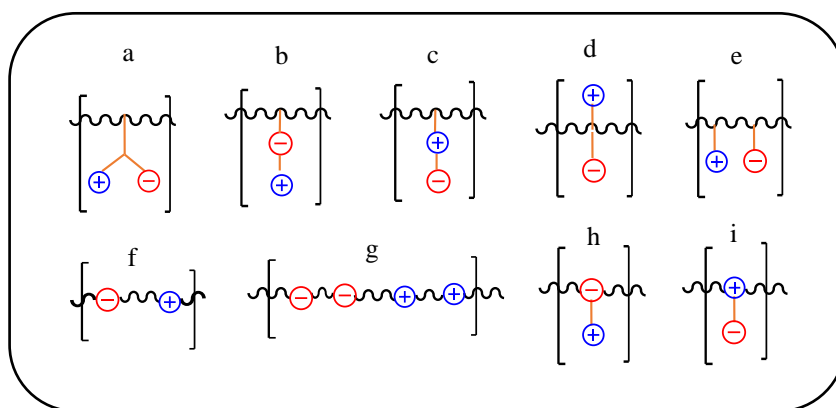


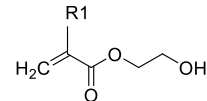
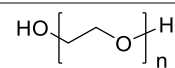
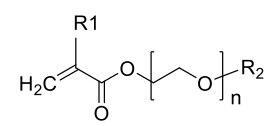

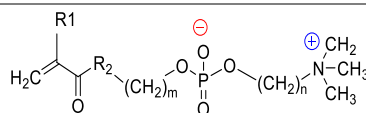
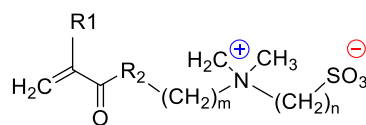
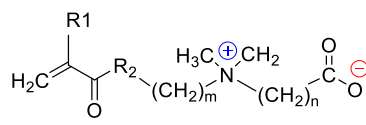
Figure 2.10. Possible distribution of ionic moieties within zwitterionic polymers. (adapted from [100]).

Type c has been recognized as the most widespread type of zwitterionic polymers. From their synthesis, it was proven that polyzwitterions containing ionic moieties in the polymer side chain (type a-e) are easier to prepare than the polyzwitterions with ionic groups in the polymer main chain (type f-i). Additionally, for polymer-analogues reaction, the required chemical functionalization is more easily and versatile accomplished for organic cationic moieties, especially for ammonium groups than for anionic moieties. Zwitterionic polymers of type c are commercially accessible and have thus attracted more interest in comparison to other zwitterionic polymers, except phosphobetaines which have been used for synthetic cell membrane [100].

After implantation of a material, the first contact will occur with the blood independent of the implantation site. Consequently, the investigation of the biomaterials blood compatibility is very important for blood-inert devices [101,102]. The improvement of non-fouling surfaces is very important in biomedical fields which contain blood-contacting devices [103,104]. However, there is very limited availability of synthetic biomaterials which have potential to be used as hemocompatible materials. Zwitterionic polymers are composed of an equal number of cationic and anionic moieties which can control non-fouling properties through a hydration layer generated from solvation of the ionic terminal moieties, in addition to hydrogen bonding

[105,106]. According to *Sin and coworkers* [102], non-fouling materials development can be divided into three groups: first generation is based on 2-hydroxyethylmethacrylate (HEMA) polymers, the second generation is based on PEGylated polymers and the third generation is polyzwitterions. In Table 2.1 their chemical structures are presented.

Table 2.1. Evolution of anti-fouling materials: a) 2-hydroxyethyl methacrylate, b) poly(ethylene glycol) or oligo(ethylene glycol), c) poly(ethylene glycol) methacrylate, d) phosphobetaine methacrylate, e) sulfobetaine methacrylate, f) carboxybetaine methacrylate. (adapted from [102]).

1 st Generation	1960s~	HEMA-based systems -OH	HEMA ^a	
2 nd Generation	1970s~	PEGlyated systems (-c-c-o) _n	PEG or OEG ^b PEGMA ^c	 
3 rd Generation	1990s~	Zwitterionic systems 	PBMA ^d SBMA ^e CBMA ^f	  

HEMA-based polymers

PolyHEMA is recognized to prevent protein adsorption due to their hydrophilicity originating from their -OH functional groups which enable it to build hydrogen bonds (H bonds) with each other and water molecules. Consequently, they have the potential to create a strongly bound hydration layer to suppress any nonspecific protein adsorption on biomaterials. However, polymers based on HEMA revealed insufficient antifouling performance in undiluted human blood plasma and serum [102,107].

PEGylated polymers

Since the early 1980s, modified surfaces with poly(ethylene glycol) (PEG) or oligo(ethylene glycol) (OEG) have been widely investigated for their antifouling properties to decrease or to prevent the non-specific adsorption of soluble proteins [108-110]. Such antifouling behavior is based on steric repulsion resulting from hydrated neutral PEG chains [111]. The key factors include the molecular weight (M_w) and graft density of PEG chains that determine the ability of PEG functionalized surface to display antifouling behavior. Another important factor is the PEG chain conformation which is related to the surface graft density [112]. Mushroom or brush conformation are typically expected for a low or high graft density, respectively [113]. The polymer chains form a pancake-like conformation at very low graft density. PEG self-assembled monolayers (SAMs) have shown to prevent nonspecific protein adsorption best when they are in the brush conformation. However, PEGylated surfaces have the chemical stability problem due to the decomposition of OEG and PEG groups in the presence of transition metal ions and oxygen detected in most biochemically related solutions. It was also reported that grafted PEG brushes show reduced protein adsorption at physiological temperature. Therefore, numerous studies have been done to find an alternative material with antifouling properties which possess higher stability in comparison to PEG/OEG systems [102].

Zwitterionic polymers

When the cationic charge of zwitterionic monomer is provided by ammonium NR_4^+ , and the negative charge are sulfonate SO_3^- , phosphonate PO_4^- or carboxylate CO_2^- groups, the zwitterionic polymers can be classified as sulfobetaine, phosphobetaine and carboxybetaine, respectively [114].

Poly(sulfobetaine methacrylate) (PSBMA) containing methacrylate as the main chain and taurine betaine analogue as a pendant group [$\text{CH}_2\text{CH}_2\text{N}^+(\text{CH}_3)_2\text{CH}_2\text{CH}_2\text{CH}_2\text{SO}_3^-$], has been widely investigated due to its facile synthesis. Previous work has shown that surfaces modified with PSBMA are good candidates for the preparation of efficient and stable antifouling materials when the chain length and surface density of the zwitterionic moieties are controlled [115]. *Chang and coworkers* [116] synthesized three types of diblock copolymers composed of PSBMA and poly(propylene oxide) (PPO) as a hydrophobic group on methyl-terminated self-assembled monolayers (CH_3 -SAM) surfaces. The copolymers were prepared by atom transfer radical polymerization (ATRP) in order to control the chain length of PSBMA with a narrow polydispersity, while the PPO chain length was fixed. Their results showed the dependence of the protein adsorption on the M_w of the copolymers. Moreover, the diblock copolymers revealed

good protein resistance when the surface densities of SBMA was well controlled. In another report [117] the influence of synthetic poly[2-(methacryloyloxy) ethyl dimethyl-(3-sulfopropyl) ammonium hydroxide] (PMEDSAH) on the self-renewal capacity of human embryonic stem cells (hESCs) was studied. The polymerization was carried out by ATRP to control the thickness of the polymer layer. By increasing the reaction time PMEDSAH thickness was enhanced retaining its overall chemical architecture while its internal hydrogel structure was modified. When the PMEDSAH coating had a 105 nm thickness, a remarkable increase in the hESCs expansion rate was observed, suggesting that the physical properties of the PMEDSAH layer have the ability to support hESC expansion.

Phosphobetaine such as poly(2-methacryloyloxyethyl phosphorylcholine) (PMPC) have attracted much attention because of their resemblance to the hydrophilic head group of the cell membrane lipid [118]. MPC can be used for drug solubilization like amphotericin B and paclitaxel [119]. A diversity of different PMPC based nano-carriers have been reported containing combined systems with DNA and other polymers like PLA to design a system with gene delivery potential. Some other systems have the potential to be used for drug-carrier application because they can self-assemble into polymersomes and micelles. They are mostly prepared by ATRP or RAFT polymerization in order to have more controlled polymer architectures and molar mass and polymer dispersity [120,121].

Carboxybetaine (CBMA) is another group of zwitterionic compounds. The difference between sulfobetaine and carboxybetaine is the negative charge from the carboxylic acid (-COOH) functional group. Therefore, CBMA has the ability to be easier functionalized with higher surface packing density [122]. *Zhang and coworkers* [123] prepared a biomimetic structure based on grafted polyCBMA on a gold surface utilizing initiators through the surface-initiated ATRP technique. This system can play two roles, first the protein resistance and second the protein immobilization. Actually, the presence of carboxyl groups within the carboxybetaine methacrylate can be used to covalently attach proteins via their amino groups. Such dual functional properties are only detected for carboxybetaine groups and are not met in other non-fouling materials like ethylene glycol, sulfobetaine and phosphobetaine.

2.4.3 Peptide based polymers

Arginine-glycine-aspartic (RGD) (Figure 2.11) defines a cell adhesion motif presented on many plasma proteins and components of ECM. The RGD peptide has attracted much attention since it was first peptide derived from fibronectin that resembles the cell adhesive properties from the fibronectin (FN) glycoprotein. Glycoproteins like fibronectin (FN), vitronectin (VN),

laminin, osteopontin or the von Willebrand factor (vWF) have been detected in the ECM. They all contain the RGD sequence within their structure as the main source of their cell adhesive properties. RGD sequences are recognized to play a fundamental role in cell recognition and cell adhesion can be utilized in tumor therapy to target integrin receptors on cancer cells and tissue engineering application such as bone cement or artificial blood vessels [124].

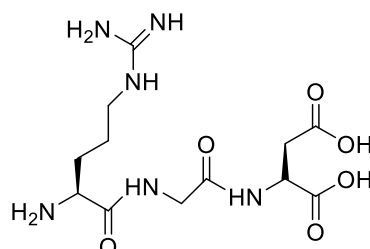


Figure 2.11. RGD sequence structure.

2.4.3.1 Chemical methods for synthesis of peptide

Solution phase synthesis (SPS) and solid phase synthesis (SPPS) are two important methods for peptide production. Solution SPS method is based on coupling of amino acids to longer peptides in solution under homogeneous conditions. The long peptides sequence can be synthesized by the fragment condensation technique. In the first step of this method, short fragments of the needed peptide are prepared before they are coupled together to form a longer peptide. The advantage of SPS method is that the desired peptide has high purity due to the fact that intermediate products can be deprotected and purified. Oxytocin (a neuropeptide and main sexual reproduction hormone), human insulin (containing 51 amino acid sequence which control the metabolism of carbohydrate in the body) and porcine gastrin releasing peptide (GRP) (a hormone which stimulating the release of gastric acid from the stomach) are examples of peptides that were fabricated by the solution SPS technique. While scaling up in SPS can be done in an inexpensive and easy manner the long reaction time is the main limitation of this method [125].

The solid-phase peptide synthesis (SPPS) technique, which was developed by *Merrifield* in 1963 enables the fabrication of short peptides with 20-30 amino acids in length. In this method *Merrifield* applied an *N*-protected amino acid generating an ester bond when reacting it with a partially chlorinated polystyrene resin. In the next step, the protecting group is removed and the free amino group is available to be attached to the next *N*-protected amino acid by using coupling agents that have been developed for the SPPS. Therefore, the SPPS method is based on a coupling-washing-deprotection-washing repeating cycles. The immobilized peptide onto the solid-phase will remain attached during this process while side products and liquid-phase

reagents are flushed away. The procedure is completed by cleaving the peptide from resin and purify it eventually by HPLC (Figure 2.12) [126,127]. In general, SPPS has the advantages to do wash cycles after each step and eliminating excess of reagents which leads to growing peptide chains remaining covalently linked to the insoluble resin. In this technique the peptide can be synthesized in a fully automated fashion utilizing peptide synthesizer. But SPPS can only be used to produce polypeptides with less than 50 amino acid residues because of some reasons: (i) low coupling efficiency when the peptide length enhances, (ii) low purity products are normally achieved when large polypeptides are prepared, (iii) to assure the maximum coupling efficiency using an excess of coupling reagents and amino acids are necessary, (iv) protected peptide solubility is often challenging and complete deprotection of long peptides is not easy to achieve [127]. Therefore, solid-phase peptide synthesis is typically limited to the preparation of polypeptides with up to 50 amino acids.

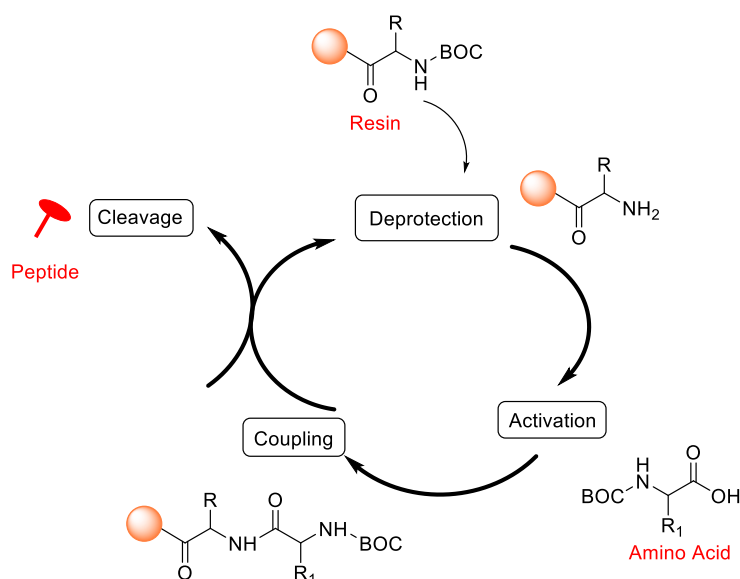


Figure 2.12. Scheme of the solid-phase peptide synthesis (SPPS) developed by Merrifield and coworker. (adapted from [127]).

2.4.3.2 RGD interaction with cell surface integrins

Cell interactions play a crucial role in numerous physiological process. They are also essential in embryonic development that is really an important period in a multicellular organism life [128,129]. Embryonic cells begin interactions with the ECM from the earliest stage of development, and these are prerequisite for cell migration and proliferation as well as cell differentiation into various lineages [130,131]. Integrins comprise a major family of cell surface receptors which are known to mediate cell-ECM interaction, and it has been reported that they

have direct or indirect influence on cell behavior [132,133]. Integrins are a large group of heterodimeric transmembrane glycoprotein receptors that consist of a non-covalent association of α and β subunits. 18 α and 8 β subunits can be expressed in mammals which can form 24 different $\alpha\beta$ dimers. Each subunit includes a large extracellular globular head, a single transmembrane helix and a mostly short cytoplasmic tail. One side of the integrin is directed to the extracellular space and can interact with particular ligands that exist on protein surfaces like LDV and RGD, whereas the other side binds to the intracellular part and is involved in propagation of signals in the interior of the cells [134,135]. Until now, nearly half of the 24 known integrins are able to bind to RGD containing protein ligands [136]. Additionally, RGD peptides have some advantages that make them attractive for practical applications and scientific research:

- compared to monoclonal antibodies the tripeptide RGD is much smaller in size, therefore RGD conjugates can eventually access tumor tissue via specific biomarkers much easier
- the RGD peptide synthesis procedure is relatively inexpensive and simple compared to the production of human antibodies

Therefore, peptide-polymer conjugates represent a very useful class of materials with the ability to be applied at the materials-biology interface. These macromolecules combine the properties of synthetic polymers like control over molecular weight, composition, architecture and stiffness with those of peptides that offer very particular biofunctionalities via well-defined amino acid sequences [137].

2.5 Polymeric Materials for Cell Culturing Applications

As has been mentioned in the previous chapter 2.2 there are many different applications of hydrogels due to the fact that their chemical, physical and biological properties can be fine-tuned by the polymer composition. One important application of hydrogels that will be explained in more detail is the use as a matrix for cell culture application [138].

Traditionally, many cell-based experiments are performed on flat and stiff materials such as polystyrene and glass dishes. Although these systems are very easy to handle, cells cultured in these environments tend to display unusual behaviors such as a flattened shape, loss of differentiated phenotype or abnormal polarization [139]. Different scientists have assumed that the reason for this behavior has to do with the two-dimensional (2D) cell culture conditions in contrast to the cells natural tissue environment that receive signals in all three dimensions. Hence, there is a huge need for culture systems that better mimic the biological environment of

cells to bridge the gap between conventional culture dishes and complex *in vivo* three-dimensional microenvironments of natural cells [140,141]. (Figure 2.13)

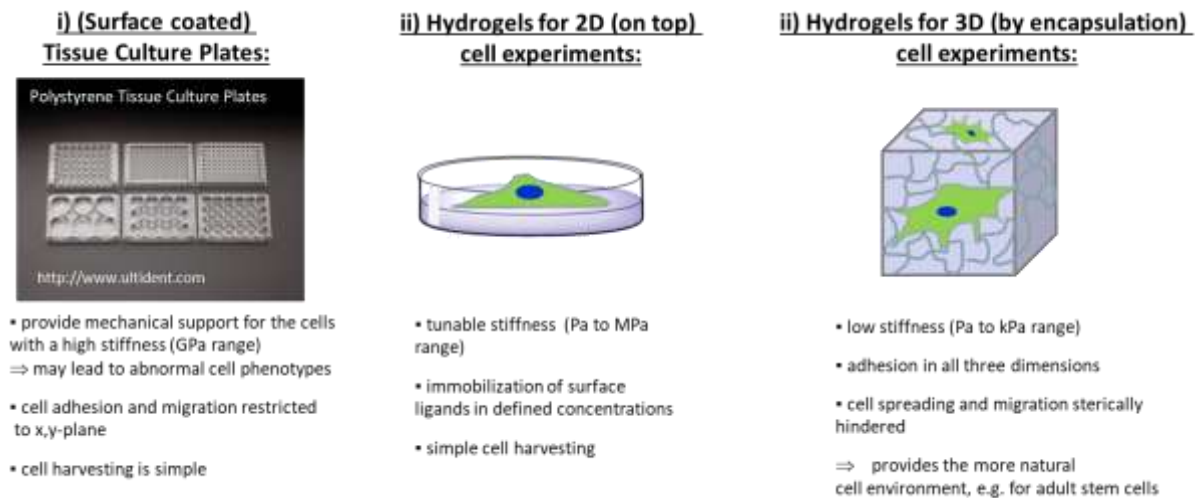


Figure 2.13. Comparison of tissue culture plates and hydrogels for cell culture applications.

The latter topic has recently attracted considerable attention in stem cell research since well-defined materials are required to store and maintain large numbers of cells in a quiescent, non-differentiated state or to provide materials that enable the reproducible differentiation into defined lineages [142-144]. Although many reports exist that culturing adult stem cells is relatively simple and can be carried out on conventional polystyrene tissue culture dishes, human pluripotent stem cells (hPSCs) require more sophisticated conditions and materials such as (i) MatriGel [145] or (ii) on top of a layer of feeder cells [146]. Especially MatriGel, that is derived from mouse tumor cells represents a rather complex protein mixture that is able to grow embryonic stem cells and retain them in an undifferentiated, pluripotent state [145]. Synthetic polymers can be a valuable alternative owing to their well-defined composition and functionalities, that are reproducible and can be easily scaled-up. More recently, *Alexander and Denning* have synthesized a large polymer library of 909 unique homo- and copolymers from 141 monomers that was screened to identify optimized polymeric substrates for cultivation of human pluripotent stem cells and induced pluripotent stem (iPSCs) cells as potential MatriGel substitutes [147]. Best results in hPSC expansion studies were obtained for poly(HPhMA-co-HEMA) coatings with the monomer. monomer *N*-(4-hydroxyphenyl)methacrylamide (HPhMA) and hydroxyethylmetharylate (HEMA) [147]. A similar approach of combinatorial polymer matrix development has been used by *Hong et al.* to fabricate optimized substrates for

iPSC derived cardiomyocytes by testing three components, poly- ϵ -caprolacton (PCL), polyethylene glycol (PEG), and carboxylated PCL (cPCL) in different ratios as synthetic substrates. Best results were obtained when iPS cells were cultured on a 4%PEG-96%PCL where each % indicates the corresponding molar ratio [148]. Although both combinatorial polymer matrix approaches were very successful to find better substrates for cell culturing in 2D these polymers cannot be used for 3D cell encapsulation experiments.

Hydrogels for cell culturing have some advantages in this respect as they can be easily synthesized with well-defined composition and functionalities [149,150] and enable cultivation in two dimensions (2D) on top of a hydrogel film and in three dimensions (3D) by encapsulation. Apart from the cell cultivation that is possible with a certain hydrogel these materials can also be divided by their origin (synthetic polymers or naturally derived polymers) and their gelation mechanism which will be explained in more detail.

In previous years, many different hydrogels have been developed for cell cultivation that are either of natural origin, either polysaccharides or proteins. Many natural-polymer based hydrogels such as alginate [151], hyaluronic acid (HA) [152,153], gelatin (denatured type I collagen) [154], chitosan [155,156], fibrin [157-159] and others are widely used due to their excellent biocompatibility and commercial availability. Table 2.2 provides a summary of important naturally derived polymers that are used as matrix for cells, their gelation mechanism and degradability. Hyaluronic acid (HA) is one of the most frequently used one in cell experiments. HA is a linear, high molar mass (6 to 8 MDa) glycosaminoglycan (GAG) found in the extracellular matrix. It contains one carboxylic acid per repeat unit and is therefore negatively charged. The half-life time in the epidermis of skin is around one to two days and in more inert cartilage tissue one to three weeks. Hence, when HA is used as a scaffold for tissue engineering application, several strategies have been developed to avoid rapid degradation such as the combination with other naturally derived polymers (e.g. gelatin, chitosan or cellulose) [160-162], chemical crosslinking [163] or the usage together with non-degradable polymers such as PEG [164]. In general, there are some notable difference between the polysaccharides and proteins mentioned in Table 2.2 Polysaccharides do not exhibit modes of specific cell engagement such as integrin-ligand interactions. Rather cells that are encapsulated in a polysaccharide gel experience a hydrated and soft matrix with some similarity to ECM physically. However, to enhance the properties of polysaccharide based gels cell-specific binding motifs derived from fibronectin, laminin or collagens need to be incorporated.

Table 2.2. Overview on naturally-derived polymers and their mechanism of gelation and degradation.

Naturally derived polymer	Origin	Description	Biological properties	Gelation mechanism	Enzymatic degradation	Chemical or other degradation
Alginate	Seaweed	a polysaccharide composed of two types of uronic acid: β -(1-4)-D-Mannuronic acid unit (M) and α -(1-4)-L-Guluronic acid unit (G)	Must be modified with adhesive ligands for cell attachment.	Complexation with Ca^{2+} or Ba^{2+} cations	- no degradation motifs for mammalian cells	The exchange of Ca^{2+} with monovalent Na^+ is the main cause of degradation of calcium cross-linked alginate hydrogels.
Hyaluronic acid	Extra-cellular matrix	an anionic, nonsulfated glycosaminoglycan (GAG)	Must be modified with adhesive ligands for cell attachment.	thermal / chemical / Schiff-base reaction / Michaeltype addition / free radical crosslinking	hyaluronidases (Hyal)	- alkaline conditions - by oxidants - by temperature (autoclave)
Gelatin	mammalian ECM	a linear protein, denatured type I collagen	Presents native cell adhesion ligands	coil-helix transition upon cooling or chemical crosslinking	degradation by proteolytic enzymes, including collagenases (e.g. matrix metalloproteinases, MMP-1; -8,-13)	
Chitosan	crustacean shells, fungal cell walls	randomly distributed β -(1 \rightarrow 4)-linked D-glucosamine (deacetylated unit) and N-acetyl-D-glucosamine (acetylated unit).	Must be modified with adhesive ligands for cell attachment.	complexation with polyanions or chemical crosslinker	<i>In vivo</i> by Chitinases and chitosanases, highly deacetylated forms (e.g. >85%) exhibit the lowest degradation rates and may last several months <i>in vivo</i>	-by different acids such HCl, phosphoric acid, or HF -by H_2O_2 - hydrogen peroxide (H_2O_2) and FeCl_3 ; UV- H_2O_2
Fibrin / (from fibrinogen and thrombin)	mammalian ECM and blood	Fibrin is a fibrous, non-globular protein involved in the clotting of blood. It is formed by the action of the protease thrombin on fibrinogen which causes it to polymerize.	Supports proliferation of human Mesenchymal SCs (hMSC) without further modification with adhesive ligands.	protease thrombin + fibrinogen = polymerization and fibrin formation	- by plasmin or matrix metalloproteinases	Weight loss of the fibrin gels was found in PBS, DMEM and DMEM/FBS, which is largely caused by the dissolution or degradation of the fibrin gels of 30 to 50 % within 9 days
MatriGel	Engelbreth - Holm-Swarm mouse sarcoma	Laminin (~60%), collagen IV (~30%), ectactin (~8%), and heparan sulfate proteoglycan + growth factors	Presents native cell adhesion ligands	gelation happens upon heating to 22°C to 35°C ; stable for a period of 14 days at 37°C	by matrix metalloproteinases	

In contrast, gelatin or fibrin based gels present native cell adhesion ligands. Besides the limited cell adhesive properties and long-term stability of almost all polysaccharides and their hydrogels other limitations are low stiffness, limited options to modify material properties, batch-to-batch variability and possible disease transmission [165,166].

On the other side many synthetic hydrogels have been developed in academia based on soluble precursor copolymers with complementary reactive functional groups and employing a bioorthogonal crosslinking reaction that does not interfere with the biological system. Typical reaction include Staudinger-Ligation [167], Cu(I) mediated click reaction between alkynes and azides [168], the metal-free click reaction between cyclooctyne and azides [169], the inverse-demand Diels-Alder with tetrazines, and the Michael-addition between thiols and α,β -unsaturated carbonyl compounds [170,171]. However, some of these reactions face limitations such as the use of metal catalysts, elaborative synthesis of functional monomers or oxygen-sensitive moieties which is probably the reason why the Michael addition is still one of the most favored crosslinking reactions for hydrogel formation. In terms of commercial availability only

polyacrylamide- and polyethylene glycol (PEG) based hydrogels among synthetic polymers can be bought in various kits, explaining their widespread application [138]. Polyacrylamide-based hydrogels can be easily fabricated from acrylamide / *N,N'*-methylene bisacrylamide with tunable mechanical properties and can be modified with peptides or proteins [149,172]. However, these gels cannot be used to encapsulate cells in 3D due to cell toxicity of the monomers and therefore are limited to 2D cell experiments. Typical parameters that can be controlled are substrate stiffness and to some extent also substrate functionalization. In contrast, PEG offers considerably more possibilities and can be employed for 2D and 3D cell experiments [173-175]. Crosslinking and hydrogel formation can be achieved under very mild conditions by mixing PEG-polymers with appropriate end groups such as thiols and maleimides or acrylates. SigmaAldrich offers more than fifty 4-arm PEG-derivatives and another forty 8-arm PEG polymers with molar masses ranging from 5 to 40 kDa and a huge variety of functional end groups (Fig. 2.14). However, introduction of functional groups is limited since PEGs carry their reactive functional groups at the α,ω -ends of the PEG chains. Moreover, the polymerization of gaseous ethylene oxide remains challenging and requires special equipment to minimize any risk of poisoning also for lab scale polymerization and thus makes it difficult to develop novel PEG-based polymers beyond commercially available ones [176].

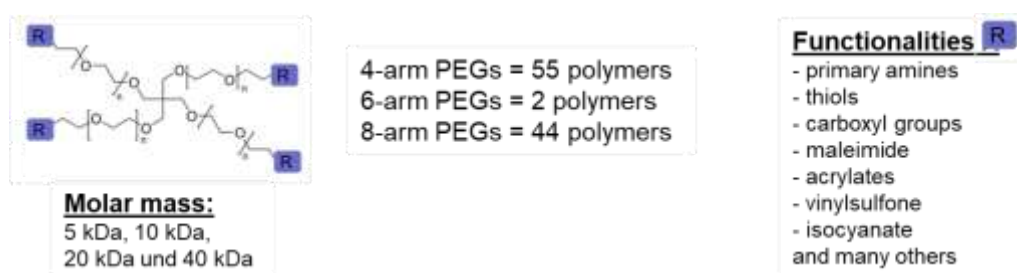


Figure 2.14. Examples for PEG polymers to form hydrogels with different functionalities and molar masses (commercially available by SigmaAldrich).

Another major difference for hydrogels being used in 3D versus 2D cell experiments is due to their crosslinking mechanism and degradability. In general, hydrogels that are used as a substrate for 2D application should be stable during the cell experiments for several days to weeks and degradation is not desirable. In contrast, when cells are encapsulated in a 3D gel, hydrogel degradability is an important feature that is required to create space for encapsulated cells to spread, migrate and generate cell-cell interactions besides other matrix properties (Fig. 2.15) [177]. In synthetic polymers this can be achieved by the introduction of cleavable sites such as ester groups [178] or specific peptide sequences [179] that enable a local degradation

of the gel via proteolytic enzymes such as matrix metalloproteinases (MMPs). Another possibility is to use gels that are not chemically but rather physically crosslinked.

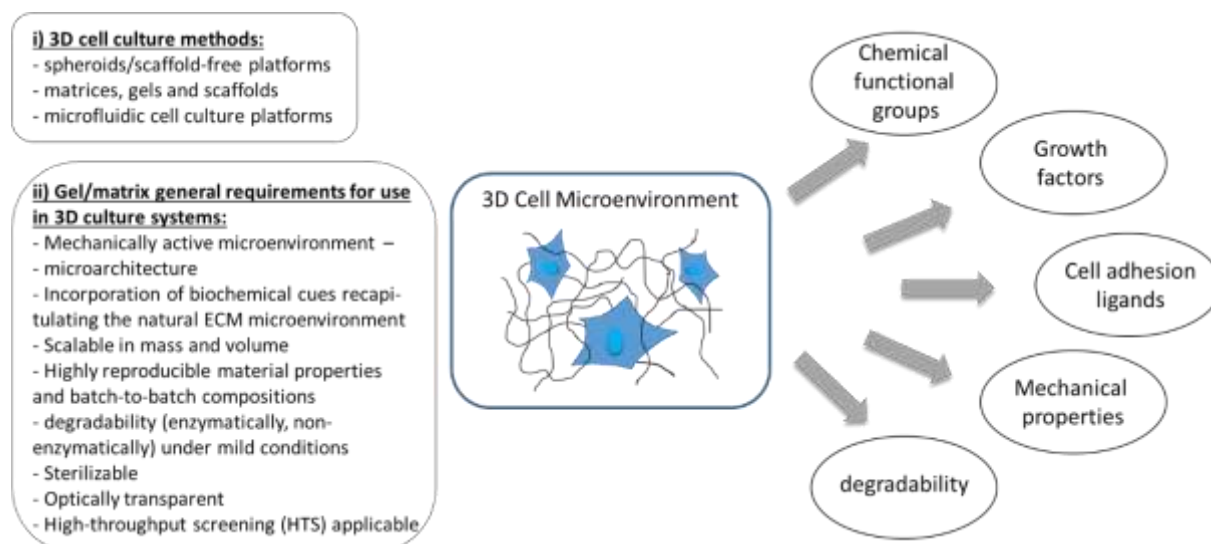


Figure 2.15. Design consideration for biomaterials to mimic a 3D cell microenvironment and general cell/matrix requirements for 3D culture systems.

Gelation methods can be based on temperature changes such as the well-known lower critical solution temperature (LCST) of poly(*N*-isopropylacrylamide), PNIPAM [180], at 32 °C in aqueous solutions, pH changes [181] or ionic interactions [182]. Other polymers that exhibit a sol-gel transition in water with increasing temperature are triblock copolymers of polyethylene glycol (PEG) in combination with polyesters such as poly(lactic-co-glycolic acid)-PEG-poly(lactic-co-glycolic acid), PEG-poly(L-lactic acid)-PEG, poly(ϵ -caprolactone)-PEG-poly(ϵ -caprolactone), poly(ϵ -caprolactone-co-lactic acid)-PEG- poly(ϵ -caprolactone-co-lactic acid) and PEG-poly(ϵ -caprolactone)-PEG. Table 2.3 gives an overview on physical, chemical and enzymatic crosslinking methods and their advantages and disadvantages. Although physically crosslinked gels seems to be favorable for 3D cell encapsulation experiments they may not be stable when such samples are processed for histology. Typical sample preparation for cryosectioning involves the hydrogel or tissue sample to be places in a sugar-based solution for some hours which may lead to dissolution of the gel structure if no fixation is done before.

Table 2.3. Methods of *in situ* gelation of biomaterials based on their gelation mechanism.

Cross-linking	Method	Advantages	Disadvantages	Example
physical	- temperature	- Mixing of cells and biomaterial at room temperature	- Reversible sol-gel transition	chitosan, poloxamer, polyNIPAAm, PEG-poly(L-lactic acid)-PEG triblock copolymer, polyphosphazene
	- pH	- Gelation under physiological conditions	- low cell viability under acidic conditions	- chitosan, <i>N</i> -palmitoyl-graft-chitosan and poly(N-isopropylacrylamide- copropylacrylic acid)
	- ionic	- Rapid gelation		- the anionic polysaccharide alginate + divalent cations, e.g. Ca ²⁺ ; - the cationic chitosan + polyanionic polyglutamate
chemical	- Schiff base	- amino groups and aldehydes	- Biocompatibility to all reagents needs to be checked	- NH ₂ -groups of gelatin and the aldehyde groups (CHO) in oxidized chondroitin sulfate
	- Michael addition	- thiols + α,β unsaturated carbonyl compound	- Biocompatibility to all reagents needs to be checked	- thiolated chitosan and poly(ethylene glycol) (PEG) diacrylate
	- Photo crosslinking	- In situ formation of gels	- Cytotoxicity of photo initiator / photo source	- methacrylated glycol chitosan
enzymatic	- enzyme	- Gelation under mild conditions	- Cell compatibility of reagents	- gelatin-PEG-tyramine and a mixture of Horseradish peroxidase (HRP) and H ₂ O ₂

Polymers that display a temperature-sensitive gelation behavior have found also increasing attention as injectable gels to improve the rather low percentage of 1 to 20 % cell survival after transplantation [183-185] *Heilshorn et al.* have summarized the challenges in stem cell survival after cell transplantation to deliver functional cells that depends mainly on the transplant phase. The reasons for the low cell survival with stem cells are manifold and include prolonged exposure to non-physiological encapsulation environment (pre-injection phase), cell damage during injection due to shear stress (injection phase), poor nutrient transport, hypoxia, cell death for anchorage-dependent cells when they detach, immune response (acute pre-injection phase) and limited proliferation, migration and differentiation (long term function). Therefore, highly sophisticated, cell protective gels are required to overcome these challenges and improve the therapeutic efficacy of stem cells [186].

Table 2.4. Selected examples of injectable gels for human mesenchymal stem cell delivery.

Polymer	Stem Cell Type	Cell retention versus saline control in brackets	Remarks
Alginate modified with RGD peptide	human mesenchymal stem cell (hMSC)	60 % (versus 9 %)	Stiffness of the alginate gel was important: hMSCs in 2 % alginate solution (~2 kPa) were found to be retained and survive 4x higher than hMSCs transplanted with saline or 1 % alginate (~700 Pa)
chitosan/ β -glycerophosphate	human mesenchymal stem cell (hMSC)	50 % (versus 9 %)	thermosensitive hydrogels may prove difficult for use in nondirect injection methods that make use of catheters because it requires the cell/gel mixture to travel a long distance through the body, which can potentially result in early gelation and failure to inject into the damaged tissue
copolymer of poly(NIPAAm-co-AA-co-HEMA) acrylic acid/PCL + collagen I	human mesenchymal stem cell (hMSC)	4 times higher compared to cells alone	Gel/hMSCs were injected hMSCs to an infarcted heart and increased heart function, increased angiogenesis, and decreased fibrous scarring

As an alternative to injectable gels, the process of microencapsulation has been developed by embedding cells in micro-sized hydrogels that enable the direct injection of the stem cells to the targeted tissue through a needle in a minimally invasive fashion [186]. Different methods have been studied to fabricate such cell loaded microcapsules either by electrospraying, droplet-based microfluidics, photolithography and emulsification. Cell supportive moieties that lead to cell-matrix binding are desirable to promote cell viability. The main gel forming materials that were used are alginate, hyaluronic acid, gelatin, agarose and PEG, either as homopolymers combinations thereof. However, many of these methods have only been developed and tested for stem cell encapsulation at a small laboratory scale and it remains unclear if they are also suitable for large scale application considering the large amount of stem cells (about 10^7 – 10^{10} cells) required for a patient.

Chapter 3. Objective of the Thesis

Hydrogels play an important role today to culture stem cells in two (2D, on top) and three dimensions (3D, by encapsulation). While it has been shown that the fabrication of well-defined 2D hydrogel coatings can be realized by many different methods, encapsulation of stem cells in a 3D hydrogel material is much more challenging. In the past, this was accomplished mainly with hydrogels that were chemically crosslinked but biodegradable to allow the cells to migrate through the hydrogels matrix. Few examples exist where physically crosslinked gels based on their thermo-responsive behavior, ionic interactions or changes in pH-value were used.

The main objective of this thesis was to investigate hydrophobically modified copolymers as a synthetic material to form physical hydrogels with tunable mechanical and biological properties for 3D cell encapsulation. In order to achieve this goal, hydrophobically modified copolymers should be prepared by free radical polymerization using *N,N'*-dimethylacrylamide (DMAM) as hydrophilic unit and lauryl (LMA) or stearyl (SMA) methacrylate as a hydrophobic comonomer. While these non-ionic copolymers should serve as a reference system, different functional moieties such as cationic groups, peptide-units and unsaturated fatty acid should be introduced in such copolymers with the goal to analyze their composition and molar mass and to elucidate effect of these functional groups on their rheological behavior in PBS buffer solution. The main focus is to better understand how solution and gel-forming properties are influenced by these functional groups.

Chapter 4. Synthesis and Rheological Studies of Functionalized, Hydrophobically Modified Cationic Polymers

4.1 Introduction

Polymeric systems bearing positive charges, which can be incorporated in the polymer backbone and/or the side chains, are defined as cationic polymers. During the past two decades cationic polymers have been subject of investigation for their application in regenerative medicine. They are promising compounds in pharmaceutical, biological and medical research such as carriers for genetic material like DNA or RNA into cells [187,188]. Poly(ethylene imine) (PEI) poly(L-lysine) (PLL) and poly(2-dimethylamino) ethyl methacrylate (PDMAEMA) are well known examples of water-soluble, cationic polymers which are able to bind and condense DNA and RNA (negatively charged nucleic acids) by ionic interaction [189], or cationic polymer such as polybrene [190] can increase significantly adenovirus-mediated transgene delivery into mesenchymal stem cells (MSCs). *Liu and coworkers* [191] demonstrated that hydrophobic modification of polycations have promising effect in gene delivery. The interaction of polycations with biological component can take place through two mechanisms: (i) electrostatic attraction between positive charges of the cationic polymers and negative charges on the surface of cells or blood, and (ii) lipid bilayers in cell membrane can interact with hydrophobic units in amphiphilic polycations via hydrophobic interactions [192].

De Rosa et al. [193] synthesized poly(hydroxyethyl methacrylate) (pHEMA) derived-polymers with different amount of 2-methacryloyloxyethyltrimethyl ammonium chloride (METAC). They showed that positively charged moieties on the polymer surface have a direct effect on the substrate adhesion of primary human fibroblast cells, as well as proliferation, triggering signals that regulate cell survival, cell cycle progression and expression of tissue-specific phenotypes. Although many research has been done to exploit Coulomb forces between charged polymers and oppositely charged biological macromolecules, many basic aspects of these interactions are not very well understood up to now. *De Luca et al.* [194] demonstrated for the first time how cationic polymer surface charge density which provide a synthetic extracellular microenvironment are able to regulate the fate of mesenchymal stromal cell (MSC), affecting cell-cell EphB₄/epharin B₂ signaling. They have illustrated that the cationic copolymer poly(HEMA-co-METAC) can modulate the interaction of potent signaling proteins like Ephs.

Although cationic polymers can be easily synthesized with great structural flexibility which makes them good candidates as non-viral gene delivery systems, undesirable cytotoxicity and low transfection properties are limitations. Different modifications have been used to overcome these disadvantages. Among various system, hydrophobic modification of polycations have become of great interest, particularly, for their potential to modify gene delivery efficacy of polycations. It can be explained by hydrophobic chains that increase cellular uptake through the lipophilic cell membrane [191]. Additionally the presence of hydrophobic groups can create associative polycations with the ability to build intermolecular interactions in aqueous solution, that results in interesting rheological properties like viscosity increase or gelation [10].

The rheological properties of associative, nonionic polymers and anionic polymers have been characterized in the literature in detail but the viscoelastic properties of cationic associative polymers are less known [195]. In the current chapter, free radical polymerization has been used to prepare hydrophobically modified cationic copolymers containing quaternary ammonium moieties in their side chain. The copolymers were characterized by ^1H NMR spectroscopy and GPC measurements. The rheology behavior in aqueous medium has been analyzed to get information about the influence of cationic charge on the thickening ability of these associative copolymers.

4.2 Results and Discussions

This chapter focuses on the synthesis and characterization of two types of hydrophobically modified copolymers via free radical polymerization in a non-blocky fashion. (i) \mathbf{P}_{ref} was prepared as a reference polymer according to a previously reported method in the literature [68], which is a non-ionic copolymer based on *N,N'*-dimethylacrylamide (DMAM) containing either lauryl methacrylate (LMA) (1.25-10 mol %) or long chain stearyl methacrylate (SMA) (1.25-2.5 mol%), (ii) cationic copolymer ($\mathbf{P1}$) which contains additional 2-methylamino ethyl acrylate (DMAEA) which was further quaternized into the cationic form. For each set of cationic copolymer, its non-ionic reference polymer was prepared in order to better understand the effect of cationic charge on the copolymer solution properties in aqueous medium.

4.2.1 Cationic copolymers preparation

Numerous cationic polymers possess the amino group and they exist in different forms (primary, secondary, tertiary and quaternary). Among these forms the quaternary ammonium groups attracted a lot of attention because they can provide a permanent positive charge. Therefore, the methylation reaction plays a key role to generate cationic polymers [72].

Polycations used in this study differ by the mole percentage and the chain length of the hydrophobic monomer. Precursor copolymer poly(DMAM-*stat*-SMA/LMA-*stat*-DMAEA) was methylated with methyl iodide to obtain **P1** (Figure 4.1). The reaction of the precursor copolymers with methyl iodide in dioxane transformed the precursor copolymer into its permanently polycationic species. This conversion was quantified with ^1H NMR spectroscopy by disappearance of the methyl protons of the tertiary amine (peak at 2.2 ppm) and the appearance of a new peak at 3.1 ppm that can be assigned to the methyl protons of the quaternary ammonium ion (Figure 4.4). The degree of quaternization was nearly quantitative for all copolymers.

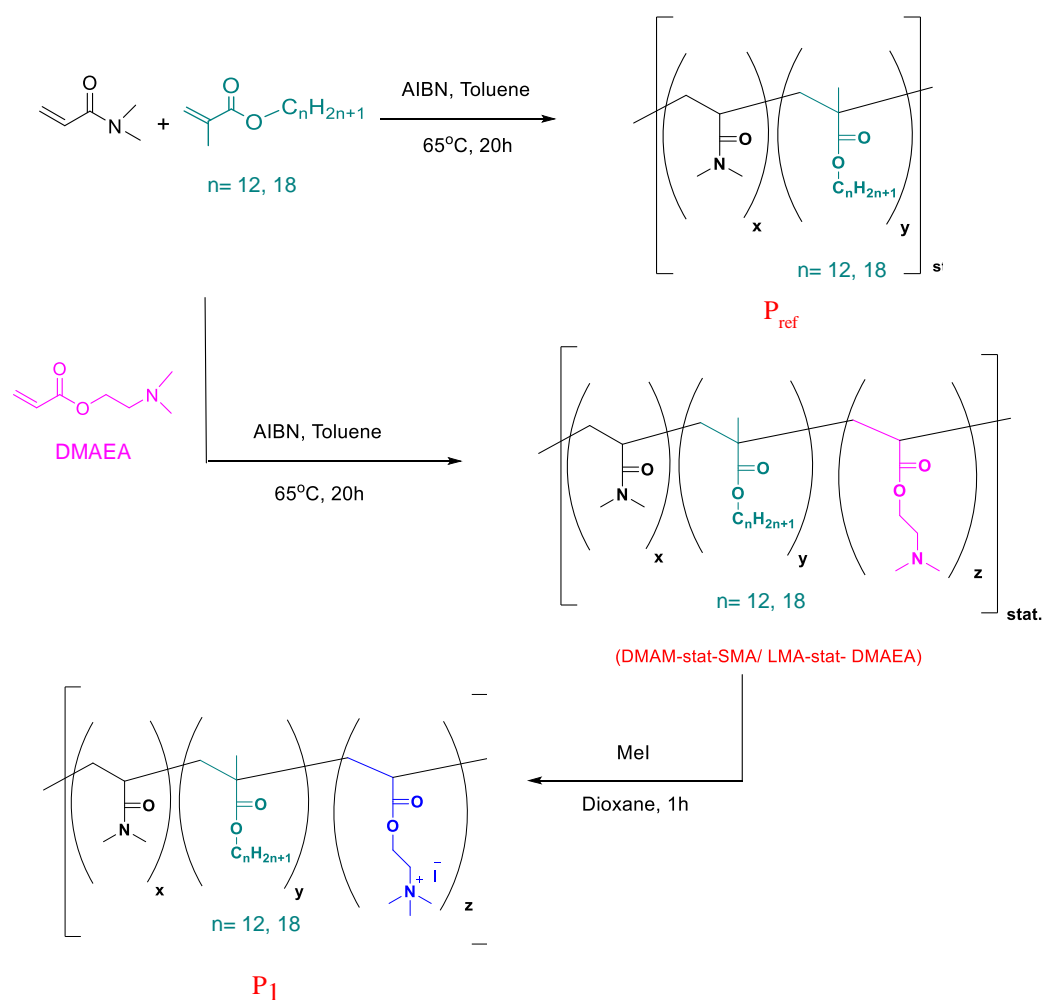


Figure 4.1. Schematic diagram for the synthesis of the precursors and **P1** copolymers of different composition.

The analytical data of the references copolymers and **P1** are listed in Table 4.1 and 4.2, respectively. Polycations that were used in this study have a constant charge density (10 mol

%) and differ by the amount of the hydrophobic comonomers (LMA, SMA). The molecular weight of all cationic copolymers has been determined by SEC in DMF. The sample code of the copolymers refers to the hydrophobic monomer LMA or SMA and its content. For example, **P1LMA1.25** stands for the cationic copolymer **P1** containing 1.25 mol% of LMA. Solution studies of the resulting cationic copolymers were carried out with a focus on the rheological behavior and compared with its references copolymers.

Table 4.1. Analytical data for the reference copolymers.

Sample	Copolymer composition (mol%) (DMAM : LMA/SMA) ^{a,b}	M _n (g/mol) ^c	D ^c	Yield (%)
P_{ref}LMA1.25	98.96 (98.75): 1.04 (1.25)	37520	2.5	84
P_{ref}LMA2.5	97.9 (97.5): 2.1 (2.5)	32290	2.2	79
P_{ref}LMA3.75	95.88 (96.25): 4.12 (3.75)	37050	2.9	85
P_{ref}LMA5.0	93.7 (95): 6.3 (5)	42620	3.1	93
P_{ref}LMA7.5	90 (92.5): 8 (7.5)	40860	2.02	87
P_{ref}LMA10	89.9 (90): 10.1 (10)	45470	2.7	84
P_{ref}SMA1.25	99.16 (98.75): 0.85 (1.25)	35550	3.3	80
P_{ref}SMA2.5	98.3 (97.5): 1.7 (2.5)	39200	2.87	88

^{a)} All polymerization were carried out with 0.01 mol/L AIBN; at T= 65 °C for 20 h, ^{b)} copolymer composition was determined by ¹H NMR, in brackets: theoretical values, DMAM (*N,N'*-dimethyl acrylamide), LMA (lauryl methacrylate), SMA (stearyl methacrylate), ^{c)} determined by SEC in DMF with 5 g L⁻¹ LiCl, T= 60 °C.

Table 4.2. Analytical data of the cationic copolymers.

Sample	Copolymer composition (mol%) (DMAM: LMA/SMS: DMAEA) ^{a,b}	M_n (g/mol) ^c	Đ ^c	Yield (%)
P1LMA1.25	86.25 (88.75): 1.65 (1.25): 12.1 (10)	25490	3.27	75
P1LMA2.5	86.5 (87.5): 2.7 (2.5): 10.8 (10)	30250	3.39	80
P1LMA3.75	85.05: 3.6 (3.75): 11.2 (10)	38580	3.37	78
P1LMA5.0	82 (85): 5 (6.1): 11.9 (10)	32260	3.35	88
P1LMA7.5	80.9 (82.5): 8 (7.5): 11.1 (10)	38360	3.41	83
P1LMA10	79.6 (80): 9.5 (10): 10.9 (10)	37120	3.17	72
P1SMA1.25	87.65 (88.75): 1.05 (1.25): 11.3 (10)	33490	3.66	86
P1SMA2.5	87.1 (87.5): 2.2 (2.5): 10.7 (10)	42600	2.36	80

^{a)} All polymerization were carried out with 0.01 mol/L AIBN; at T= 65 °C for 20 h. ^{b)} copolymer composition was determined by ¹H NMR, in brackets: theoretical values, DMAM (*N,N'*-dimethyl acrylamide), LMA (lauryl methacrylate), SMA (stearyl methacrylate), DMAEA (2-dimethylamino ethyl acrylate), ^{c)} determined by SEC in DMF with 5 g L⁻¹ LiCl, T= 60 °C.

Figure 4.2 illustrates the ¹H NMR spectra of the precursor copolymers with different mole percentage of LMA. The final hydrophobic monomer content of LMA (mol%) was obtained by comparing the integration of backbone methylene groups of DMAM with LMA methylene groups in the side chains (Figure 4.3). The results show relatively good agreement of the mole percentage of LMA in the final products and the reaction feed.

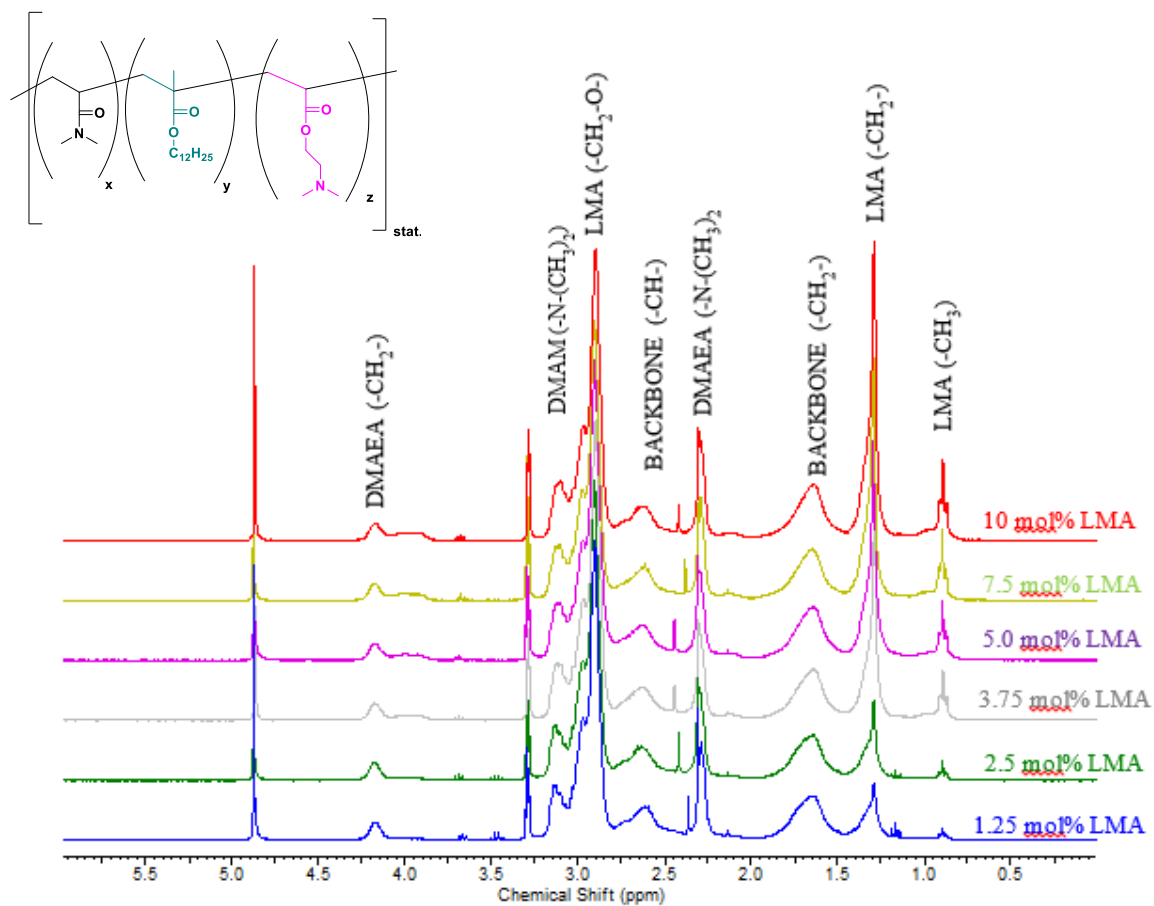


Figure 4.2. ^1H NMR of precursor copolymers with various mole percentage of LMA (d-MeOD).

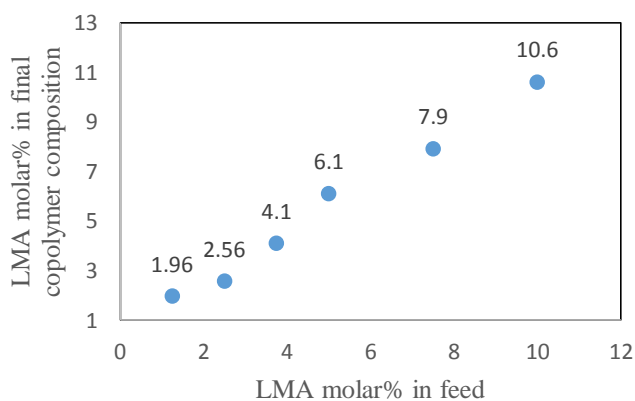


Figure 4.3. ^1H NMR analysis of LMA (mol%) as a function of initial molar percentage of LMA in monomer feed in precursor copolymers.

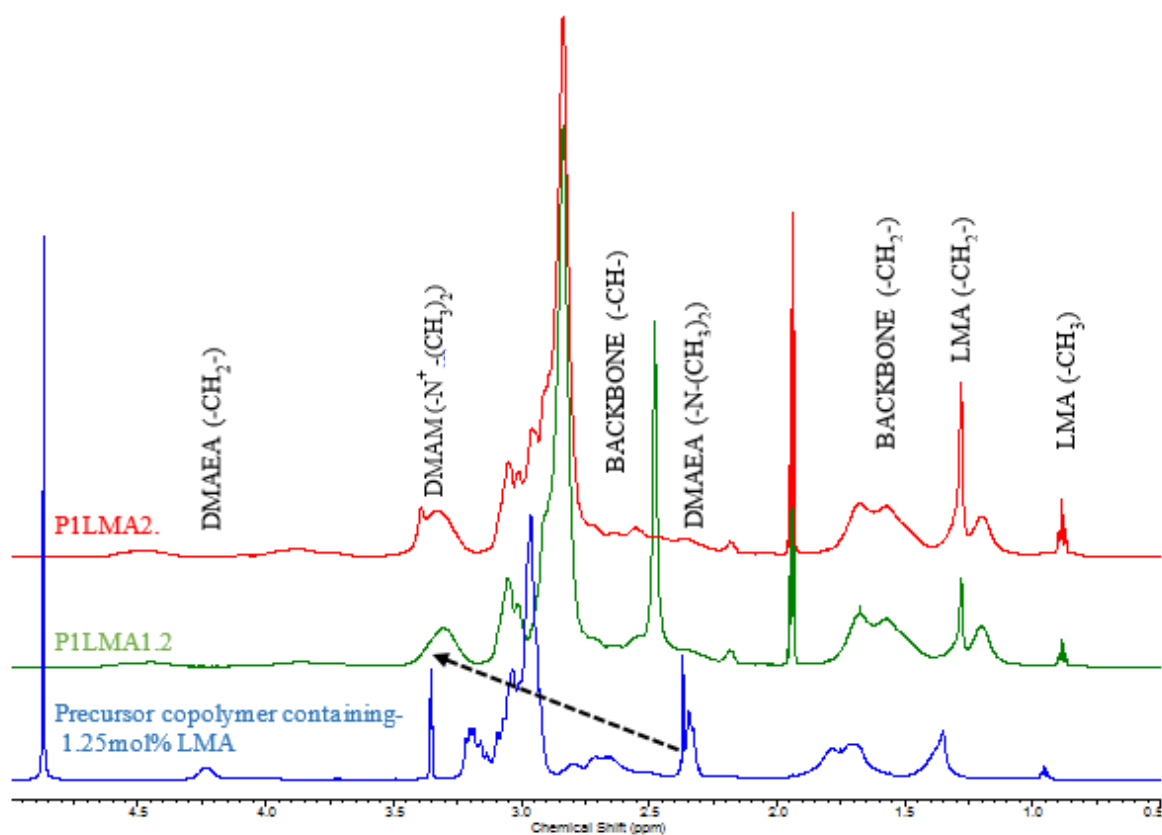


Figure 4.4. ^1H NMR of **PILMA1.25** and **PILMA2.5**, the conversion was quantified by comparing peak integrals at 2.2 ppm (methyl groups of the tertiary amine) and 3.3 ppm (methyl groups of the quaternary ammonium group).

4.2.2 Solubility of the copolymers

In this part, solubility characteristics of reference copolymers and their cationic analogue were compared in the concentration range from 1 to 25 wt% in phosphate-buffered saline solution (0.01 M molar PBS buffer) at room temperature. For all samples, the final desired copolymers were directly prepared in a screw-capped vial and the proper amount of buffer solution was added, the samples were kept at room temperature without stirring and heating. In Table 4.3 the copolymers solubility after 48 h are summarized. According to the literature [68], the solubility of the reference copolymers in buffer solution decreases with increasing hydrophobicity of the samples. It can be seen that the hydrophobe content and chain length, copolymer concentration and positive charge are the main parameters which have an effect on copolymer solubility. With respect to the hydrophobe content, the reference copolymers are water soluble up to 5 mol% LMA, this amount decreased to 2.5 mol % for long chain stearyl methacrylate, confirming the more hydrophobic character of the side chains in the SMA samples. Furthermore, the maximum

polymer concentration that could be dissolved in an aqueous buffer solution decreased with increasing hydrophobe content. For example, **P_{ref}LMA1.25** (with 1.25 mol% hydrophobic monomer) can be dissolved up to 22.5 wt% while it decreases to 7.5 wt% for **P_{ref}LMA5.0** (with 5.0 mol% hydrophobic monomer). The obtained results illustrate that the whole set of polycations are soluble in buffer solution. It can be seen from Figure 4.5 that **P1SMA1.25** is soluble in buffer solution up to 40 wt % at room temperature whereas the maximum solubility is just 12.5 wt% for its reference polymer. Additionally, **P_{ref}LMA7.5** and **P_{ref}LMA10** were insoluble even after they were heated to 100 °C, therefore more investigation on these two copolymers were not done.

Table 4. 3. Solubility of **P_{ref}** and **P1** copolymers in aqueous buffer solution.

Reference copolymer	Max. solubility of references copolymers (wt%)	Cationic copolymers	Cationic copolymers (wt%)
P_{ref}LMA 1.25	22.5	P1LMA1.25	> 40
P_{ref}LMA 2.5	15	P1LMA 2.5	> 40
P_{ref}LMA 3.75	12.5	P1LMA 3.75	> 40
P_{ref}LMA 5.0	7.5	P1LMA 5.0	> 40
P_{ref}LMA 7.5	Insoluble	P1LMA 7.5	> 40
P_{ref}LMA 10	Insoluble	P1LMA 10	> 40
P_{ref}SMA 1.25	12.5	P1SMA 1.25	> 40
P_{ref}SMA 2.5	7.5	P1SMA2.5	> 40

The final desired copolymers were prepared in a screw-capped vial and the proper amount of PBS buffer solution was added. The solubility was determined by visual inspection at room temperature without stirring after 48 h.



Figure 4.5. P1SMA1.25 in aqueous PBS buffer solution from 15 to 40 wt%.

4.2.3 Rheological Studies

In this part, the effect of cationic charge, hydrophobe content and the length of hydrophobic chains on the rheological properties of aqueous copolymer solutions is discussed. The viscoelastic properties of **P1** series were compared with their reference non-ionic copolymer **P_{ref}** in the concentration range of 1 to 25 wt%. The difference in charge and hydrophobic monomer resulted in significant changes in the solution characteristics when going from liquid to gel-like samples (Figure 4.6). Therefore, the viscosities of the liquid and low viscous copolymer solution were measured with an Ubbelohde viscometer situated in a thermostat-control water bath at 37 °C whereas high viscous samples were measured by oscillatory rheometry with a 150 mm cone-plate and 1000 mm plate-plate geometry for gel-like samples. For all rheological studies, the desired copolymers were directly prepared in a screw-capped vial and the proper amount of buffer solution was added, the samples were kept at room temperature without stirring. For homogenization, the copolymers were heated to 100 °C before conducting the rheological measurements.

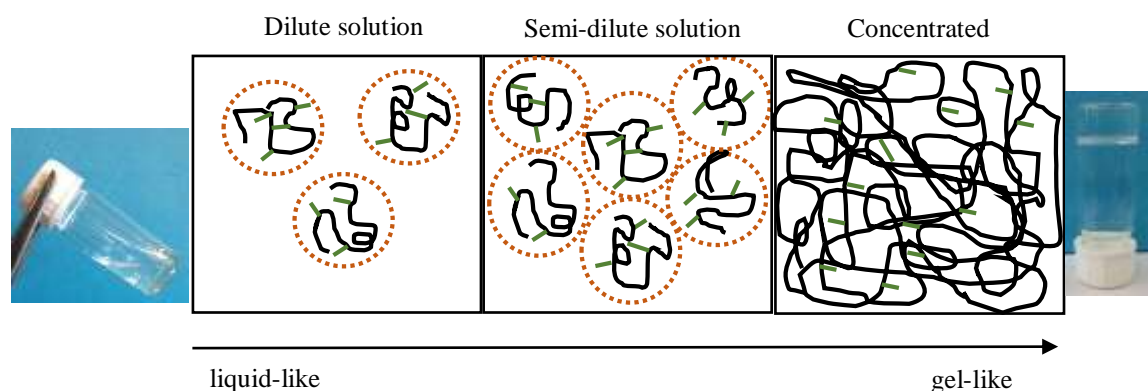
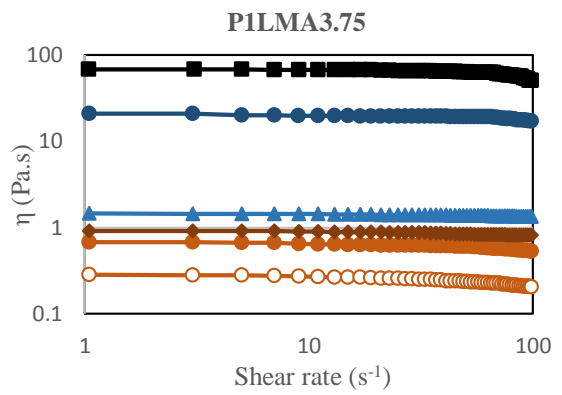
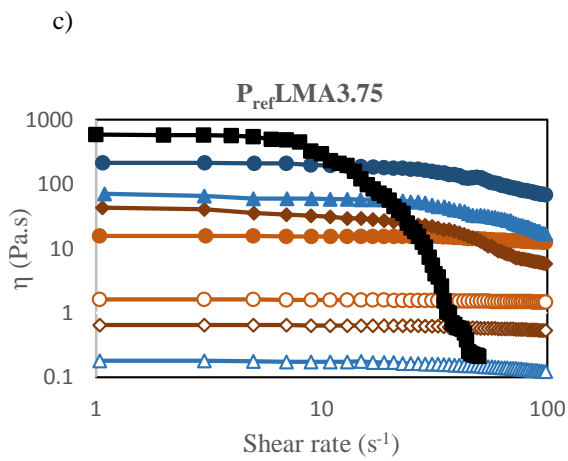
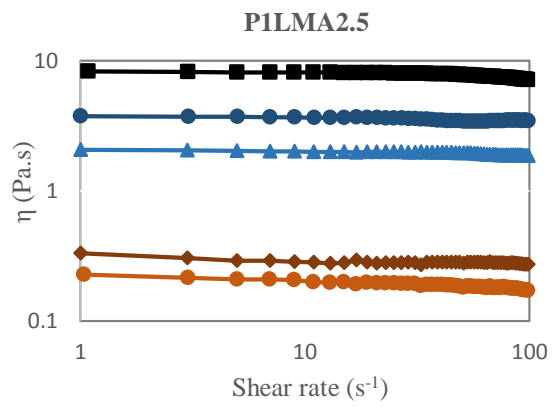
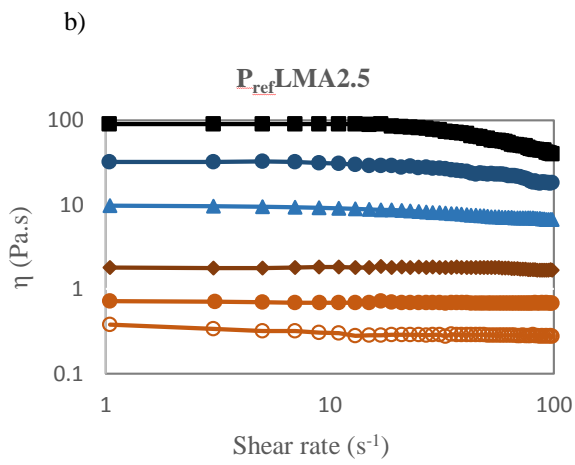
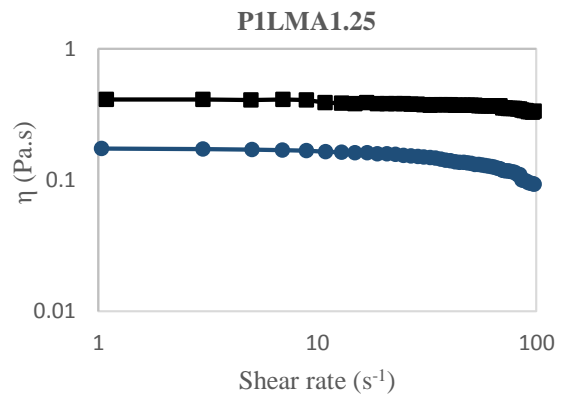
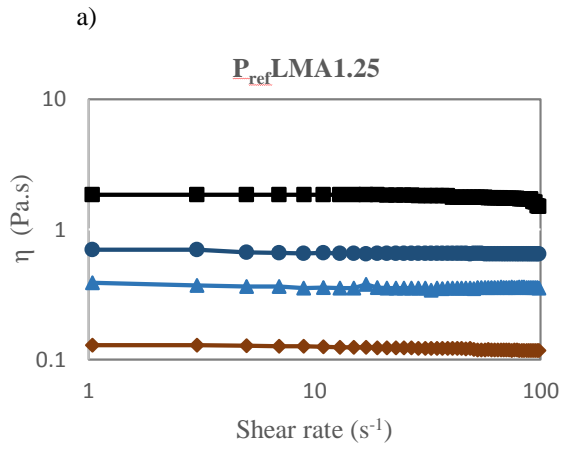


Figure 4.6. Schematic diagram of the conversion from a dilute to concentrated solution for a hydrophobically modified polymer.

4.2.3.1 Steady Shear Flow Measurements

The viscoelastic behavior of hydrophobically modified polymers appear in semi-dilute regime above the critical concentration when intermolecular associations start to dominate. In aqueous solutions steady shear flow measurements can be useful to recognize the semi-dilute regime by observing the steady-state viscosity as a function of shear rate at various concentrations. Figure 4.7 summarizes the shear rate dependency of the polymer viscosity for **P1LMA1.25**, **P1LMA2.5**, **P1LMA3.75** and **P1SMA1.25** in comparison to their references analogue. All copolymers show a significant concentration dependence of the viscosity. With increasing concentration of the non-ionic and ionic copolymers, shear viscosity showed a trend to increase suggesting the formation of a three-dimensional transient network in these concentration regime through the extensive associations of LMA and SMA hydrophobic side chains. Unlike non-ionic macromolecular coils, cationic copolymers begin to overlap at extremely high concentration. Consequently, the transition between dilute and semi-dilute regime spans up to very large concentration range, for instance for **P_{ref}LMA1.25** the intermolecular association starts at 12.5 wt% while it is 20 wt% for **P1LMA1.25**. Below these concentrations the viscosity was measured by Ubbelohde viscometer. It can be seen that the viscosity increases with increasing mole fraction and length of the hydrophobic groups. In this study, the solutions demonstrate Newtonian behavior which means that there is no variation in viscosity as a function of shear rate. No remarkable shear thinning was observed over the shear rate range examined (up to 100 s⁻¹) for most copolymers solutions. This can be explained by the effect of the molecular weight of the copolymer solution properties. For copolymers with higher molecular weight the disruption of overlapping chains is faster than their capability to the formation of associations when the shear rate enhances. For example *Volpert and coworkers* [49] showed for HM (hydrophobically modified) copolymers that were synthesized by a micellar polymerization technique with molecular weights of 10⁶ g/mol shear thinning effect in copolymers containing 1 mol% hydrophobic monomer, depending on the number of hydrophobe per micelle (N_H) and copolymer concentration [196,197]. But for this system with a molecular weight around 10⁵ g/mol a Newtonian behavior was observed. Actually, lower molecular weight copolymers (10⁵) have shorter relaxation times, therefore the shear thinning effect would be expected to appear in a wider range of our shear rate measurements. The interesting observation is that the **P_{ref}LMA3.75** and **P_{ref}SMA1.25** in the high concentration (20, 22.5 and 25 wt%) regime exhibit peculiar shear thinning behavior. For these compounds the disorientation and disentanglement of the intermolecular associations become more pronounced upon increasing the shear rate.



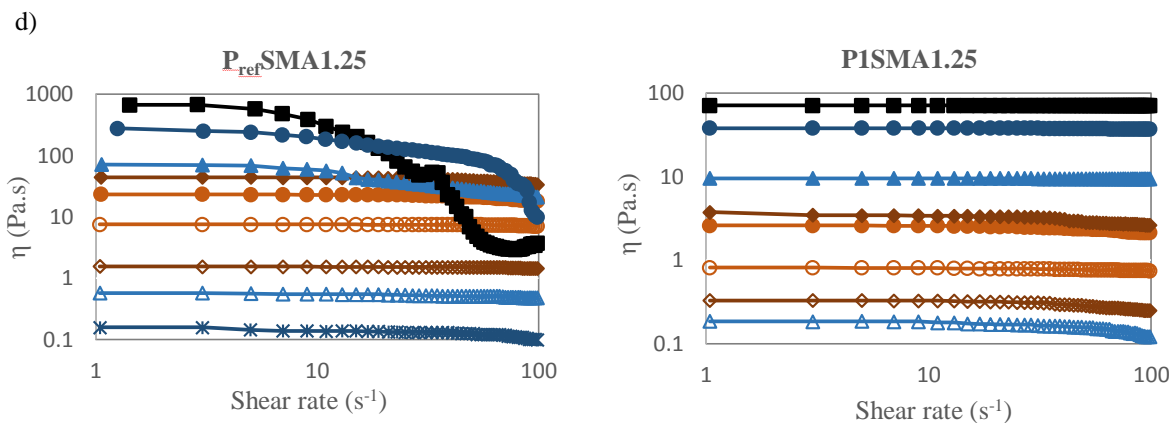


Figure 4.7. Viscosity as a function of shear rate at various concentration (wt%): 25 % (—■—), 22.5 % (—●—), 20% (—▲—), 15% (—◆—), 12.5% (—●—), 10% (—○—), 7.5% (—◇—), 6% (—△—), 5% (—*—) for a) $P_{ref}LMA1.25$ and $P1LMA1.25$ b) $P_{ref}LMA2.5$ and $P1LMA2.5$, c) $P_{ref}LMA3.75$ and $P1LMA3.5$, d) $P_{ref}SMA1.25$ and $P1SMA1.25$, demonstrating the effect of hydrophobic content and chain length.

4.2.3.2 Effect of copolymers concentration on viscosity

The aggregation behavior of the copolymers was further investigated by studying the viscosity as a function of polymer concentration. Typically, the concentration dependence of the specific viscosity can be divided in three concentration regimes:

$$\text{Dilute regime } \eta_{sp} \sim c^a, c < c^*$$

$$\text{Semi-dilute unentangled regime } \eta_{sp} \sim c^b, c^* < c < c^{**}$$

$$\text{Semi-dilute entangled regime } \eta_{sp} \sim c^c, c > c^{**}$$

The specific viscosity of copolymers solution was obtained using equation [4.1]:

$$\eta_{sp} = (\eta_{\text{solution}} / \eta_{\text{solvent}}) - 1 \quad \text{eq. [4.1]}$$

The variations of the specific zero-shear viscosity as a function of polymer concentration for both types of copolymers are shown in Figure 4.8. **In dilute regime**, where the rheological behavior of the copolymers is generally controlled by intramolecular association, the viscosity of the mixture is low corresponding basically to the concentration and differences between cationic and reference copolymers are insignificant. Coefficient for concentration dependencies demonstrate that for all copolymers, the viscosity increases by a factor of $C^{-0.9}$ in dilute regions. After this region, when the possibility of intermolecular interactions enhances, the viscosity of

solutions increases dramatically. Moreover, in the **semi-dilute unentangled regime**, the reference copolymer viscosity rises very steeply in comparison to the cationic one in the same concentration range. This can be seen e.g. for **P_{ref}LMA1.25**. The onset of the concentrated regime is at 12.5 wt% while **P1LMA1.25** possesses a higher onset of the concentrated regime of 20 wt%. In the investigated concentration range (1-25 wt%), there is not enough information to distinguish three different regimes for **P_{ref}LMA1.25** and **P1LMA1.25**. Therefore, more concentrations are required to obtain quantitative interpretations for copolymers containing 1.25 mol% LMA. The value of C^* is 7.5 wt% for **P_{ref}LMA2.5** with a power law exponent of 5.8, while only two regions for **P1LMA2.5** can be recognized. The concentrated regime starts at 10 wt % for **P1LMA2.5** and the viscosity increases with scaling coefficient of 6.6. However, as *Gillet et al.* [198] mentioned the distinction between semi-dilute unentangled regime (C^*) and semi-dilute entangled regime (C^{**}) is not always visible from the graphs. The critical association concentration decreases to 5 wt% for **P_{ref}LMA3.75** and 6 wt% for **P1LMA3.75** and their viscosity indicates a scaling law of the concentration with an exponent 6 and 4.3 respectively. Finally, for samples containing SMA with longer chain length, more intermolecular association form at lower concentration of 4 wt% and 5 wt% for **P_{ref}SMA1.25** and **P1SMA1.25**, respectively. For these copolymers only two regions can be identified, the viscosity of **P_{ref}SMA1.25** enhances by a factor of $C^{5.3}$, whereas the viscosity of **P1SMA1.25** augments more slowly by a factor of $C^{4.6}$. It should be noted for **P_{ref}LMA2.5**, **P_{ref}LMA3.75** and **P1LMA3.75**, with a visible semi-dilute unentangled regime, their power law exponents are in good agreement with the first two cases of the sticky Rouse model (explained in literature review chapter, section 2.3). According to *Cram et al.* [68] in **semi-dilute entangled** regime, the power law exponents were found to be around 5 while the viscosity increases with a power law exponent of 7.6, 5.6 and 7.5 for **P_{ref}LMA2.5**, **P_{ref}LMA3.75** and **P1LMA3.75**, respectively. The deviation between the obtained results and theoretical results expected from sticky Rouse model can be explained by the limited set of data in this concentration regime.

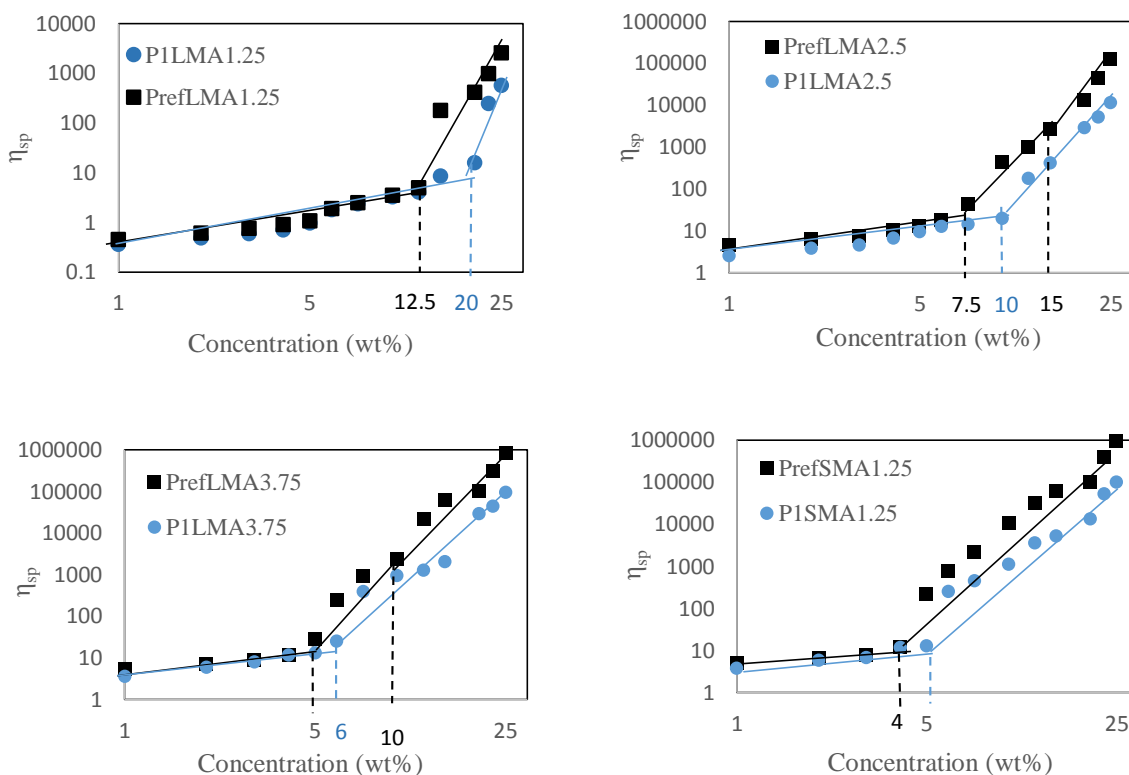


Figure 4.8. Specific zero shear viscosity as a function of concentration, demonstrating the significant effect of charge, hydrophobic content and chain length on solution properties.

To better observe the effect of hydrophobe content and chain length on the viscosity of copolymer solution, Figure 4.9 displays the concentration dependences of the zero shear specific viscosity for cationic copolymers. With increasing the copolymer concentration, intermolecular aggregation was strengthened due to the shortening of distance between polymer chains, therefore viscosity rises sharply in all samples. It was observed that the viscosity increases and the transition concentration (from intramolecular associations to intermolecular one) decreases with the increase of hydrophobic monomer content. This suggests that higher density of hydrophobic moieties along the DMAM chain, led to a larger probability of hydrophobic parts that participated in aggregation. In comparison, **PILMA1.25** and **PISMA1.25** show the strong effect of the length of the hydrophobic chain on the viscosity. The critical concentration decreases from 20 wt% for **PILMA1.25** to 5 wt% for **PISMA1.25**. This is attributed to the stronger intermolecular association by the longer hydrophobic C₁₈ side chain.

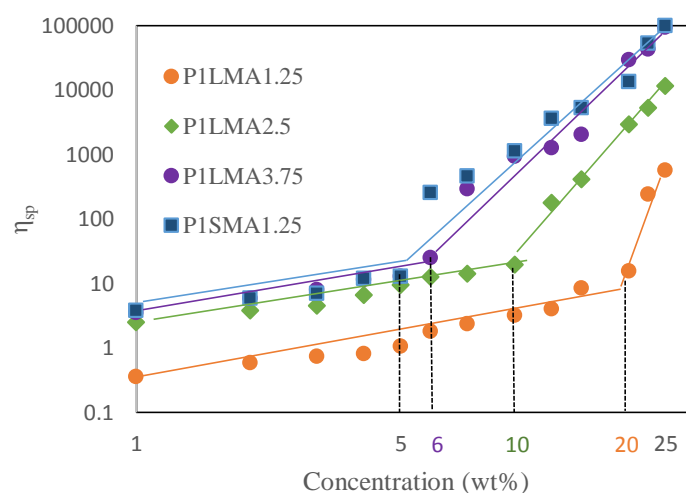


Figure 4.9. Zero shear viscosity as a function of concentration for cationic copolymers.

4.2.3.2 Complex modulus

To gain further insight in the properties of the aqueous copolymers solutions, dynamic viscoelastic measurements were carried out. Plots of the rheological parameters G' and G'' , the shear storage modulus and shear loss modulus versus the oscillation frequency for the most viscous samples of **PILMA1.25**, **PILMA2.5**, **PILMA3.75**, **PISMA1.25** and their references polymers were measured but only **PILMA2.5** and **PISMA1.25** and **PISMA2.5** at 20 wt% are presented in Figure 4.10, respectively. The typical viscoelastic, liquid-like behavior was observed for the copolymer solutions (except **PrefSMA2.5**), storage modulus G' and loss modulus G'' make a cross-over, denoted ω_{cross} , that is accompanied with an increase in both moduli. Moreover, at lower frequencies the value of G'' exceeds G' but at high frequencies the value of G' is larger than G'' . Therefore, ω_{cross} determines the transition from a liquid-like dominated behavior ($G'' > G'$) to a solid-like dominated behavior of the aqueous polymer mixtures ($G' > G''$), hence, **PrefLMA2.5**, **PILMA2.5**, **PrefSMA1.25**, **PISMA1.25** and **PISMA2.5** behave as a weak viscoelastic gel, at high frequencies above ω_{cross} .

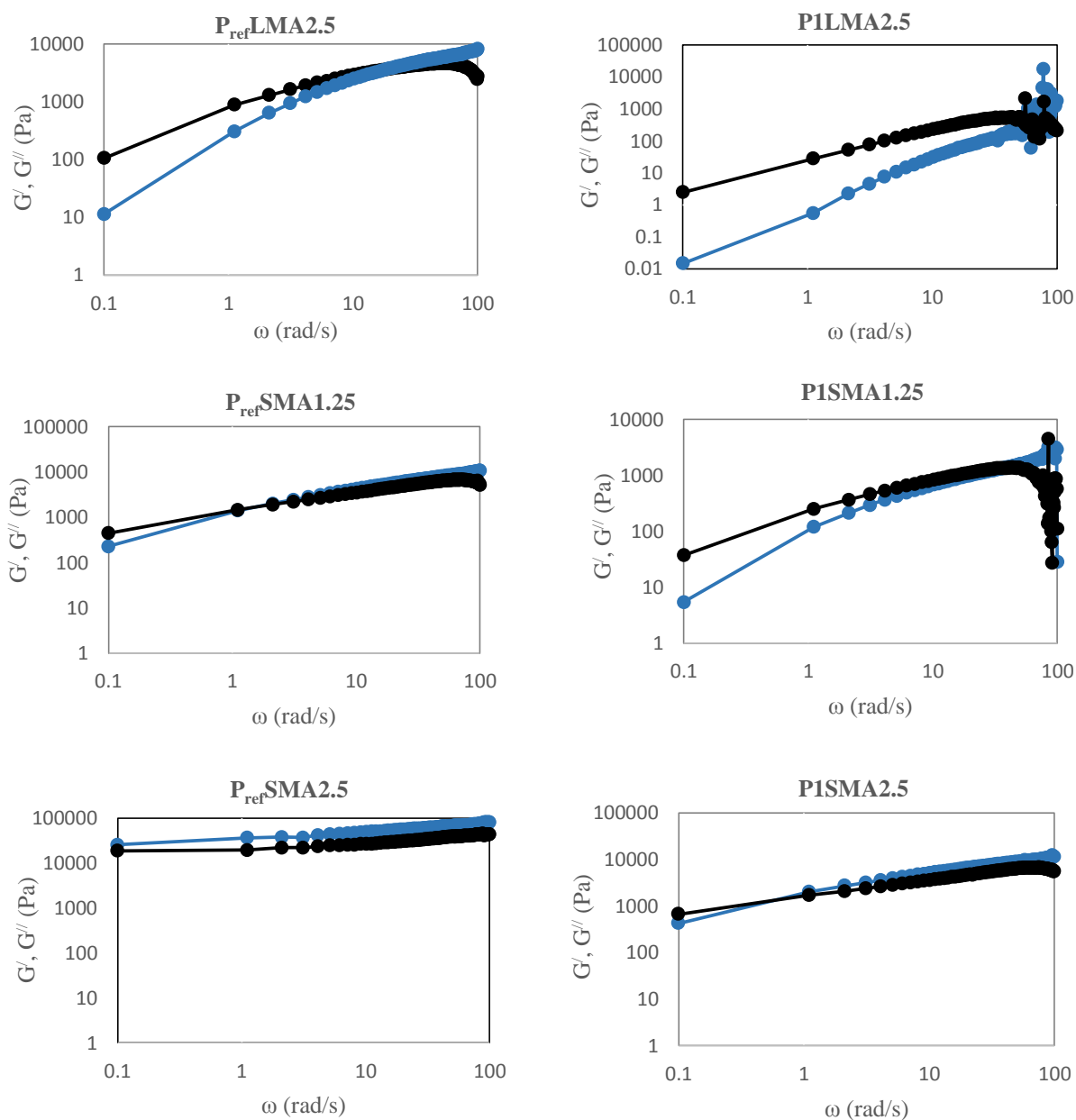


Figure 4.10. Plots of storage modulus G' (—●—) and loss modulus G'' (—●—) against frequency for **P1LMA2.5**, **P1SMA1.25**, **P1SMA2.5** and their reference copolymers at 20 wt%.

Interestingly, incorporation of 2.5 mol% SMA into the DMAM backbone resulted in solid-like behavior for the reference copolymer (**P_{ref}SMA2.5**) at 10 wt% solution. The storage moduli G' is greater than loss moduli G'' in the entire measurements and a strong gel-like behavior is observed. The longest relaxation time is too long to be characterized within the observation timescale of 300 s corresponding to frequencies $\omega=0.1-100$ rad/s. This behavior can be understood by the strong hydrophobic interactions between long chain stearyl methacrylate that

slow down the dynamics of physical interactions. Within the observation window, the pendant chains don't leave its associate, the gel structure is not allowed to relax and the alkyl chains stay associated to the same domains. Physical crosslinked materials do not possess a permanent network structure but rather present elasticity if the relaxation time of the network is much longer than the application time of stress. For these samples, G' is larger than G'' over the entire frequency range which is consistent with the solid-like, elastic nature of the hydrogels. There is a weak dependency of the elastic and loss modulus on frequency because of the physical and nonpermanent nature of the network [199,200]. When the network undergoes some creep which results in a viscous, energy dissipative response, the gels are still elastic at room temperature due to the long relaxation time of the physical hydrophobic association for the most part.

The cross-over frequencies for **P1LMA2.5** at 20 and 25 wt% and for **P1SMA1.25** at 15, 20 and 25 wt% were compared with their reference copolymers and are summarized in Table 4.4. The shift of ω_{cross} to lower frequencies is the evidence of a slowing system dynamics. The relaxation time λ is an important parameter which is affected by the molecular motions of the physical networks. The relaxation time is defined as the time that is required by the polymer chains to return to the equilibrium state after being stressed. For information about the relaxation time of the system equation [4.2] was used [47]:

$$\lambda = (G' \cdot [\eta']) \cdot (\omega \cdot [\eta^*])^{-1} \quad \text{eq. [4.2]}$$

With storage modulus (G'), dynamic viscosity (η') and complex viscosity (η^*). As can be seen from Table 4.4 all copolymers display a similar behavior and with increasing copolymer concentration cross-over frequencies, ω_{cross} , decrease. This can be explained by an increase of the elastic character of copolymers. According to equation 4.2, increasing G' leads to higher relaxation time and lower frequency. Moreover, another parameter which has direct influence on relaxation time is the hydrophobic chain length, the relaxation time ($1/\omega_{\text{cross}}$) increases with alkyl chain length and decreases with frequency. It shows that, for SMA the elastic part (G') of the system increases with the length of alkyl chain consequently, the relaxation time increases. Therefore, **P_{ref}SMA1.25** at 25 wt% has a lowest frequency with high value of relaxation time. In contrast, cationic copolymers with lower dynamic viscosity and LMA with shorter chain length displays a lower λ value.

Table 4.4. Cross-over frequency, ω_{cross} , for a range of cationic copolymers and their reference copolymers with various hydrophobicities and concentrations.

Sample	Concentration (wt%) ^{a)}	ω_{cross} (rad s ⁻¹) ^{b)}
P _{ref} LMA2.5	20	19.27
	25	12.21
P1LMA2.5	20	64.6
	25	58.6
P _{ref} SMA1.25	15	14.23
	20	3.12
	25	1.1
P1SMA1.25	15	37.44
	20	18.26
	25	9.5

^{a)} Two different concentrations (20 and 25 wt%) for **P_{ref}LMA2.5** and **P1LMA2.5**, three different concentrations (15, 20 and 25 wt%) for **P_{ref}SMA1.25** and **P1SMA1.25**. ^{b)} cross-over frequency obtained from storage (G') and loss moduli (G'') as a function of oscillating frequency of 0.1-100 rad/s, at a constant strain ($\gamma=10\%$) at 37 °C.

4.2.3.3 Modulus as a function of time

The storage and loss modulus as a function of time at constant frequency (1Hz) are shown in Figure 4.11. The same trend was observed for all compounds. Both moduli increase with increasing polymer concentration as well as increasing the hydrophobic content and chain length. In comparison, a significant lower modulus has been found for cationic copolymers in comparison to their reference polymers in the same concentration regime. For the copolymers with shorter alkyl side chains (LMA) and 1.25 mol% SMA, liquid like ($G'' > G'$) behavior was detected, while gelation ($G' > G''$) can be seen for **P_{ref}SMA2.5**. The increase of storage modulus G' suggests an enhancement of the elastic strands and expansion of a more complete network.

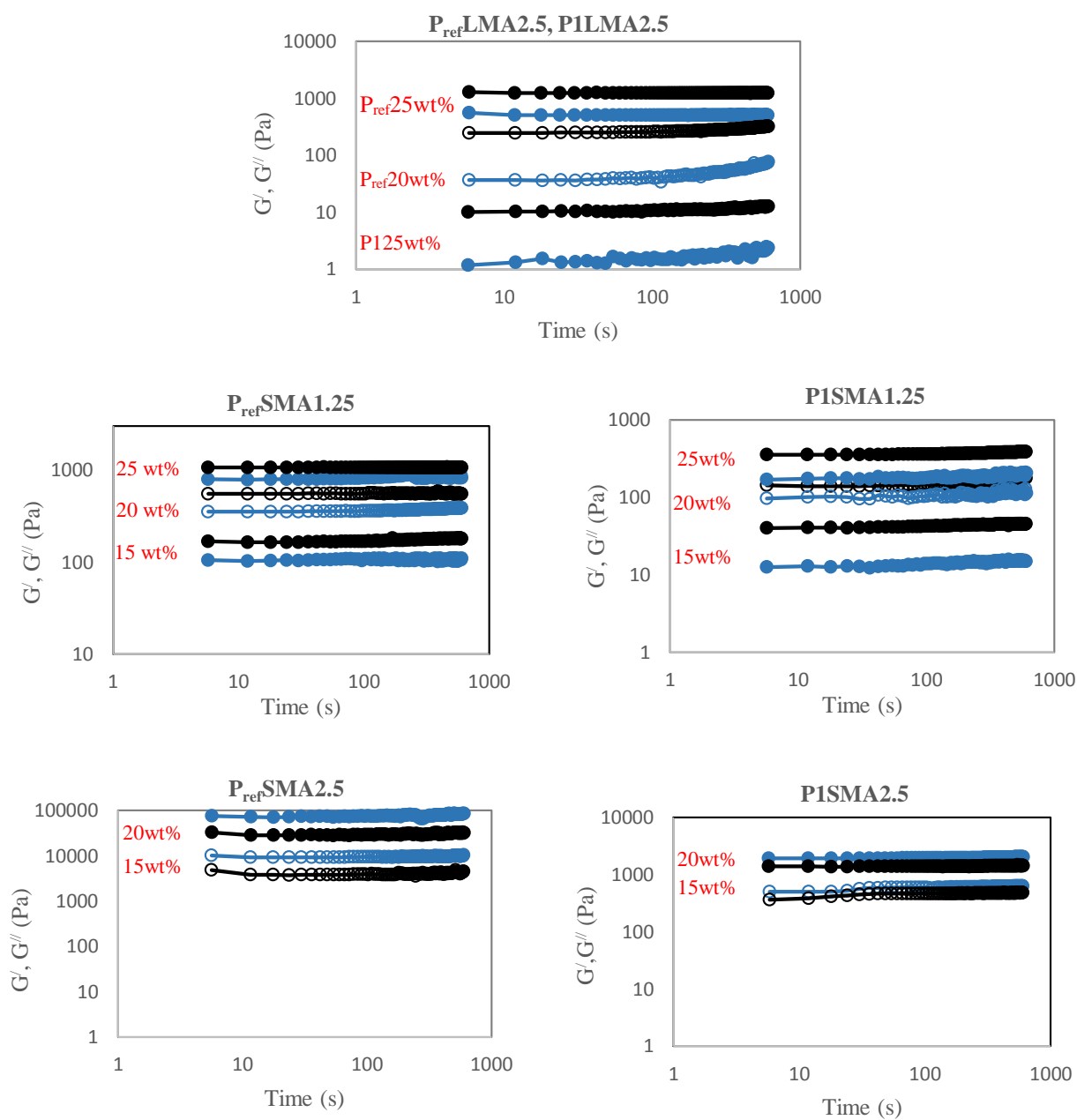


Figure 4.11. Elastic moduli G' (blue symbols), the viscous moduli G'' (black symbols) as a function of time at constant frequency (1Hz) for $P_{ref}LMA2.5$, $P1LMA1.25$, $P_{ref}SMA1.25$, $P1SMA1.25$, $P_{ref}SMA2.5$ and $P1SMA2.5$ at different concentration.

4.2.3.4 The impact of temperature on the modulus

The effect of temperature on the rheological behavior of hydrophobically modified polymers is the main factor to be taken into account for various applications such as oil recovery processes and cell experiments. The temperature effect on the behavior of the aqueous copolymer solutions was studied with the variation of the complex modulus as a function of time at various temperatures ranging from 25 °C to 80 °C to 25 °C at constant frequency (1Hz).

As shown in Figure 4.12, temperature effect on modulus behavior was investigated with samples **P1LMA2.5** at 22.5 and 25 wt%, **P_{ref}SMA2.5** at 10 and 12.5 wt% and **P1SMA2.5** at concentrations of 20 and 25 wt%. **P_{ref}SMA2.5** and **P1SMA2.5** at both concentrations are characterized by an initial decrease of both loss and storage modulus with increasing the temperature. Obviously, even with temperature enhancement the solutions behave like elastic solid ($G' > G''$) but the cross-over between G' and G'' is obtained around 72 °C and 55 °C for **P_{ref}SMA2.5** and **P1SMA2.5** respectively. After the cross-over point the solutions behave like a viscous fluid ($G'' > G'$) and an elastic solid is obtained again with decreasing the temperature. The decrease in elastic behavior of the hydrogels is accompanied by increase in the viscous modulus. At sufficiently high temperature, storage and loss modulus become equal and finally the two quantities cross-over and G'' , the viscous character of the gels becomes dominant. In the case of a viscous sample such as **P1LMA2.5**, the loss modulus has the same behavior and decreases with increasing temperature from 25 °C to 80 °C and increases again with decreasing temperature, while storage modulus was lower than G'' in the whole range of the time-temperature investigated. The cross-over point exhibits the transition from solid-like to liquid-like character of the gel, which could be due to a disruption of the physical network composed of hydrophobic interactions. The most of theoretical studies on crosslinked polymers noticed that the characteristic time of the network (τ_N) is proportional to the hydrophobe lifetime in the micellar junction (τ_b) [201,202]. This can be explained by equation [4.3]:

$$\tau_N \sim \tau_b = \tau_0 \exp (W/kT) \quad \text{eq. [4.3]}$$

With τ_0 is a microscopic time, which is related to the hydrophobe diffusion and W is the potential barrier corresponding to the additional activation barrier and binding energy. This equation illustrates the dynamics of the network will slow down either by decreasing the temperature or by the hydrophobicity of the sticker (binding energy). The aqueous or organic amphiphilic polymer solutions, which are subjected to temperature changes, show this general

feature; the relaxation time and viscosity reduce when the temperature increases. The higher the binding energy, the greater would be the viscosity decline with temperature enhancement.

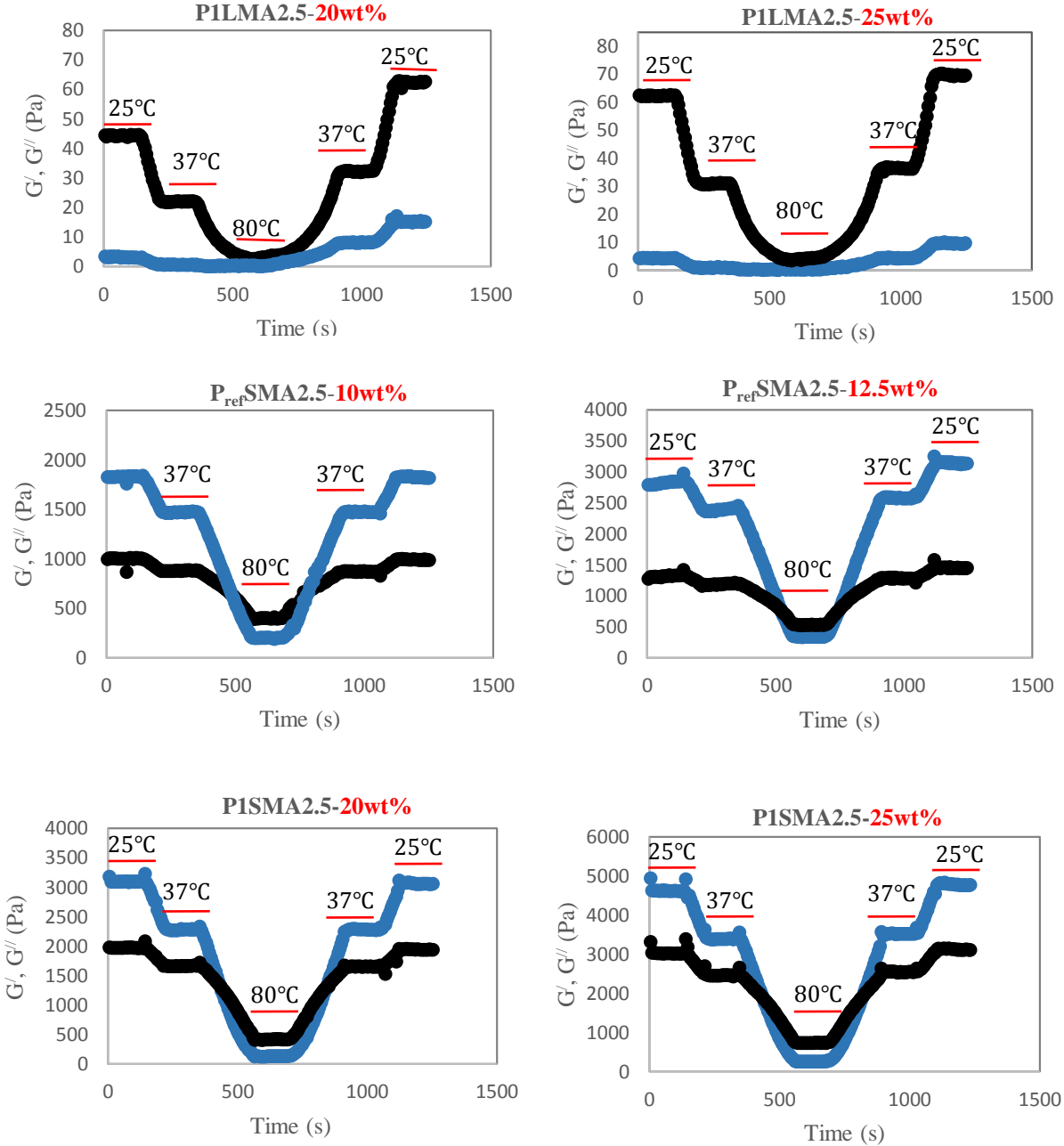


Figure 4.12. Temperature dependence of the storage G' (—●—) and loss modulus G'' (—●—) between 25 and 80 °C at constant frequency (1 Hz) for **PILMA2.5**, **P_{ref}SMA2.5** and **PISMA2.5**.

4.2.4 Fluorescence measurements of the hydrophobic domains

The sensitivity of pyrene to the polarity of the host microenvironment and long lifetime make it a good candidate to probe the formation of hydrophobic domains [203,204]. The information about the micropolarity, where the probe is located, can be obtained by the ratio of the first (I_1) to the third (I_3) vibronic peak in the pyrene emission spectrum (polarity index I_1/I_3). Figure 4.13 compares the intensity ratio I_1/I_3 for **P1SMA2.5** and **P1LMA1.25** as a function of polymer concentration. For **P1SMA1.25** the I_1/I_3 ratio remains rather constant up to 1.5 wt% of the polymer concentration and decreases afterwards with increasing copolymer concentration to a value I_1/I_3 of around 1.1 suggesting that the pyrene environment becomes more hydrophobic with increasing polymer concentration. The value of 1.1 is very typical for pyrene in a hydrophobic environment in agreement with results found for micellar solutions [205,206]. The higher I_1/I_3 value of ≈ 1.3 for aqueous **P1LMA2.5** solutions can be attributed to a decrease in hydrophobicity with decreasing the length of hydrophobic side chain.

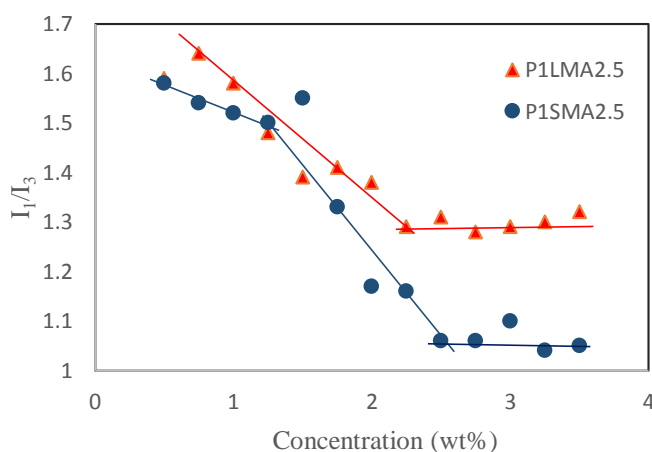


Figure 4.13. I_1/I_3 intensity ratio as a function of polymer concentration for **P1SMA2.5** and **P1LMA2.5**.

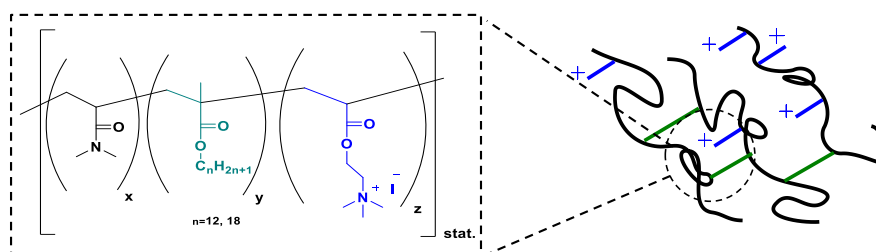
4.3 Conclusions

Cationic hydrophobically modified copolymers were prepared by free radical polymerization in excellent yields and their solution properties were compared to their non-ionic references copolymers (DMAM-stat-LMA/SMA) to investigate the influence of positive charge on the solution behavior and rheological properties. Precursor copolymers (DMAM-stat-SMA/LMA-DMAEA) were methylated with methyl iodide. The conversion induces significant changes in polymer solution properties such as solubility in aqueous medium. Apart from the solubility, drastic changes in rheological behavior was observed compared to their references analogue. It

was found that **P1** produced a significant lower viscosity compared to the non-ionic reference copolymers **P_{ref}**, but both copolymers exhibit typical associative behavior of hydrophobically modified copolymers. Above a certain copolymers concentration threshold the dynamics of the copolymer solution is generally controlled by the transformation from intra- to intermolecular hydrophobic association. The length of hydrophobic side chain was modified by using SMA, resulting in samples with higher viscosity and more elastic character compared to samples with LMA side chains.

4.4 Experimental

4.4.1 Synthesis of cationic copolymers



Non-ionic copolymers were synthesized according to a previously reported method in the literature [68]. Copolymers were prepared by free radical polymerization in toluene in Schlenk flasks with freeze- pump-thaw cycles to obtain oxygen-free atmosphere at room temperature. Different amounts of lauryl methacrylate (1.25- 10 mol%) and stearyl methacrylate (1.25 -2.5 mol%) and 0.01 mol/L AIBN were added to the polymerization flasks to 1 M solution. The polymerization was carried out at 65 °C for 20 h. Before the resulting copolymers were precipitated in diethyl ether the solutions were let to cool down to room temperature. The precipitated copolymers were dried under vacuum for at least 48 h.

To obtain cationic copolymers a series of random precursor copolymers were prepared by altering the mole ratio of LMA (1.25-10 mol %) and SMA (1.25 and 2.5 mol %), while the total amount of DMA and DMAEA (10 mol%) was kept constant. The polymerizations were carried out as it was already described. The yield of all precursors copolymers were more than 80 %. ¹H NMR (500 MHz, MeOD, δ): 0.88 (t, CH₃, SMA/ LMA), 1.29 (brs, -CH₂- SMA/ LMA), 1.57 (brs, -CH₂- backbone DMAM and DMAEA), 2.3 (brs, -N-(CH₃)₂, DMAEA), 2.59

(brs, -CH- backbone DMAM, DMAEA), 3.04 (m, -N-(CH₃)₂-, DMAM, -CH₂-O- SMA/LMA), 4.18 (brs, -CH₂-O-, DMAEA). The variation of hydrogen was gained according to the variation of SMA or LMA, which quantitative analysis of the ¹H NMR proved close results to the monomer mixture utilized for each polymerization. To calculate the molecular weight in the range of ($M_n = 25000-43000 \text{ g mol}^{-1}$) and polydispersity ($\text{Đ} = 2.3- 3.7$), SEC was used in DMF. According to the literature [207], the quaternization were done by adding iodomethane to all eight different copolymers. 2 mmol DMAEA were dissolved in 8 to 10 ml of dry dioxane and 2.4 mmol of methyl iodide was added dropwise over 20 min at room temperature and the solution stirred for some minutes. The final yellow copolymers were precipitated in diethyl ether and dried under vacuum. The quaternization was confirmed by the disappearance of the methyl protons attached to the tertiary amine (2.3 ppm) and the appearance of new peak at 3.3 ppm, without residual signs of di-methyl group. All copolymers were carefully purified by dialysis against distilled water and dried by freeze-drying before ¹H NMR measurement. ¹H NMR (500 MHz, D₂O, $\delta = 4.75$): 0.88 (t, CH₃, SMA/ LMA), 1.29 (brs, -CH₂- SMA/ LMA), 1.57 (brs, -CH₂- backbone DMAM and DMAEA), 2.59 (brs, -CH- backbone DMAM, DMAEA), 3.04 (m, -N-(CH₃)₂-, DMAM, -CH₂-O- SMA/LMA), 3.34 (brs, -N⁺(CH₃)₃I⁻). The cationic copolymers yields were more than 70%. The molecular weight was in the range of ($M_n = 25000-43000 \text{ g mol}^{-1}$) and polydispersity ($\text{Đ} = 2.3- 3.7$), SEC was carried out in DMF.

Chapter 5. Synthesis and Rheological Study of Functionalized Hydrophobically Modified zwitterionic Polymer

5.1 Introduction

Today it is well known that implanted devices can be recognized as a foreign object by the immune system and encapsulated by a dense collagen layer due to the body self-protection mechanism. Proper implant functioning can be prevented by this layer, because it is impermeable to nutrients and metabolites, resulting very often in implant failure [208,209]. The event of nonspecific protein adsorption onto the implant surface has been suggested to help the immune system to recognize the implant upon implantation into the body, and this identification is regarded to the first step in the foreign body reaction. Therefore, the protection resistance property of biological materials has a fundamental role *in vivo* in avoiding macrophage identification and the following isolation from the body. Thus, for *in vivo* medical application, this property is the most important factor [210]. During the past few years, *Jiang and coworkers* detected polyzwitterions as compounds that illustrated ultralow-fouling properties in terms of nonspecific protein adsorption [211,212]. The zwitterionic nature of the sulfobetaine groups resulted only in $<0.3 \text{ ng/cm}^2$ protein adsorption, even in pure blood [213,214]. The structure in the body is glycine betaine like and the highly bionic structure make them safe for *in vivo* applications. Moreover, the facile synthesis method and excellent biocompatibility [215], non-fouling properties [216] and salt sensitivity behavior [217] make the sulfobetaine group one of the most widely known zwitterionic moieties. Additionally, the zwitterionic hydrogels can lead to a reduced foreign body reaction comparable to PEG hydrogels and inhibit the formation of collagenous capsule *in vivo* for 3 months [218].

Polysulfobetains are zwitterionic polymers containing sulfonic anions and ammonium cations connected by alkyl groups. This dipolar pendant functional groups are responsible for strong inter- and intramolecular interactions, which makes polyzwitterionic polymers attractive materials due to their salt-responsive behavior (polymer chains have collapsed conformations and stretched conformations in water depending on the salt concentration), photoelectric activity, anti-fouling property and biocompatibility [219,220].

Diaz and coworkers [221] synthesized six polymer coatings (Figure 5.1) by surface-initiated graft polymerization and reported that these polymers have the ability to promote attachment and proliferation of undifferentiated human embryonic stem (hES) cells. They

obtained the best results for poly[2-(methacryloyloxy) ethyl dimethyl-(3-sulfopropyl) ammonium hydroxide] (PMEDSAH), which demonstrated the ability to support long-term culturing of undifferentiated, pluripotent hES cells. *Ye and coworkers* [214] also showed that the starch-based zwitterionic (3-[2-(methacryloyloxy) ethyl] (dimethyl)-ammonio]-1-propanesulfonate) hydrogel exhibited excellent biocompatibility suggesting that this is a promising material for future *in vivo* applications, like cartilage regeneration. On the other hand [2-(methacryloyloxy)]dimethyl-(3-sulfopropyl)ammonium hydroxide with the persistent charged state of the quaternary ammonium and sulfonate groups gives sulfobetaine-functionalized copolymers to retain a constant near net-zero charge irrespective of the pH of the medium.

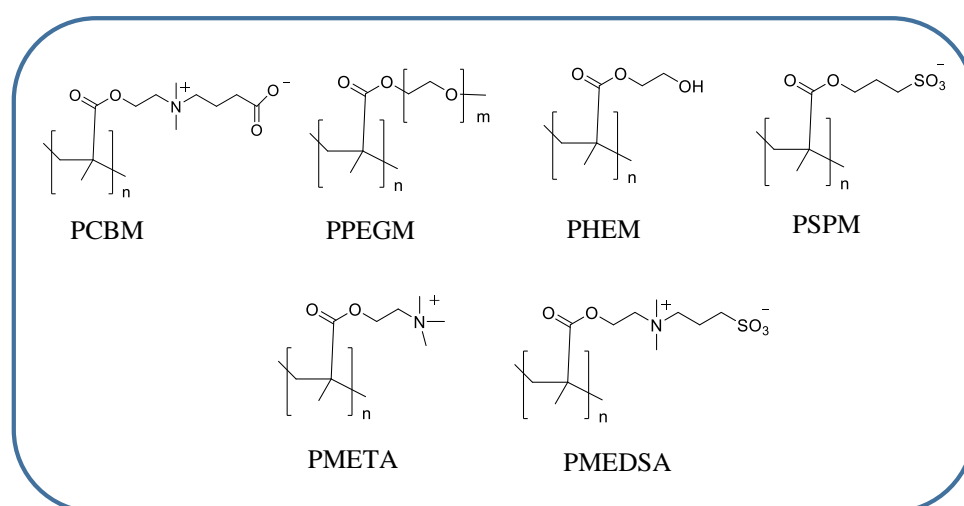


Figure 5.1. The chemical structure of synthetic polymers for long-term growth of hES. Poly[carboxybetaine methacrylate] (PCBM), poly[poly(ethylene glycol) methyl ether methacrylate] (PPEGM), poly[2-hydroxyethyl methacrylate] (PHEM), poly[3-sulfopropyl methacrylate] (PSPM), poly[[2-(methacryloyloxy) ethyl] trimethylammonium chloride] (PMETA), poly[2-(methacryloyloxy) ethyl dimethyl-(3-sulfopropyl) ammonium hydroxide] (PMEDSAH).

The rheology of polyelectrolyte solutions has witnessed increasing interest because of a wide variety of practical applications such as viscosity control additives. The molecular conformation of polyelectrolyte can be modified by manipulating temperature, pH and addition of low-molecular weight electrolytes or ionic species with the potential to have electrostatic interactions with polyelectrolytes (PEs). In aqueous polyelectrolyte solutions increasing the ionic strength causes usually the polymer coil to shrink due to the decrease of intramolecular repulsion between similar charges along the polymer backbone. This phenomenon can lead to less stretched or extended conformation, which is accompanied by a viscosity decrease of

polyelectrolyte solutions, known as the *polyelectrolyte effect* [222]. In contrast to PEs, polyezwitterions (PZs) solutions show an *anti-polyelectrolyte effect* in which the physical attraction between equivalent cations and anions are weakened and the zwitterionic polymer extends therefore to a random coil conformation, with the addition of salt the PZs viscosity increase and makes PZs good candidates as salt-tolerant viscosifiers (Figure 5.2) [223,224]. Additionally, the salt concentration and ion types [225] affect such salt responsive behaviors of zwitterionic polymers, providing many applications for membrane separations [226], protein transport [227,228], controlled release [229,230] self-cleaning surfaces [231,232] and lubricant surfaces [233,234].

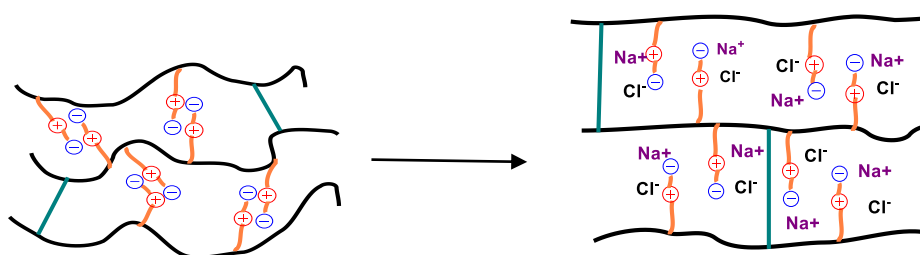


Figure 5.2. Structural dependence of salt-responsive polyezwitterionic brushes with an *anti-polyelectrolyte* effect.

In this chapter, the synthesis and characterization of hydrophobically modified zwitterionic copolymers has been studied, and their rheological properties in aqueous medium have been compared to the cationic and non-ionic hydrophobically modified copolymers.

5.2 Results and Discussions

A random terpolymer composed of *N,N'*-dimethyl acrylamide (DMAM), [2-(methacryloyloxy)] dimethyl-(3-sulfopropyl) ammonium hydroxide (MEDSAH) and stearyl methacrylate (SMA) were prepared via free radical polymerization (**P2**) (Figure 5.3). Different solvent mixtures were examined, however, the best results were obtained in a solvent mixture containing methanol and toluene, 70/30 (v/v), respectively and just few drops of water to solve the MEDSAH monomer. Analytical data of **P2** are listed in Table 5.1 and the successful copolymerization of the three monomers was confirmed by ¹H NMR (Figure 5.4).

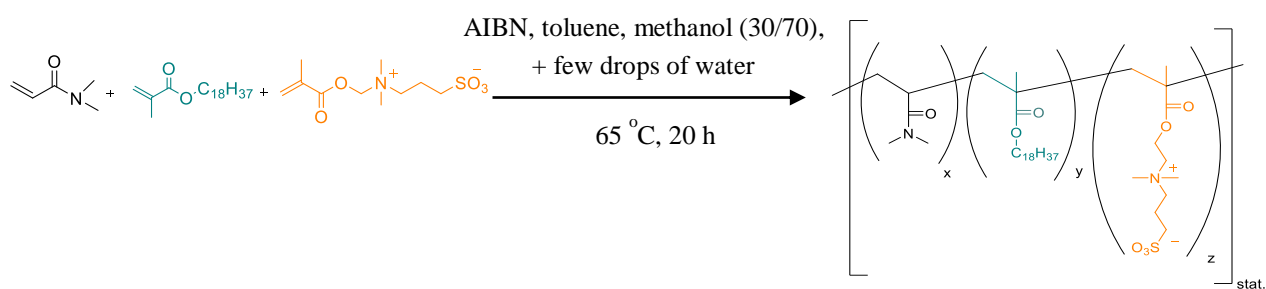


Figure 5.3. Synthetic route of **P2** copolymer.

Table 5.1. Analytical data of **P2**.

Sample ^{a)}	Copolymer composition (mol%) (DMAM: SMA: MEDSAH) ^{b)}	M _n (g/mol) ^{c)}	Đ ^{c)}	Yield (%)
P2	89.18 (88.75): 1.82 (1.25): 9 (10)	23890	2.58	88

^{a)} The terpolymer has been prepared by free radical polymerization with 0.1 mol/L AIBN at T= 65 °C for 20 h, copolymer composition was determined by ¹H NMR, in brackets: theoretical values; ^{c)} polymer dispersity Đ determined by SEC measurements with PMMA standards in DMF with 5 g·L⁻¹ LiBr at T= 60 °C.

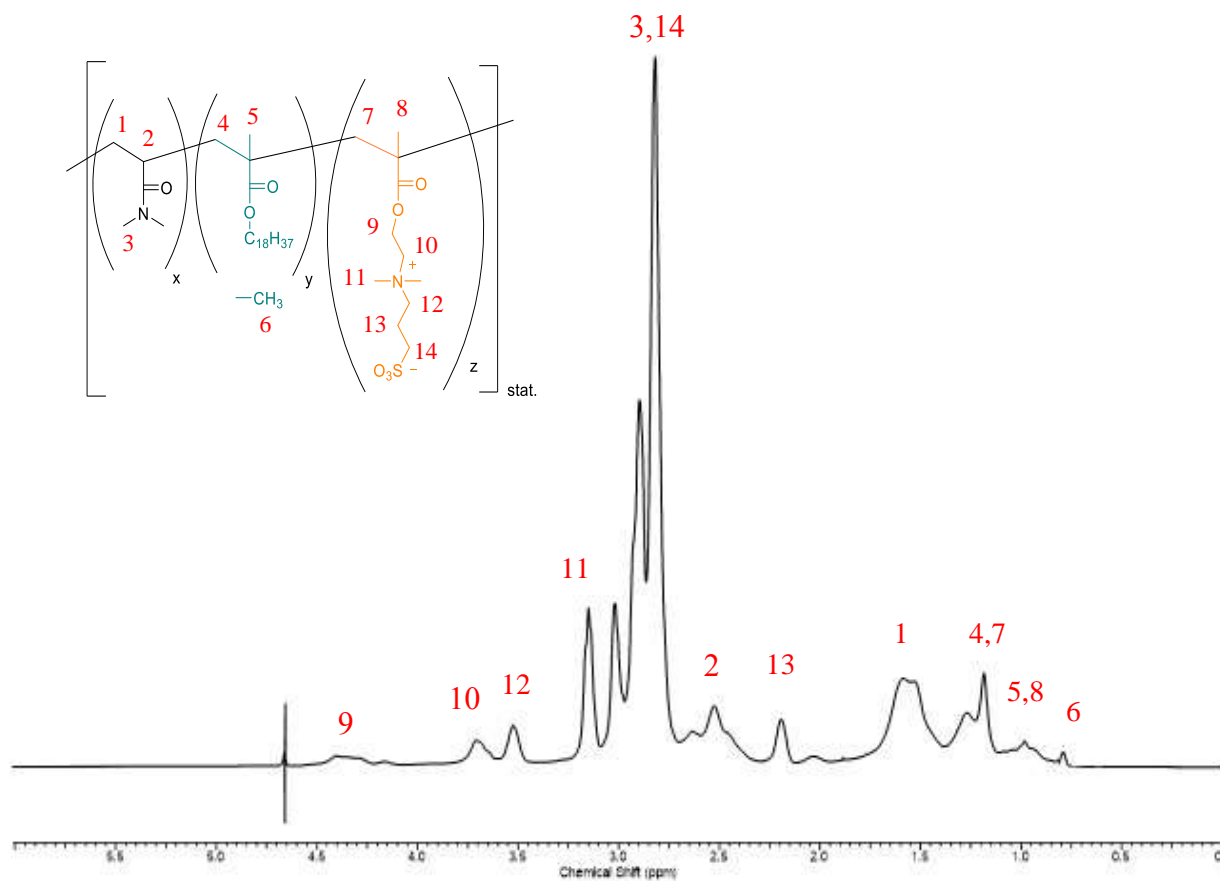


Figure 5.4. ¹H NMR spectrum of **P2** in D₂O.

5.2.1 The rheological behavior of **P2**

The results from each rheological measurements are shown in the following section along with the discussion of the observed behavior based on the copolymers compositions and structures. The rheological study of **P2** in buffer solution illustrates the similar solution behavior when compared to the non-ionic copolymer **P_{ref}SMA1.25**. **P2** is zwitterionic polymer, containing a cationic and anionic moiety within the same monomer side chain. The existence of two different charges as pendant side chain functionality may cause two different effects. First, the hydrophilic nature of the zwitterionic charges should increase hydrophilicity of the copolymer and therefore prevent hydrophobic aggregations between side chains. As a results, the viscosity of the solution is expected to be lower compared to copolymers based on hydrophobic side chains only with similar structure but without charge. On the other hand, the solution viscosity could rise because of the repulsion between the charged groups which encourages coil expansion. Therefore, polyelectrolyte solution behavior may be determined by a combination of these two effects [222].

The viscoelastic properties of **P2** were compared with **P_{ref}SMA1.25** and **P1SMA1.25** in the concentration range from 1 to 25 wt%, the difference in concentration resulted in significant changes in solution characteristics from liquid to gel-like samples. Therefore, the viscosities of liquid and low viscous copolymers solutions were measured via Ubbelohde viscometer situated in a thermostat-control water bath at 37 °C and high viscous samples were measured by oscillatory rheometry with a 150 mm cone-plate and 1000 mm plate- plate geometry for gel-like samples. For all rheological studies, the final desired copolymers were directly prepared in a screw-capped vial and the proper amount of buffer solution was added, the samples were kept at room temperature without stirring. For preparing the gels for rheology measurements the copolymer solutions were heated to 100 °C.

5.2.1.1 Viscosity as a function of shear rate

Viscosity profile of the HM zwitterionic terpolymer and **P_{ref}SMA1.25** and **P1SMA1.25** are shown in Figure 5.5. **P2** illustrates the greatest increase in viscosity with increasing the concentration, which is the normal behavior for associative polymers. The solutions of 7.5 to 20 wt% polymers presented nearly Newtonian behavior, but significant changes in the flow behavior were observed for 20 and 25 wt% polymer solutions. In these concentration at higher shear stress the viscosity profiles were characterized by a low shear Newtonian plateau follow by shear thinning effect. Shear thinning is observed when disentanglement of alkyl chains can occur faster than the rate of formation of entanglements. For **P2** and **P_{ref}SMA1.25** in more concentrated solution the aggregation between overlapping chains become stronger and their disruptions is faster than the reformation. Therefore, a shear thinning behavior was identified. Generally, a comparison between **P2** and **P_{ref}** copolymers exhibits not so much differences in their viscosities, however, **P2** shows little higher solution viscosity. *Peiffer and Lundberg* [235] and *Johnson and coworkers* [224] reported that hydrophobically modified acrylamide-based copolymers bearing charge density of less than 10 mol% betaine generally associate intermolecularly, while the high charge density polybetaine systems (greater than 10 mol%) associate intramolecularly. For **P2** with 10 mol% zwitterionic monomer incorporation, the results suggest intermolecular association between similar charges and therefore the polymer coils expanded and the viscosity increased above the overlapping concentration. Visual inspection (inverted-vial test) can also prove the close viscosities of the solutions. The charge influence on the copolymers properties was further studied by comparison between **P2** and **P1SMA1.25**. A large viscosity enhancement for **P2** is detected compared to **P1SMA1.25**. For

instance, at each concentration the viscosity of zwitterionic copolymer is ~ 10 times larger than the cationic polymer. *Elmalem and coworkers* [14] also showed poly(fluorine phenylene) when carrying zwitterions in their side chains (1,4- butane sultone) can form hydrogel above 1.1 wt%, however, when it possesses cationic charges in the side chains (2-bromoethan-1-ol) the same polymer cannot form hydrogels even at 10 wt%.

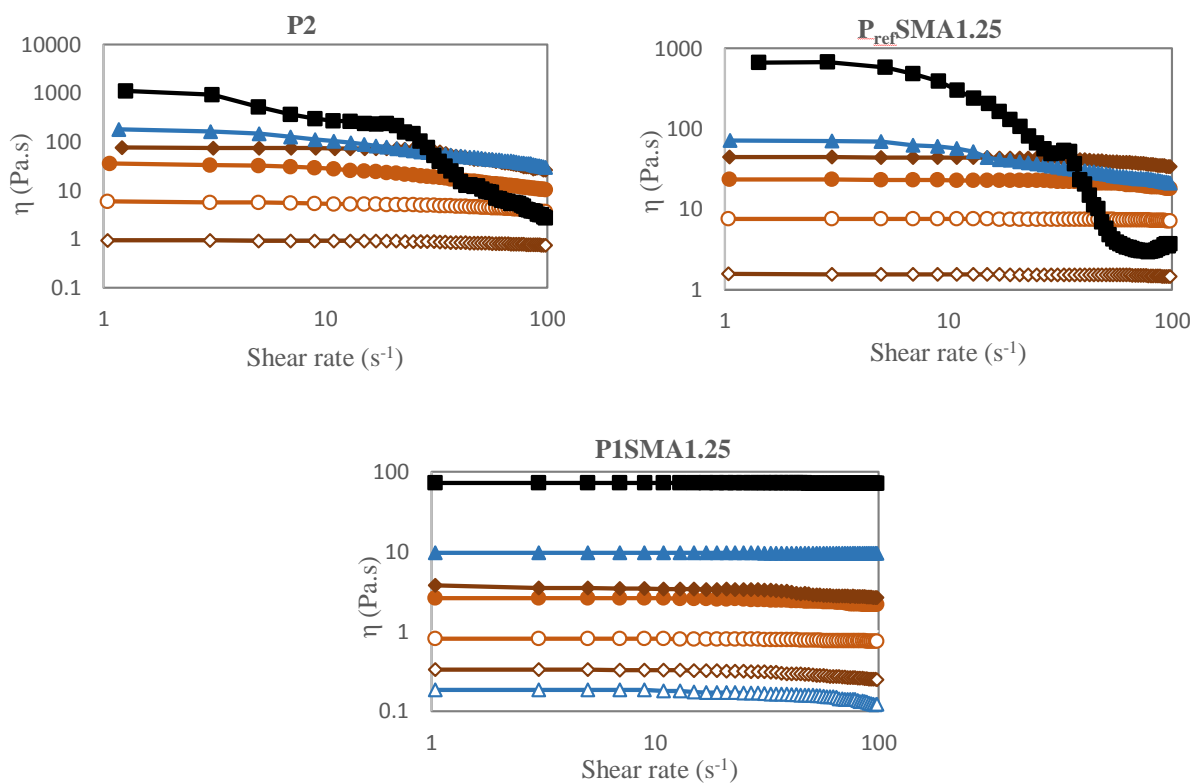


Figure 5.5. Presents a plot of the viscosity as a function of shear rate at various concentration (wt %): 25 % (—■—), 20 % (—▲—), 15% (—◆—), 12.5% (—●—), 10 % (—○—), 7.5% (—◇—) for P2, P_{ref}SMA1.25 and P1SMA1.25.

5.2.1.2 Viscosity as a function of concentration

The dependence of the viscosity on polymer concentration of **P2** has been compared with **P_{ref}SMA1.25** and **P1SMA1.25** (Figure 5.6).

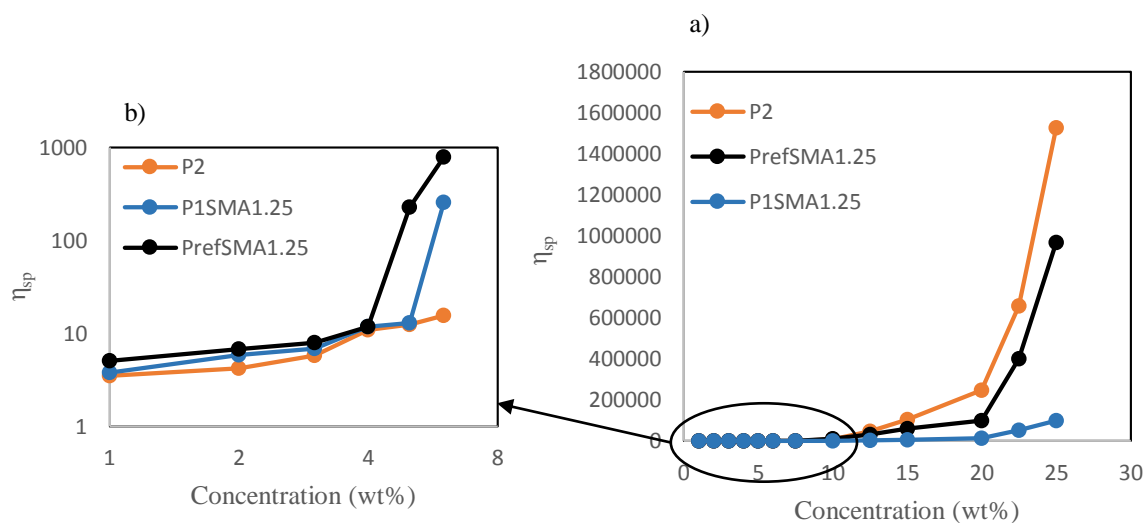


Figure 5.6. Zero shear specific viscosity as a function of concentration for **P2**, **P_{ref}SMA1.25** and **P1SMA1.25** in a) semi-dilute and concentrated regime b) in dilute regime, demonstrating the effect of zwitterion incorporation on the viscosity.

As expected, the specific viscosity of **P2** increases with increasing polymer concentration and above a critical concentration, when the behavior of the solution is controlled by the influence of intermolecular associations the viscosity increases sharply, showing the same behavior like **P_{ref}** and **P1**. In the dilute regime, the viscosity of copolymers increases by a factor of $c^{0.96}$, $c^{0.85}$ and $c^{0.8}$ for **P_{ref}SMA1.25**, **P1SMA1.25** and **P2** respectively. As is shown in Figure 5.6b the lowest viscosity value was measured for **P2**. One explanation could be the intramolecular zwitterion association between opposite charges and drop in coil size, which leads to viscosity decrease for **P2**. With increasing the concentration, where the intermolecular association of stearyl methacrylate starts, copolymers showing typical behavior for a semi-dilute unentangled regime. An increase in viscosity occurs with concentration dependence $c^{5.3}$ for **P_{ref}**, $c^{4.6}$ for **P1** and $c^{7.12}$ for **P2**. The results from the graph 5.6a show only two regions for **P2** as was observed for **P_{ref}SMA1.25** and **P1SMA1.25**. According to the obtained data from rheology, **P2** has higher viscosity in comparison to its reference analogue and **P1SMA1.25**. The viscosity enhancement with incorporation of zwitterionic monomer in the concentrated regime can be attributed to the coil expansion due to the repulsion of similar charges. The results are in a good

agreement with results from *Che and coworkers* [236]. They synthesized acrylamide-based hydrophobically modified copolymers containing polysulfobetaines and stearyl methacrylate (SMA). To determine the influence of sulfobetaine monomer a copolymer with only acrylamide and SMA (AS) was prepared. In the dilute polymer regime, the viscosity of copolymer containing zwitterionic monomer was lower than that of AS copolymer, but above the critical concentration, the zwitterionic copolymer shows higher viscosity. Therefore, the incorporation of zwitterionic monomer can promote intramolecular association in dilute regions and intermolecular aggregation at high concentration.

5.2.1.3 Complex modulus

Figure 5.7 depicts the variation of the storage and loss modulus as a function of frequency, for **P2** at 20 and 25 wt% and compared with their references and **P1SMA1.25** at the same concentrations. When the concentration is increasing, there is an overall increase in storage and loss modulus for all copolymers. The results indicate that the frequency dependence of the shear moduli corresponds to a viscous-like behavior since at low frequencies the loss modulus is higher than the storage modulus and only above cross-over point ω_{cross} G' exceeds G'' . The shift of the cross-over point between G' and G'' to lower frequencies prove a more elastic solution character. The longer mean relaxation time for the formation and breakup of the fluid microstructure is responsible for this cross-over frequency shift. The interesting behavior is observed for **P2** at 25 wt% that the solution behaves as an elastic solid since G' and G'' are frequency independent in the entire frequency range of experiment. The elasticity arises from chain expansion of the zwitterionic units. Therefore, the hydrogel that is formed from **P2** at 25 wt% is defined by $G' > G''$ while **P_{ref}SMA1.25** and **P1SMA1.25** display at 25 wt% still a viscous character.

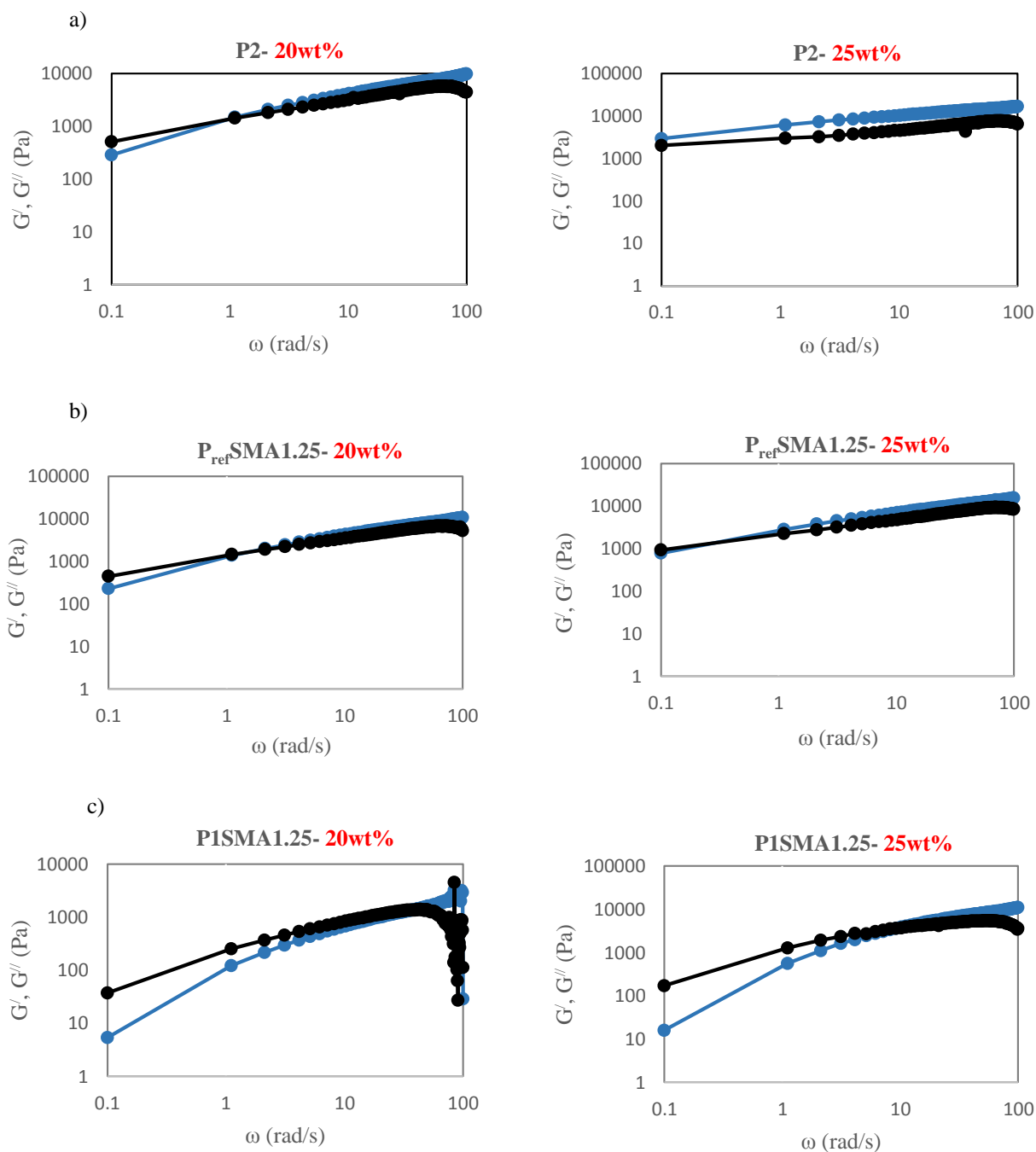


Figure 5.7. Elastic moduli G' (—●—) and viscous moduli G'' (—●—) as a function of frequency for a) **P2** b) $P_{ref}SMA1.25$ and c) **P1SMA1.25** at 20 wt% and 25 wt%.

5.2.1.4 Complex modulus as a function of time

Dynamic oscillatory measurements (time sweep experiments) were carried out for **P2** to get more information about the stiffness of the hydrogel network in aqueous medium. Figure 5.8 shows the elastic and viscous modulus as a function of time at 37 °C, 10 % strain and constant

frequency (1Hz) were applied for **P2**, **P_{ref}SMA1.25** and **P1SMA1.25**. The results show an increase in storage and loss modulus with increasing copolymers concentration. It is clear that the values of G' and G'' for **P2** in these concentrated regime are higher than their references analogue and cationic copolymers. These schematic diagrams illustrate that **P2** formed a gel at 25 wt% due to the predominant elastic character while below 25 wt % and also for the other polymers **P_{ref}SMA1.25** and **P1SMA1.25** G'' is always higher than G' . Visual inspection (inverted-vial test) indicate also that the zwitterionic polymer forms a hydrogel at 25 wt%, whereas **P_{ref}SMA1.25** does not at the same concentration and is still liquid-like.

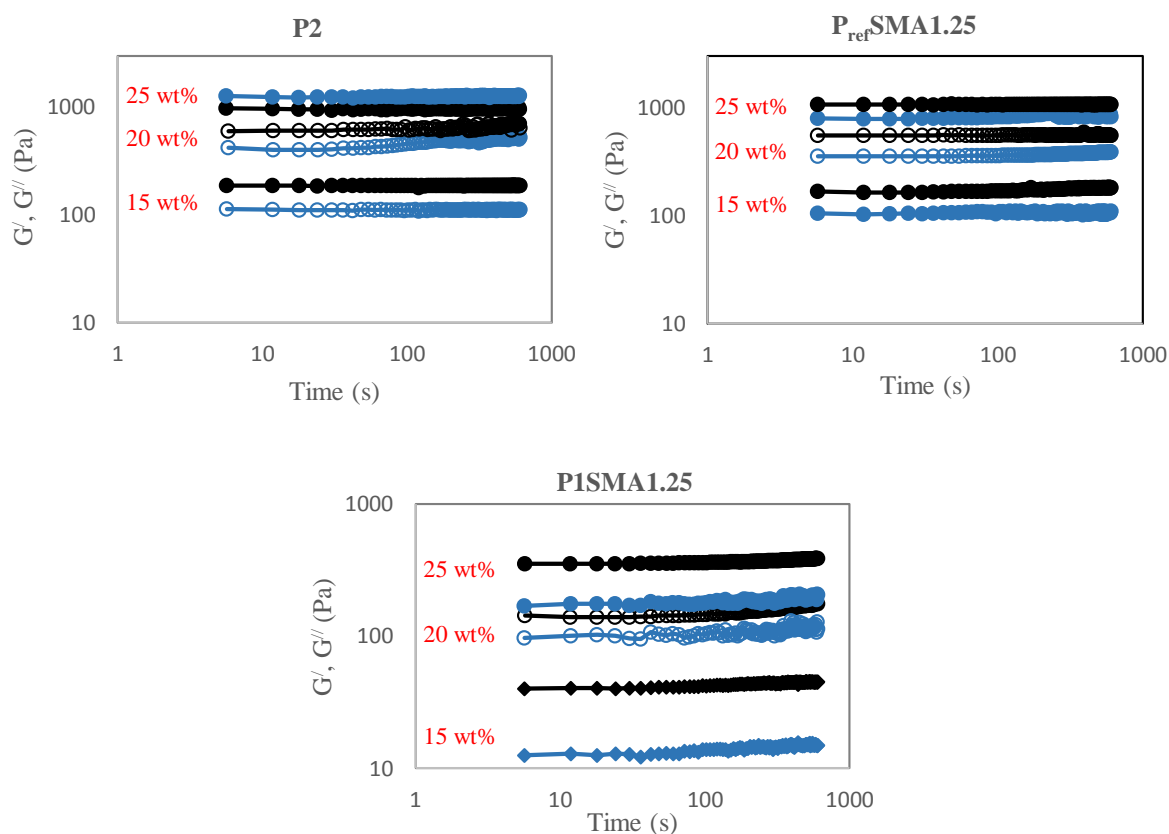


Figure 5.8. Elastic moduli G' (blue symbols), the viscous moduli G'' (black symbols) as a function of time for **P2**, **P_{ref}SMA1.25** and **P1SMA1.25**, showing the solid-like behavior of **P2** at 25 wt%.

When comparing **P2** and **P_{ref}SMA1.25**, it is reasonable to conclude that the hydrophobic (SMA) association moieties have a greater effect on solution rheology than the electrostatic interactions of the zwitterionic moieties.

5.3.1 Effect of salt

5.3.1.1 Viscosity as a function of shear rate

In the following subchapter the effect of 2 and 4 molar NaCl solution on the solution viscosity of **P2** at 7.5, 10, 12.5 and 15 wt% was studied. The polymer solutions showed significant increase in viscosity with increasing polymer concentrations when salt was added as well as salt-free solutions. Interestingly, in the same polymer concentration, the viscosity of the solution increase with increasing of salt.

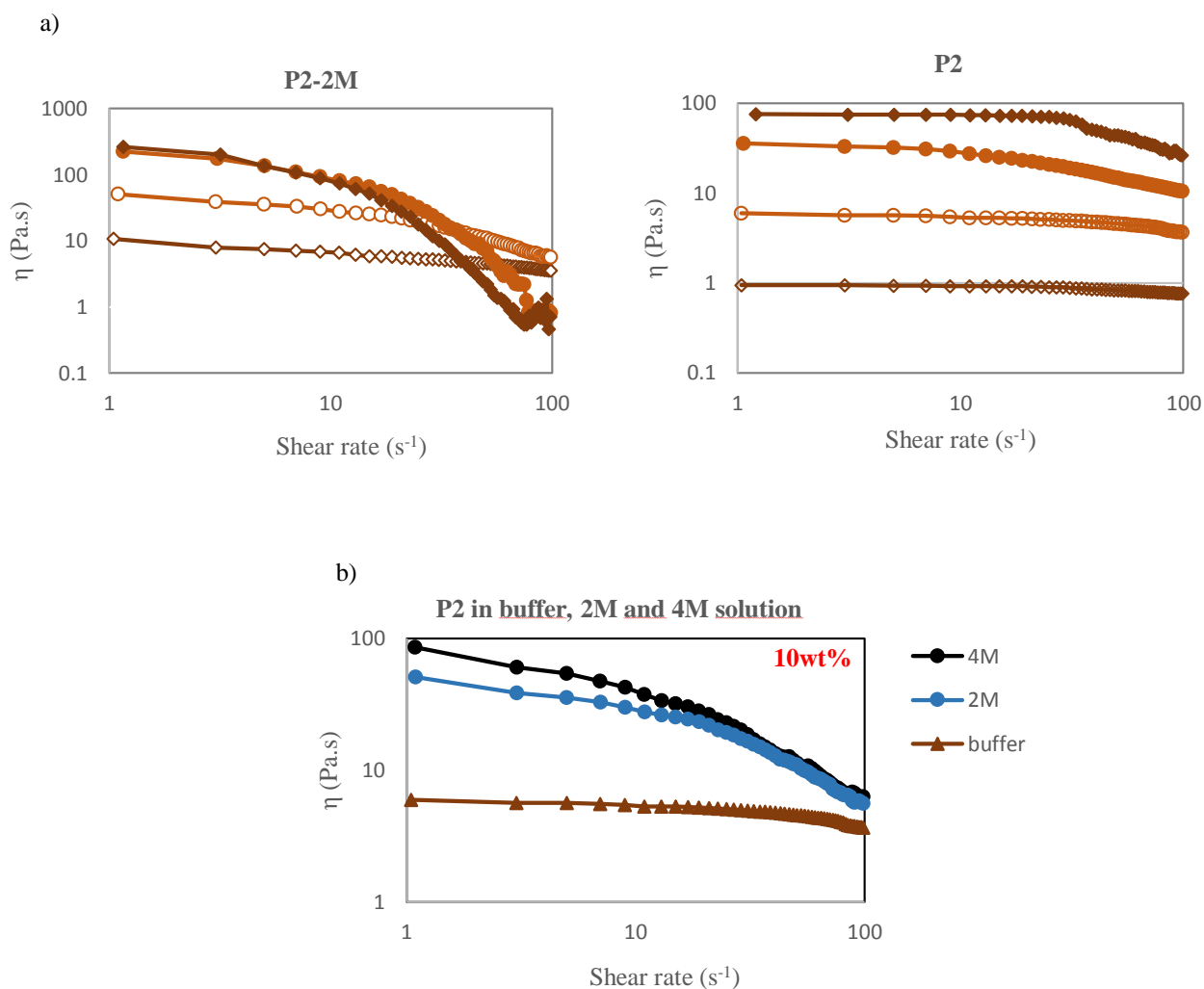


Figure 5.9. Zero shear viscosity as a function of shear rate for a) **P2** in PBS buffer compared with **P2** in 2M NaCl solution at 15% (—◆—), 12.5% (—●—), 10% (—○—), 7.5% (—◇—) (wt%), b) **P2** in PBS buffer compared with **P2** in 2M and 4M NaCl solution at 10 wt%.

The zero shear viscosity of **P2** in PBS buffer, 2 and 4 M NaCl solutions is plotted against shear rate. Comparison of the diagrams in Figure 5.9a shows the higher viscosity for **P2** in 2M

solution than **P2** in buffer solution. In Figure 5.9b the viscosity of **P2** in buffer, 2M and 4M solution at 10 wt% was compared, the result shows that the viscosity is higher at 4 M solution followed by the 2M and the buffer solution, respectively. It should be noted, that the 4M solution at a higher concentration than 10 wt% **P2** form solid-like polymer gels with infinite viscosity. Actually, the salt addition is favorable for the molecular expansion of the side chains due to the shielding of the charges of the polymers and the viscosity of the solutions enhances correspondingly (Figure 5.2).

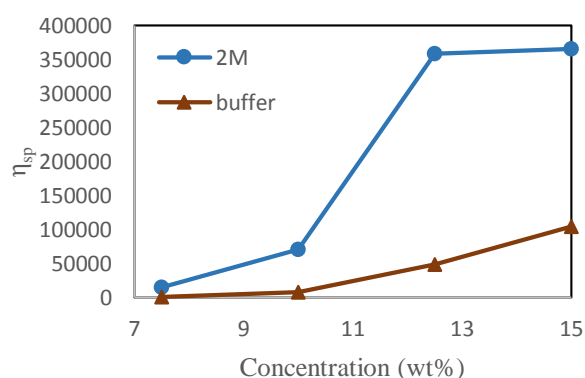


Figure 5.10. Specific viscosity at zero shear rate as a function of concentration for **P2** in buffer and 2M solution.

The influence of salt addition on the solution viscosity of zwitterionic polymers can be observed more clearly in Figure 5.10. **P2** exhibits a significant viscosity increase at 2M NaCl solution as a consequence of an extension of the polymer chains. *Che* [236] and *Chen* [237] investigated the effect of different salt concentrations on acrylamide-based hydrophobically modified copolymers containing sulfobetaine and the hydrophobic monomer SMA. They also found that the copolymers illustrate higher viscosity in NaCl solution and the viscosity of the copolymers enhances with the increase of the salt concentration.

5.3.1.2 Modulus as a function of time

The elastic and viscous moduli as a function of time at constant frequency (1Hz) and temperature (37 °C) was measured for **P2** in buffer, 2M and 4M NaCl solutions. The addition of electrolyte (NaCl) results in an increase of storage and loss modulus. A comparison between **P2** in buffer (Figure 5 .8), 2M and 4M NaCl solutions shows higher modulus for 4M followed

by 2M and buffer solutions respectively (Figure 5.11a). Additionally, it can be seen that the 4M polymer solution forms a gel ($G' > G''$) above 10 wt% (at 12 and 15 wt%) whereas in 2M NaCl solution only the 15 wt% **P2** solution displays a solid-like response and in buffer solution gel formation was observed at 25 wt%. It illustrates that in the presence of salt, solid-like behavior occurs at lower polymer concentration. This can be explained by the *anti-polyelectrolyte effect* which leads to the expansion of the copolymers side chains and consequently facilitates intermolecular aggregation. In Figure 5.11b shows the comparison of the elastic modulus (G') at 15 wt% for **P2** in three different solutions, the addition of 4M NaCl causes a significant increase of the storage modulus.

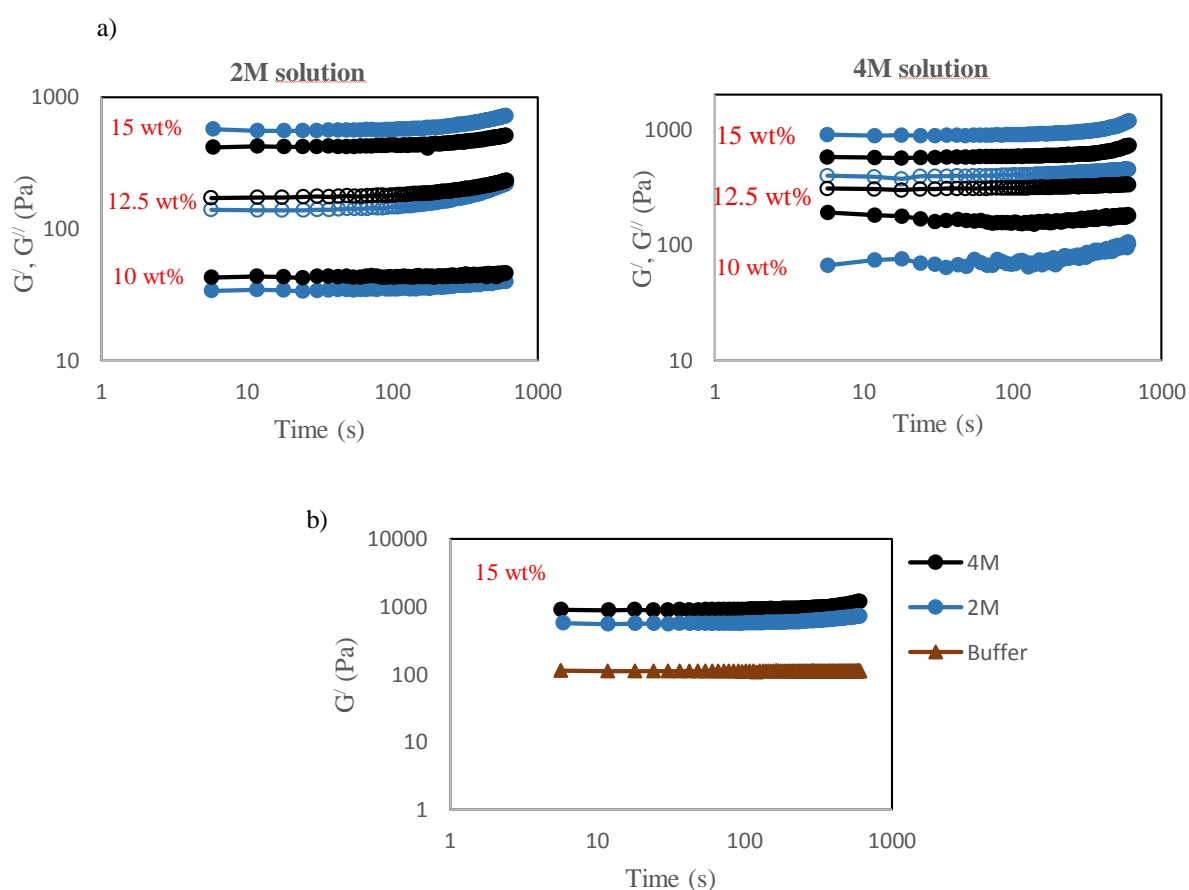


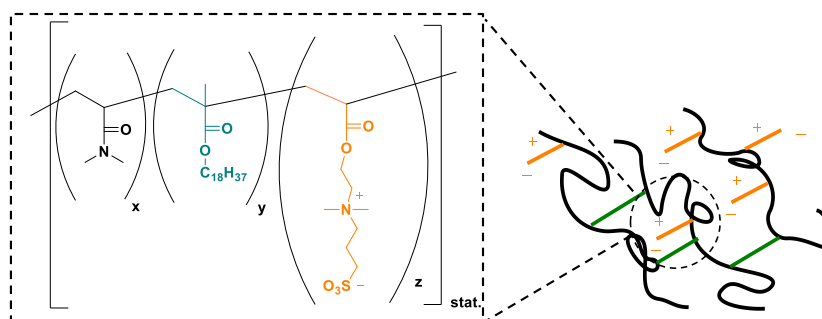
Figure 5.11. a) Elastic modulus (blue symbols) and viscous modulus (black symbols) as a function of time for **P2** in 2M and 4M NaCl solution at 10, 12.5 and 15 wt%, b) elastic modulus as a function of time for **P2** in buffer, 2M and 4M solutions.

5.4 Conclusion

Hydrophobically modified copolymer (**P2**) containing 1.25 mol% SMA functionalized with the zwitterionic MEDSAH monomer was prepared by free radical polymerization. Addition of 10 mol% zwitterionic monomer resulted in electrostatic interaction between the opposite charges and led to the expansion of the molecular side chains and thus increased the viscosity and modulus compared to its reference copolymer. The anti-polyelectrolyte behavior and noticeable increase in viscosity and modulus with the addition of salt were also detected. Consequently, a variety of rheological properties can be achieved with the incorporation of the zwitterions in a copolymer.

5.5 Experimental

5.5.1 Synthesis of zwitterionic copolymer



2-(Methacryloyloxy)ethyl dimethyl-3sulfopropyl ammonium hydroxide (MEDSAH) (10 mol %), SMA (1.25 mol%), DMA (88,75 mol%), initiator AIBN (0.01 mol/L) and methanol-toluene (70/30 vol%) with few drops of water were combined in a flask equipped with stir bar. Oxygen-free atmosphere was achieved with several freeze-pump-thaw cycles before the flask was placed into oil bath at 65 °C for 20 h. The copolymer was isolated as a white powder by precipitations in diethyl ether followed by drying in vacuum. The reaction yield was 88%. Quantitative analysis of the ¹H NMR resulted in a relatively good agreement with the monomer mixture used for the polymerization. ¹H NMR (500 MHz, D₂O, δ = 4.75): 0.79 (brs, CH₃, SMA), 0.98 (brs, -CH₃-, MEDSAH, SMA), 1.18 (brs, -CH₂-, backbone MEDSAH and SMA), 1.53 (brs, -CH₂-, backbone DMAM), 2.19 (brs, -CH₂-CH₂-N⁺-(CH₃)₂-, MEDSAH), 2.53 (brs, -CH-, backbone DMAM), 2.82 (brs, -N-(CH₃)₂, DMAEA, -CH₂-SO₃⁻, MEDSAH), 3.15 (brs,

$-\text{N}^+(\text{CH}_3)_2$, MEDSAH), 3.53, 3.71 (brs, $-\text{CH}_3)_2\text{-N}^+$, MEDSAH), 4.30 (brs, $-\text{CH}_2\text{-O-C=O}$, MEDSAH). SEC in DMF was applied to calculate molecular weight ($M_n = 23888 \text{ g mol}^{-1}$) with dispersity ($\mathcal{D} = 2.58$).

Chapter 6. Synthesis and Rheological Characterization of Cationic, Hydrophobically Modified Copolymers containing Peptide moieties in the side chain

6.1 Introduction

Today there are a large number of synthetic polymeric compounds accessible for medical application with adequate mechanical stability and elasticity as well as favorable stability concerning degradation and nontoxicity. However, one of the most important problem remains the insufficient interaction between polymers and cells, causing *in vivo* foreign body reactions which can lead to inflammation, implant encapsulation, local tissue waste, thrombosis and embolization [238]. Hence, controlled interactions between cells and synthetic materials can be achieved by immobilizing cell recognition motifs to the polymeric substrates. The initial interaction between cells and biomaterials is shown in Figure 6.1. Chemical composition, surface energy, stiffness, roughness and biomaterial surface topography are the factors which control cell-biomaterial interactions [239]. RGD peptides are known to promote cell adhesion via specific RGD-integrin interaction, in addition, these interactions have shown to evoke also certain cell responses [240].

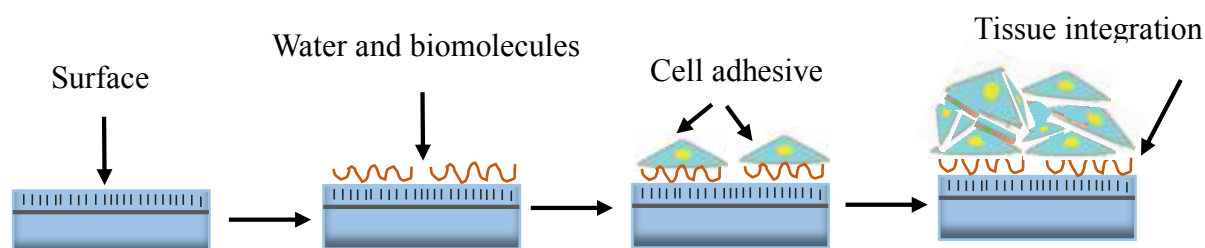


Figure 6.1. The surface properties of biomaterials control the interaction of cells with biomaterials [241].

Schaffer and coworkers [242] engineered an interpenetrating polymer network (IPN) (from acrylamide (AAm), poly(ethylene glycol) 1000 monomethyl ether monomethacrylate (pEG 1000MA), and acrylic acid (AAc) which was modified with the RGD or the laminin derived peptide motif IKVAV to regulate the behavior of adult neural stem cells (aNSCs) (Figure 6.2). They could show, that peptide-modified IPN can control adult NSCs self-renewal and differentiation while the IKVAV-functionalized IPN had only a modest influence on NSCs

differentiation. They also studied the effect of stiffness on cell behavior [243]. IPNs with variable moduli (vmIPN) were synthesized in order to control the modulus within a range of 10-100,000 Pa. The results demonstrated that the self-renewal and differentiation of aNSCs can occur on RGD peptide modified vmIPN with an elastic modulus of at least 100 Pa.

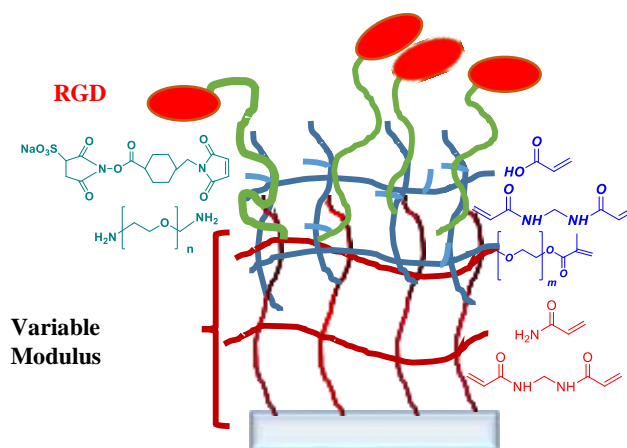


Figure 6.2. The vmIPN structure with monomers used for sequential polymerization [243] .

Missirlis and coworkers [244] prepared poly(ethylene glycol) based hydrogels functionalized with RGD peptide and other ECM proteins. They showed that the cell behavior can be controlled by hydrogel elasticity and biochemical properties. Physically crosslinked polymers based on peptides have also attracted much attention and rheological measurements were considered to be an important tool to gain more information about the flow and viscoelastic properties of peptide-based hydrogels [245]. In the following chapter, a hydrophobically modified DMAM copolymer containing a RGD peptide functionalized comonomer as the most widely applied synthetic binding motif with the ability to enhance cell adhesion efficiently [135], was synthesized and its solution properties characterized and compared to previous reported copolymers in this thesis.

6.2 Results and discussion

A random copolymer composed of DMAM with 1.25 mol% SMA functionalized by grafting peptide Phe-Ser-**Asp-Gly-Arg**-Gly-6Ahx-6Ahx with the bioactive sequence Arg-Gly-Asp (RGD) was prepared via free radical polymerization.

The peptide monomer (Figure 6.3) was synthesized on a 2-CLtrt resin. After the resin was swollen in toluene with distilled acetyl chloride (1ml/g resin) at 60 °C for 3 h, the amino acid

sequence was coupled stepwise according to the general principle of solid-phase peptide synthesis with repeated cycles of deprotection-washing-coupling-washing by using piperidine in DMF (1:4) to deprotect the Fmoc group and HBTU/HOBT for the activation/coupling reaction with the next Fmoc-protected amino acid. To obtain the peptide monomer methacryloyl chloride was added to the amino terminus of the peptide. The cleavage step was done with a mixture of 95% TFA, 2.5% triisopropylsilane and 2.5% water for 3.5 h at room temperature. The obtained peptide solution was precipitated in cold diethyl ether. The crude product was separated by centrifugation and purified by HPLC. The peptide monomer composition was verified by ^1H NMR and mass spectrometer.

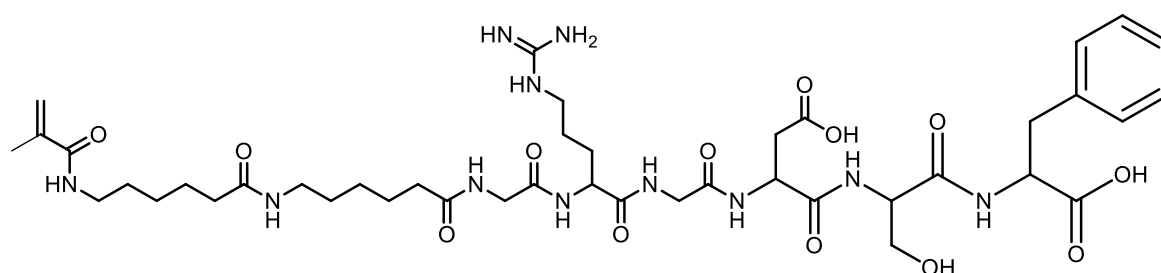


Figure 6.3. Peptide monomer structure.

Free radical polymerization was carried out in a solvent mixture of toluene and methanol (20/80) with AIBN as an initiator. To remove any dissolved oxygen, the freeze-pump-thaw cycle was carried out before starting the reaction at 65 °C for 20 h. The obtained copolymer was dissolved in water and after dialysis for 72 h, the water was removed by freeze-drying. The peptide modified copolymer was characterized by ^1H NMR and GPC. (Figure 6.4)

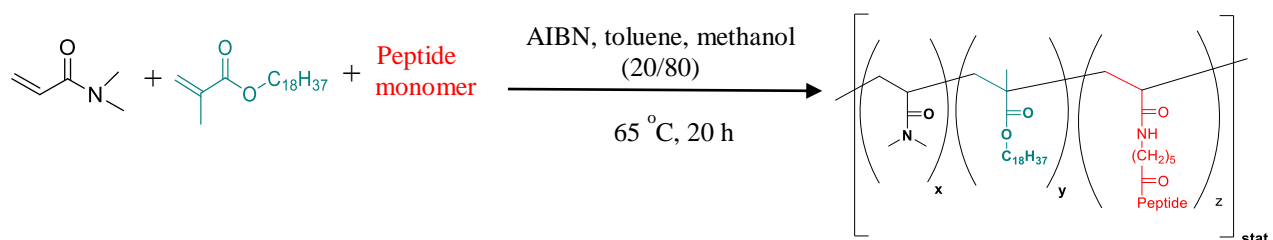


Figure 6.4. Synthesis route of copolymer containing peptide.

Table 6.1. Characterization data of copolymer containing peptide.

Sample ^a	Copolymer composition (mol%) (DMAM: SMA: Peptide) ^{a,b}	M _n (g/mol) ^c	Đ ^c	Yield (%)
Peptide-based polymer	97.51 (97.75): 1.58 (1.25): 1 (0.91)	28650	2.55	86

^{a)} The copolymer has been prepared by free radical polymerization with 0.1 mol/L AIBN at T= 65 °C for 20 h, ^{b)} copolymer composition was determined by ¹H NMR, in brackets: theoretical values; DMAM (*N,N'*-dimethyl acrylamide), SMA (stearyl methacrylate), ^{c)} determined by SEC in DMF with 5 g L⁻¹ LiCl, T= 60 °C.

The copolymer characterization data are presented in Table 6.1. The incorporation of peptide monomer into the polymer backbone can be verified in ¹H NMR with the aromatic moiety related to the phenylalanine amino acid. Figure 6.5 presents the ¹H NMR spectrum of copolymer containing peptide, the aliphatic signals 1 and 2 can be assigned to -CH₂- and CH- groups of polymer backbone whereas signal 4 corresponds to the aromatic protons of the peptide monomer.

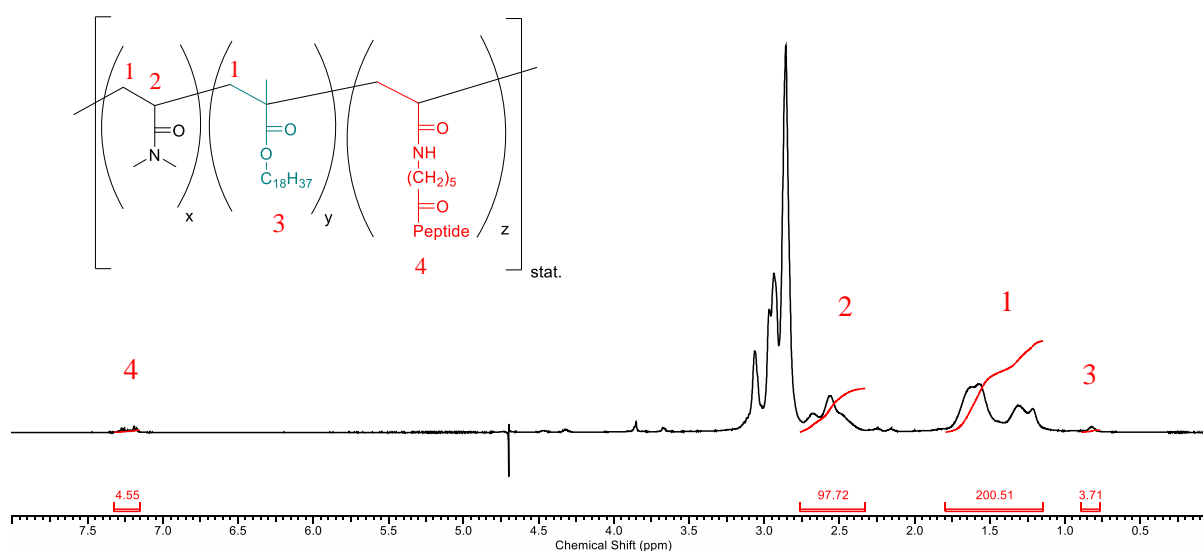


Figure 6.5. ¹H NMR spectrum of peptide copolymer (in D₂O).

In order to study the solubility of the copolymer, the samples were prepared in a screw-capped vial in the concentration range from 1 to 25 wt% in PBS buffer solution. The samples were kept at room temperature without stirring and heating. After 48 h polymer solutions up to 5 wt% were soluble. Therefore, the samples were heated to 100 °C and allowed to cool to room

temperature, however, there was no improvement in the copolymer solubility for the higher copolymer concentrations.

6.2.1. Copolymer containing peptide and cationic functional groups (P3)

As has been discussed before the incorporation of 1 mol% peptide in the hydrophobically modified copolymer resulted in a strong reduction of the solubility. One way to improve water-solubility can be the addition of a cationic monomer to the copolymer. **P3** was synthesized like the previous work but only methacryloyloxyethyl trimethyl ammonium chloride (MADQUAT) (10 mol%) was used as a cationic comonomer in addition to 1.25 mol% SMA with two different amounts of peptide monomer, **P3-1**, **P3-2** containing 1 and 2 mol% peptide monomer respectively. Copolymers characterization are listed in Table 6.2.

Table 6.2. Analytical data of **P3-1** and **P3-2**.

Samples	Copolymer composition (mol%) (DMAM: SMA: MADQUAT: Peptide) ^{a,b)}	M _n (g/mol) ^{c)}	Đ ^{c)}	Yield (%)
P3-1	86.7(87.75): 2.07(1.25): 10.24(10): 0.99(1)	23820	2.19	81
P3-2	82.87(86.75): 1.8(1.25): 13.66(10): 1.67(2)	32590	2.79	79

^{a)} The polymerizations were carried out with 0.01 mol/L AIBN; at T= 65 °C for 20 h, ^{b)} copolymer composition was determined by ¹H NMR spectroscopy, in brackets: theoretical values; DMAM (*N,N'*-dimethyl acrylamide), SMA (stearyl methacrylate), MADQUAT (methacryloyloxyethyl trimethyl ammonium chloride), ^{c)} determined by SEC in DMF with 5 g L⁻¹ LiCl, T= 60 °C.

The copolymers **P3-1** and **P3-2** were dialyzed in water for 72 h and the water was removed by freeze-drying before characterization. Figure 6.6 shows the ¹H NMR spectra for **P3-1** and **P3-2**, the signals for peptide and the cationic residues can be clearly assigned. The aliphatic signals from the backbone as well as the quaternary ammonium (8) and methylene groups (6, 7) correspond to the MADQUAT group with aromatic protons corresponding to the peptide residue (9), verifying the copolymers structure. The analysis of the copolymer composition of **P3-1** and **P3-2** by ¹H NMR is in good agreement with the monomer mixtures used for both polymerizations.

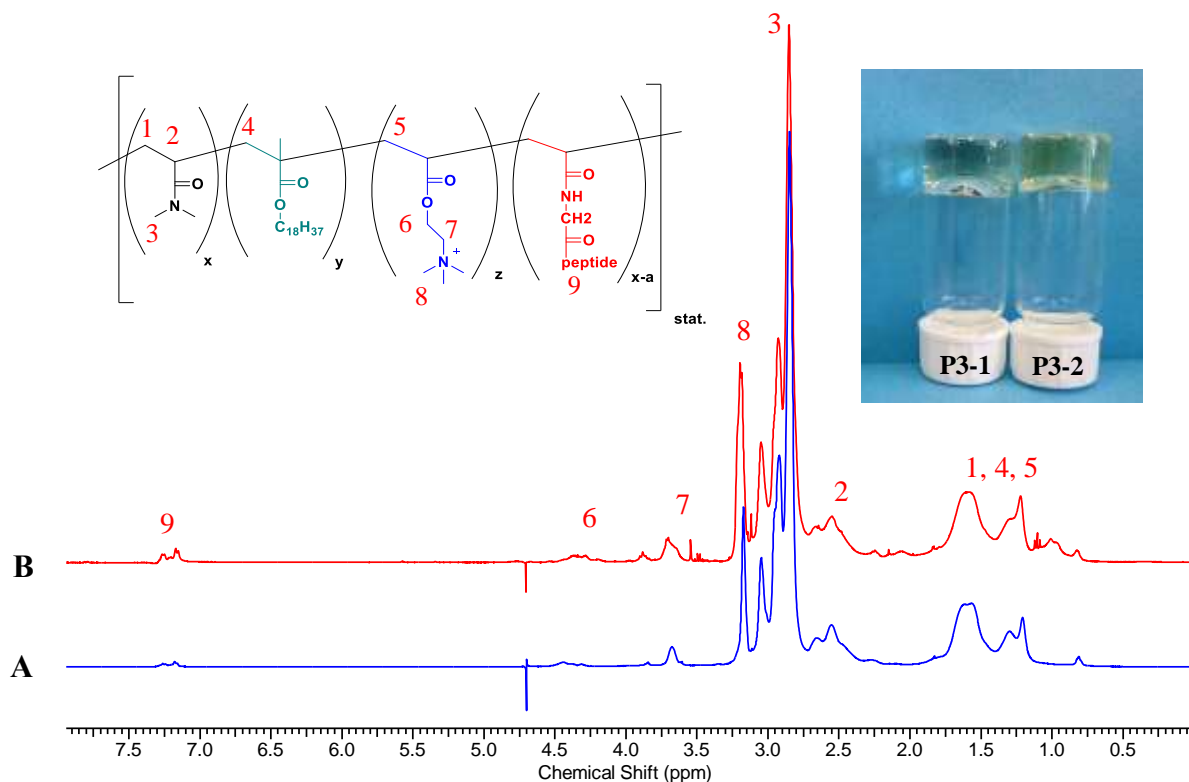


Figure 6.6. ^1H NMR spectrum of (A) **P3-1** and (B) **P3-2** recorded (in D_2O).

6.2.2 Rheological Study

The rheological studies for **P3-1** and **P3-2** were performed at three different concentrations (10, 15 and 20 wt%). The solutions were directly prepared in a screw-capped vial and the samples were kept at room temperature without stirring for 48 h to dissolve the copolymers. For preparing the gels for rheology measurements, the copolymer solutions were heated to 100 °C and cooled down and the copolymer rheology was measured by oscillatory rheometry with a 150 mm cone plate at 37 °C.

6.2.2.1 Viscosity as a function of shear rate

Figure 6.7 shows the zero shear viscosity data obtained for **P3-1** and **P3-2** at three different concentrations (10, 15, 20 wt%). Both copolymers show increasing viscosities with increasing polymer concentration. Additionally, it was observed that an increase in peptide content resulted in an increased viscosity at a given shear rate. In Figure 6.8 the viscosity as a function of shear rate is compared between **P_{ref}SMA1.25**, **P1SMA1.25**, **P2**, **P3-1** and **P3-2** at 20 wt%. The results suggest that the incorporation of 1 mol% peptide with 10 mol% cationic moiety caused a viscosity reduction compared to **P_{ref}SMA1.25** while the addition of 2 mol% peptide

increased the viscosity even higher than the reference copolymer. The results also show clearly a significant difference between the cationic copolymers **P1SMA1.25** and other copolymers. Moreover, the highest viscosity was obtained for the zwitterionic copolymer (**P2**) in this concentrated regime. Such a high value displays the effect of coil expansion in **P2** due to the repulsion between ionic groups.

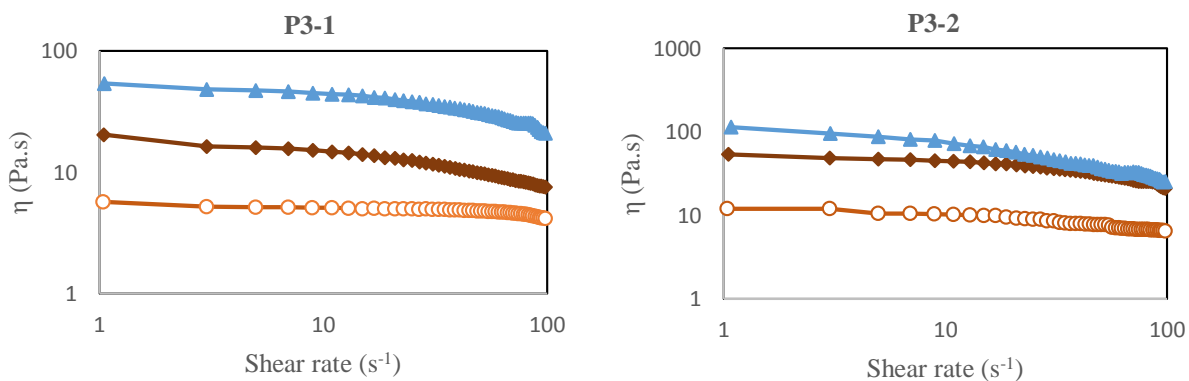


Figure 6.7. The viscosity as a function of shear rate for **P3-1** and **P3-2** in 20 (—▲—), 15 (—◆—) and 10 (—○—) wt%.

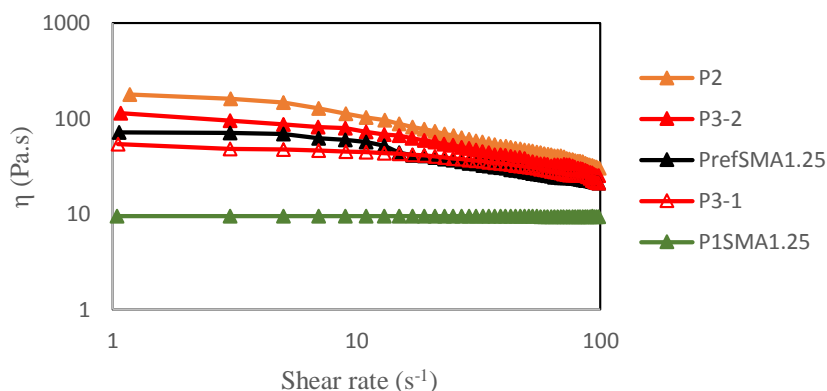


Figure 6.8. Viscosity as a function of shear rate for **P1SMA1.25**, **P_{ref}SMA1.25**, **P2**, **P3-1** and **P3-2** at 20 wt%.

6.2.2.2 Complex modulus

The variation of the storage (G') and loss (G'') modulus as a function of frequency is illustrated for **P3-1** and **P3-2** in Figure 6.9. The comparison of the linear viscoelastic data in both cases

show that the frequency dependence of the shear moduli corresponds to a typical viscoelastic fluid in which G' exceeds G'' above a certain frequency which corresponds to the relaxation time of the chains in an associative polymer. Compared to **P_{ref}SMA1.25**, **P1SMA1.25** and **P2** (Figure 5.7) a similar trend in behavior was observed in all copolymers.

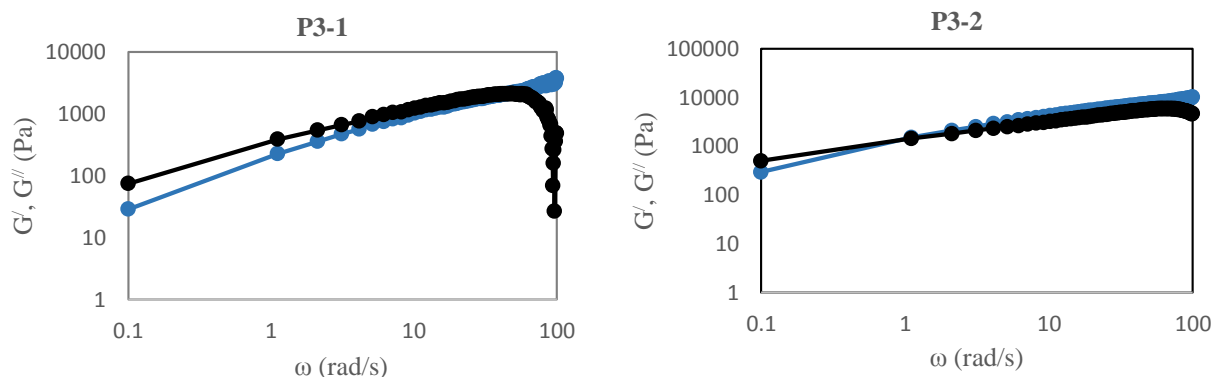


Figure 6.9. Elastic modulus (—●—) and viscous modulus (—●—) as a function of frequency for **P3-1** and **P3-2** at 20 wt%.

In Figure 6.10 the storage and loss moduli are illustrated as a function of time at a frequency of 1 Hz at 20 wt%. As can be seen, a liquid-like response was observed for both copolymers. In both cases, the loss modulus is higher than the storage modulus over the entire frequency range investigated. The obtained results demonstrate a liquid-like behavior in both samples similar to **P_{ref}SMA1.25**, **P1SMA1.25** and **P2**.

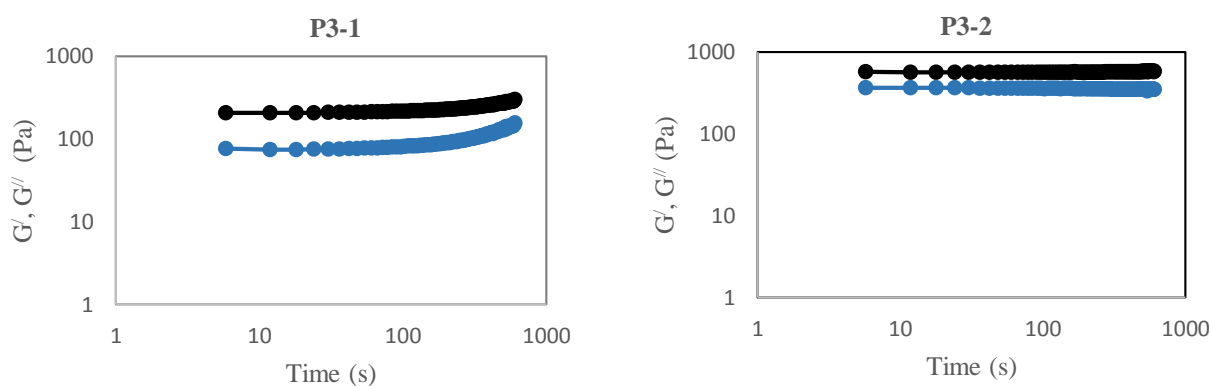


Figure 6.10. Elastic modulus (—●—) and viscous modulus (—●—) as a function of time at 20 wt%.

6.3 Conclusion

DMAM-based associating polymer containing 1.25 mol% SMA functionalized with 2 mol% peptide monomer was prepared by free radical polymerization in a non-blocky fashion. The solubility study indicated that the copolymer can be dissolved in aqueous PBS buffer only up to 5 wt%. In order to increase the solubility of the copolymer, a cationic monomer was incorporated into the copolymer backbone. Thus, two peptide-functionalized, cationic copolymers with 1 (**P3-1**) or 2 mol% peptide (**P3-2**) and 10 mol% cationic MADQUAT monomer were synthesized. Furthermore, the influence of the incorporation of 1 and 2 mol% peptide on the rheological properties was studied. The results show a higher viscosity for **P3-2** compared to **P3-1**. A comparison between the viscosity of **P3-1** and **P3-2** with **P_{ref}SMA1.25** displays a higher viscosity for **P3-2** following **P_{ref}SMA1.25** and **P3-1** respectively. Although **P3-2** shows a higher elastic (G') and viscous (G'') modulus, both copolymers show viscous dominated response ($G'' > G'$).

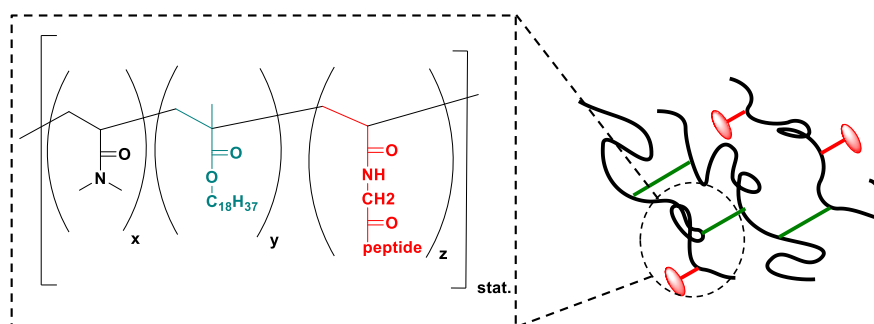
6.7 Experimental

6.7.1 Peptide monomer synthesis

RGD peptide monomer with sequence of Phe-Ser-Asp-Gly-Arg-Gly-6Ahx-6Ahx and theoretical mass of 932 was prepared by standard Fmoc chemistry procedure in a solid-phase peptide synthesis vessel. The peptide was synthesized on 1 g 2-ClTrt resin. The resin was swollen in toluene with distilled acetyl chloride (1 ml/g resin), the reaction was allowed to stay at 60 °C for 3 h. Upon completion, the reaction was cooled down to reach room temperature again and the resin was subsequently washed with DCM (6 x times). Fmoc-protected phenylalanine (1.6 mmol) was used as first amino acid, followed by solving in dry DMF (in the minimum amount of DMF necessary) and DIPEA (3.2 mmol) prior to adding to the resin. The solution mixture was stirred over night at RT, then the solution filtered and washed with DCM/MeOH/DIPEA (17:2:1, 3 x 20 ml) and DMF (3 x 10 ml). For coupling with next amino acid, the resin was treated with 40% (v/v) piperidine in DMF to remove the Fmoc group and the resin was washed with DMF (6 x 5 ml). Coupling of the next amino acid (serin, 1,87 mmol) was performed for at least 1h with a mixture of HBTU (2.51 mmol) and HOBt (2.33 mmol) in DMF (in the minimum amount of DMF necessary) and DIPEA (11.04 mmol) in NMP (8.82 ml) and deprotection was done as described above. The same coupling and deprotection method like serin was applied for Asp-Gly-Arg-Gly-6Ahx-6Ahx (1.87 mmol) amino acids. After the

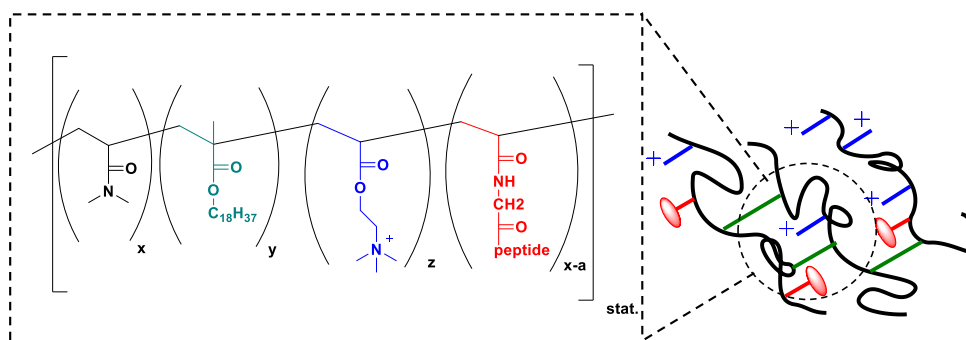
final deprotection, DIPEA (2 mmol) with dry and cold DMF (20 ml) was added to the peptide under argon atmosphere. Methacryloyl chloride (1 mmol) in cold and dry DMF (10 ml) was added dropwise to the peptide mixture. A cleavage cocktail mixture of 95% TFA, 2.5 % TIS and 2.5 % deionized water for 3.5 h at RT (room temperature) was utilized for cleavage of the peptide from the resin, followed by filtration. In the last step, the peptide was cleaved from the resin and precipitated in cold diethylether, resolubilized in deionized water and dried with freeze drying. The crude peptide was purified by high performance liquid chromatography (HPLC) using water/acetonitrile (50/50 v/v) co-solvent. The purified peptide monomer was freeze-dried for future use. The aromatic ring of phenylalanine was considered in order to confirm the incorporation of peptide to the copolymers. In addition to ^1H NMR (Figure 11.1), peptide monomer was verified by mass spectrometry (Figure 11.2).

6.7.2 Copolymer containing peptide



The copolymer was prepared by free radical polymerization in methanol-toluene (80/20 v/v) in a Schlenk flask with freeze- pump-thaw cycles to obtain dry atmosphere at room temperature. DMAM, SMA (1.25 mol%), peptide monomer (2 mol%) and 0.01 mol/L AIBN were added to the flask to 1 M solution. The reaction carried out at 64 $^{\circ}\text{C}$ for 20 h. The target copolymer cooled to room temperature before precipitation in cold diethyl ether. The copolymer was purified by dialysis against deionized water for at least 72 h and a yellow powder obtained after freeze drying. The reaction yield was 86%. Quantitative analysis of the ^1H NMR was in good agreement with the monomer mixture used for the polymerization. SEC in DMF was applied to determine the molecular weight ($M_n = 28656 \text{ g mol}^{-1}$) and its dispersity ($\mathcal{D} = 2.55$).

6.7.3 Cationic copolymer containing peptide



P3-1 and **P3-2** were synthesized as described above with the addition of 10 mol% MADQUAT as a cationic comonomer. Therefore, **P3-1** is containing DMAM, 1 mol% peptide, 1.25 mol% SMA and 10 mol% MADQUAT, the only difference for **P3-2** is related to 2 mol% peptide monomer. The copolymers were characterized after being purification by dialysis and freeze dried. The reaction yield was 81% and 79% for **P3-1** and **P3-2**, respectively. Quantitative analysis of the ^1H NMR was in good agreement with the monomer mixture used for the polymerization. ^1H NMR (500 MHz, D_2O , $\delta = 4.75$): 0.81 (brs, CH_3 , SMA), 1.21, 1.57 (brs, $-\text{CH}_2-$, backbone, DMAM, SMA, MADQUAT), 2.55 (brs, $-\text{CH}-$, backbone, DMAM), 2.85 (brs, $-\text{N}-(\text{CH}_3)_2$, DMAM), 3.17 (brs, $-\text{N}^+(\text{CH}_3)_3$, MADQUAT), 3.68 (brs, $-\text{CH}_2-\text{N}^+(\text{CH}_3)_3$, MADQUAT), 4.47 (brs, $-\text{CH}_2-\text{O}-\text{C}=\text{O}$, MADQUAT), 7.18 (brs, aromatic protons of peptide residue). SEC in DMF gave molecular weights of (**P3-1**, $M_n = 23820$ and **P3-2**, $M_n = 32589$ g mol^{-1}) with dispersities of (**P3-1**, $\text{Đ} = 2.19$ and **P3-2** $\text{Đ} = 2.79$).

Chapter 7. Synthesis and Characterization of Hydrophobically Modified Polymers Based on Fatty Acid monomers

7.1 Introduction

Growing awareness and environmental concerns, along with the dwindling of crude oil reserves (according to predict of Energy Information Administration's 2016 report the global energy consumption will enhance by 48% in 2012-2020) [246] and the increasing cost of petroleum derived chemical commodities have sparked the interest of many researchers to think about a new alternative pathways for materials based on renewable resources [247,248]. Fatty acids (FA) and their derivatives are advantageous in this regard due to their renewability, availability in large quantities, biocompatibility and relative low cost which are the reasons why they find many applications in diverse field [249].

Depending on the degree of saturation/unsaturation of the carbon chain, FA can be classified in: saturated fatty acids (SFA), without any double bond and unsaturated fatty acids (USFA) which bear double or triple bonds. Additionally, USFA can also be divided into monounsaturated fatty acids (MUSFA) if only one double bond is present and polyunsaturated fatty acids (PUSFA) with two or more double bonds.

The incorporation of renewable resources like FA in the polymer chain allows to design bio-based polymers with widespread applications, but one limitation is that the rather low reactivity of their unsaturated aliphatic chains make them not very useful for further chemical modification. This problem can be solved by functionalization with polymerizable moieties. For example, *La Scala and coworkers* [250] used methacrylate to make a fatty acid based monomer, which can be applied as styrene replacement in vinyl ester resins leading to lower viscosity, volatility and costs. Other studies have also been worked on the functionalization of FA by addition of vinylic, acrylic and styrenic groups [251], generally involving esterification reaction. Moreover, introduction of fatty acids into the polymer chain leads to better compound properties such as low melting point, improved handling, flexibility, with providing a better release profile and degradation compares to the simple physical mixture of polymers with fatty acid [252]. For example, a series of fatty acid functionalized norbornenes were prepared by the ring-opening metathesis polymerization (ROMP) with potential to control the thermal property by changing the chain length of the fatty acid [249]. The objective of this chapter is to prepare hydrophobically modified polymers via mono and polyunsaturated fatty acids to combine the

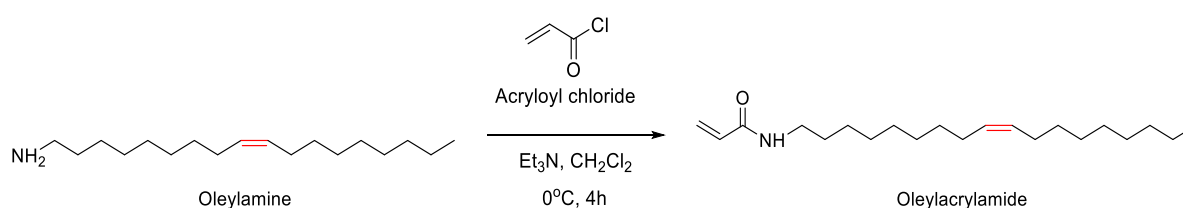
properties of long alkyl chains with the flexibility and functionality of fatty acids. Additionally, the copolymer containing polyunsaturated double bonds has the potential to change from a viscoelastic physically crosslinked hydrogel to an elastic chemically crosslinked one for providing a model to better understand *in vivo* cellular processes, such as the irreversible cross-linking that occurs during aging and diabetes [253].

7.2 Results and Discussion

This chapter focuses on the synthesis and characterization of hydrophobically modified polymers based on fatty acids, using oleic acid (*cis*-9-octadecenoic acid) and linoleic acids (*cis*, *cis*-9,12-octadecadienoic acid). A comparison of the rheology between copolymers made from oleic and linoleic acid and those containing the saturated SMA side chains was done to assess how and to what extent the presence of the double bond affects the gel forming properties in aqueous medium.

7.2.1 Synthesis of oleyl acrylamide copolymer (POA)

This section elaborates the experimental results obtained for the synthesis of the precursor monomer, oleyl acrylamide (OA). The reaction involves a nucleophilic reaction of the oleylamine with acryloyl chloride and formation of the desired oleyl acrylamide. This reaction is shown in the following scheme.



Scheme 7.1. Synthesis of the oleyl acrylamide (OA) monomer.

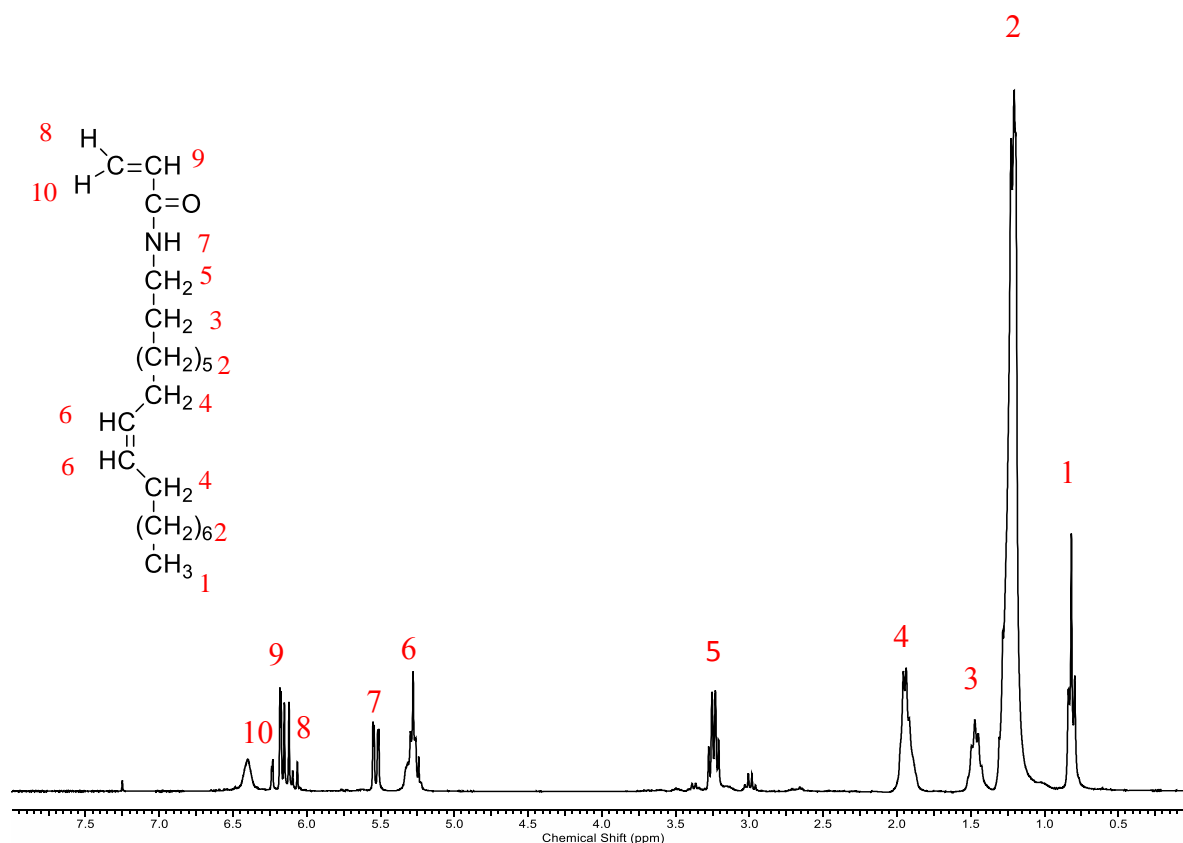


Figure 7.1. ¹H NMR spectrum of oleylacrylamide monomer (CDCl₃).

As can be seen from the ¹H NMR spectrum (Figure 7.1), successful synthesis was achieved with a yield of 86%. The signals corresponding to the double bond appear between 5.0-5.5 ppm and those from the remaining functional groups can be easily identified and are in agreement with the results from *Shiono and coworkers* [254].

With the aim of studying hydrophobically modified polymers using fatty acid monomers with unsaturated bonds in the side chain, a copolymer **POA** consisting of dimethylacrylamide and oleyl acrylamide was synthesized. For this purpose, three varying copolymer compositions using 1.25 mol% (**POA1.25**), 2.5 mol% (**POA2.5**) and 3.75 mol% (**POA3.75**) of oleyl acrylamide were synthesized. The polymerizations were initiated by AIBN and proceeded in degassed toluene at 65 °C for 20 hours. The copolymers were then obtained by precipitation in diethyl ether. The copolymers were characterized by ¹H NMR and SEC measurements.

The molecular weight and dispersity of the copolymers was determined by size exclusion chromatography (SEC) in DMF. The analytical data are listed in Table 7.1.

Table 7.1. Analytical data of the oleyl acrylamide (OA) containing copolymers.

Samples	Copolymer composition (mol%) (DMAM: OA) ^{a,b)}	M _n (g/mol) ^{c)}	D ^{c)}	Yield (%)
POA1.25	98.43 (98.75):1.57 (1.25)	35900	2.77	81
POA2.5	97.05 (97.5): 2.95 (2.5)	32940	2.81	78
POA3.75	96.62 (96.25): 3.38 (3.75)	42800	2.99	73

^{a)} The polymerizations were carried out with 0.01 mol/L AIBN; at T= 65 °C for 20 h, ^{b)} copolymer composition was determined by ¹H NMR spectroscopy, in brackets: theoretical values, DMAM (*N,N'*-dimethyl acrylamide), ^{c)} determined by SEC in DMF with 5 g L⁻¹ LiCl, T= 60 °C.

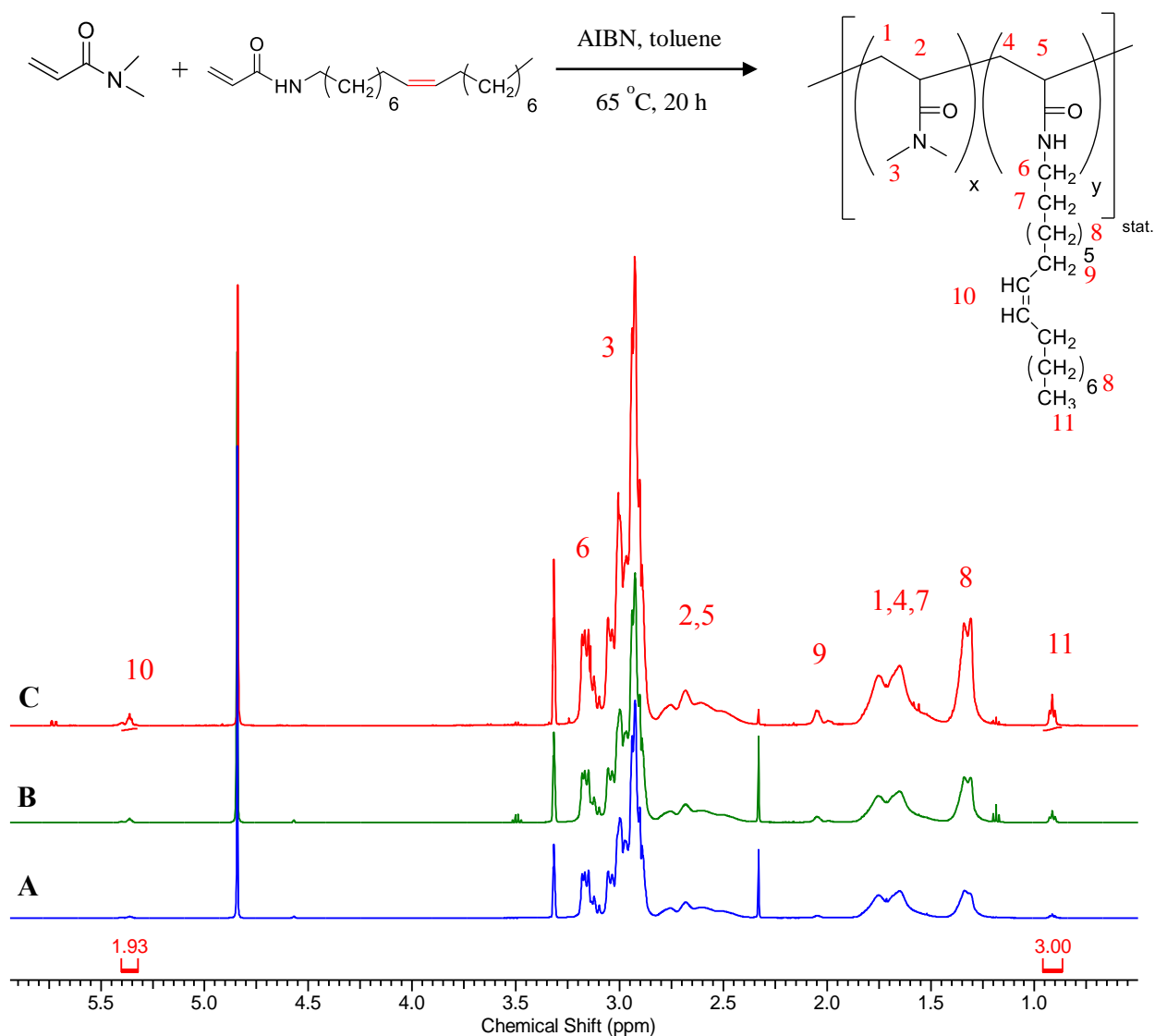


Figure 7.2. ¹H NMR spectra of A) POA1.25, B) POA2.5 and C) POA3.75 (in MeOD).

^1H NMR spectroscopy (Figure 7.2) reveals that the copolymerization was successful with the OA double bond peak appearing between 5.0-5.5 ppm. This peak becomes significantly larger as the amount of OA in the copolymer is increased, whereas those corresponding to the remaining functional groups are in agreement with the expected chemical shifts.

7.2.2 Rheological Study

In order to distinguish the effect of the presence of the double bond in the copolymer side chain, a comparison of the rheological properties of the copolymer containing oleyl acrylamide was made with those copolymers with stearyl methacrylate (SMA) side chains, that contain also 18 carbon atoms in the side chain, however, as a saturated chain.

The aqueous PBS-buffer solutions of the copolymers were prepared in a screw-capped vial at varying concentration of 10, 12.5 and 15 wt%.

7.2.2.1 Viscosity Measurements

In Figure 7.3a the viscosity of the copolymers consisting of 1.25 and 2.5 mol% oleyl acrylamide at 37 °C at varying shear rates are shown. It is apparent that the viscosity increases with increasing the concentration for both copolymers, but a comparison between the viscosities reveals a rather drastic difference. For each sample there is an almost twenty fold increase in the viscosity; for example, at 10 wt% the initial value jumps from approximately 0.5 (**POA1.25**) to 9 (**POA2.5**) Pa.s. For the next concentration (12.5 wt%), it changes from approximately 1.05 to between 25-30 Pa.s and the same observation is made for the final concentration with a change from about 3 to 80-90 Pas.

Figure 7.3b elucidates the effect of the copolymer composition on solution properties. Viscosity enhances with increasing OA content. A comparison of shear viscosity between the copolymers at 10 wt% shows a significant viscosity increase from approximately 0.5 for **POA1.25** to around 230 Pa.s for **POA3.75**. The copolymer viscosity is made through transient oleyl acrylamide side chain association. **POA3.75** consisting of 12.5 and 15 wt% form hydrogels, therefore the shear viscosity measurements were not performed for these two samples.

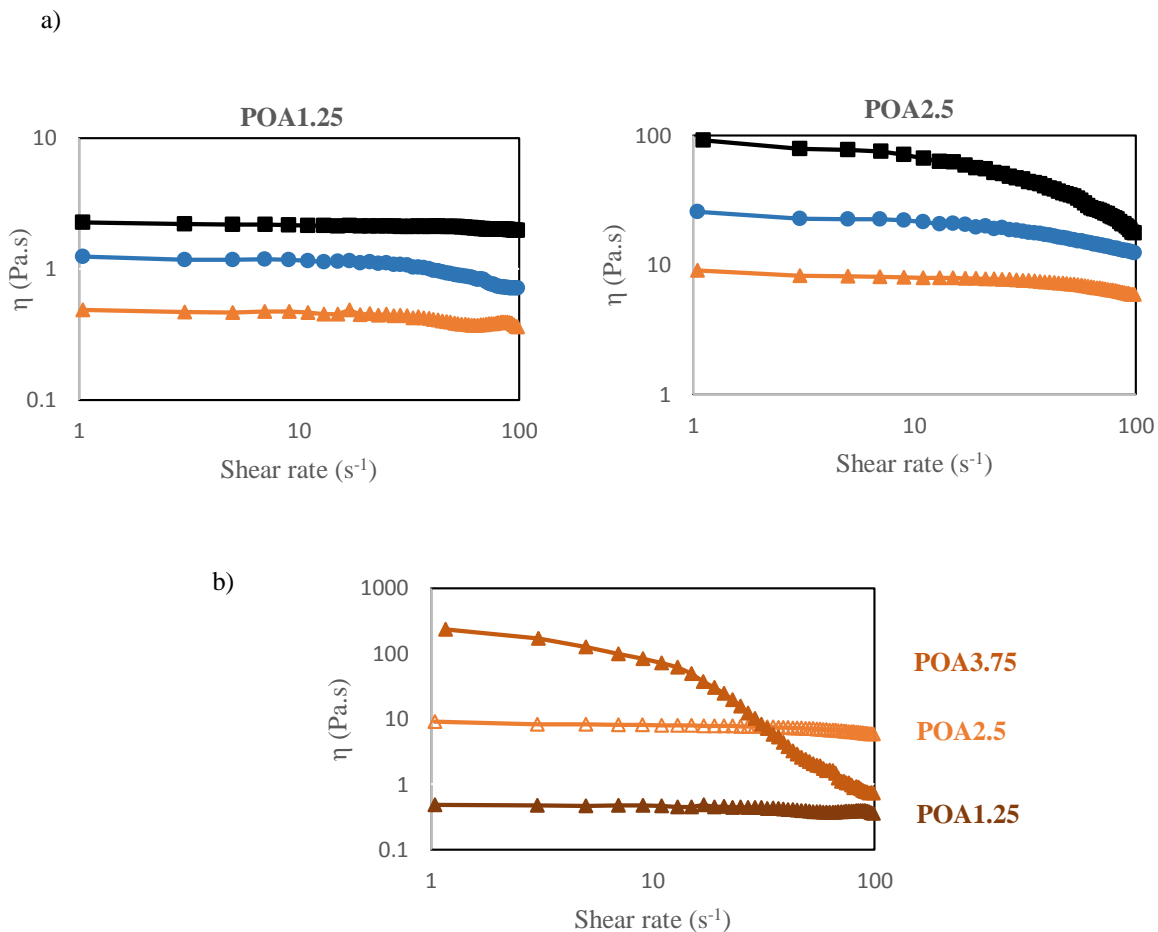


Figure 7.3. Copolymer viscosity as a function of shear rate a) at various concentration of 15 (—■—), 12.5 (—●—) and 10 (—▲—) wt% for **POA1.25** and **POA2.5**; b) for **POA1.25**, **POA2.5** and **POA3.75** at 10 wt%.

The copolymer viscosity change was also visually assessable as can be seen through the decrease in fluidity of the solutions in Figure 7.4 (based on the solution consisting of 15 wt%) and leads to the conclusion that an increasing amount of oleyl acrylamide in the copolymers results in an increase in the viscosity of the resulting copolymers solution.



Figure 7.4. Visual inspection for **POA1.25** and **POA3.75** at 15 wt%.

As can be seen from Figure 7.5, the viscosity of the copolymers comprising OA is significantly lower compared to those copolymers with SMA as the comonomer. The values for OA remain well below 10 Pa.s with relatively larger jumps in the viscosity as the polymer concentration in the sample is increased, however, the values are clearly lower than their reference analogue with a saturated C18-alkyl chain. This change in properties can be attributed to the presence of the double bond. The stearyl side chain of **P_{ref}SMA1.25** can crystallize, while the oleyl pendant group of **POA1.25** cannot because of the cis double bond in the alkyl sequence.

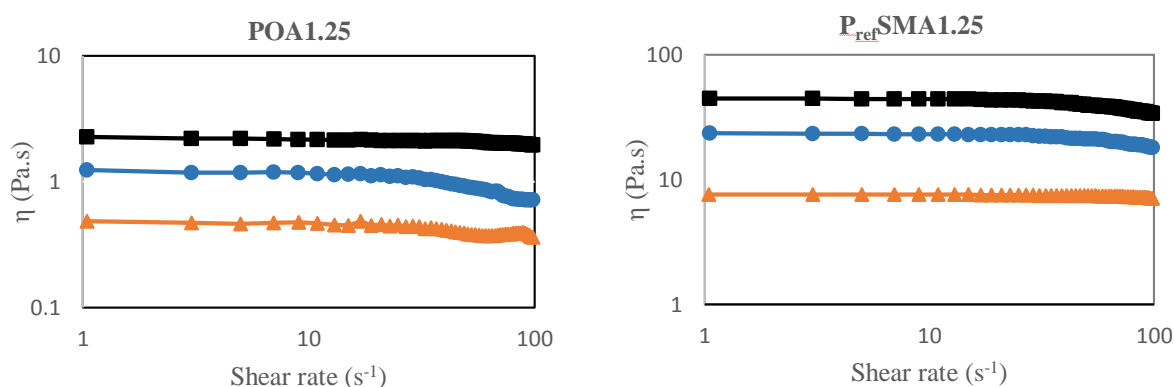


Figure 7.5. **POA1.25** and **P_{ref}SMA1.25** viscosities at various concentration of 15 (—■—), 12.5 (—●—) and 10 (—▲—) wt% and various shear rates.

7.2.2.2 Modulus as a function of frequency

In this part the effect of oleyl acrylamide content and chain regularities were examined in order to depict the effect of molecular architecture on crystalline structure and consequently on the stiffness by performing dynamic rheological measurements for the copolymers. The results are shown in Figure 7.6 for **POA2.5**, **POA3.75** and **P_{ref}SMA2.5** at 15 wt%. The obtained data support clearly the well-known behavior of physical cross-linked copolymers for **POA2.5** in which G' becomes larger than G'' at a certain frequency showing the importance of the elastic part, meaning the solution has fluid character. The viscoelastic behavior of **POA3.75** is different over the entire frequency range since the cross-over concentration between G' and G'' disappeared for **POA3.75** and G' is larger than G'' in the entire frequency range, denoting a gel-like behavior. The increase of hydrophobe content (from 2.5 to 3.75 mol%) gives rise to stronger and more dense intermolecular associations, reflected by the solid-like response of **POA3.75**.

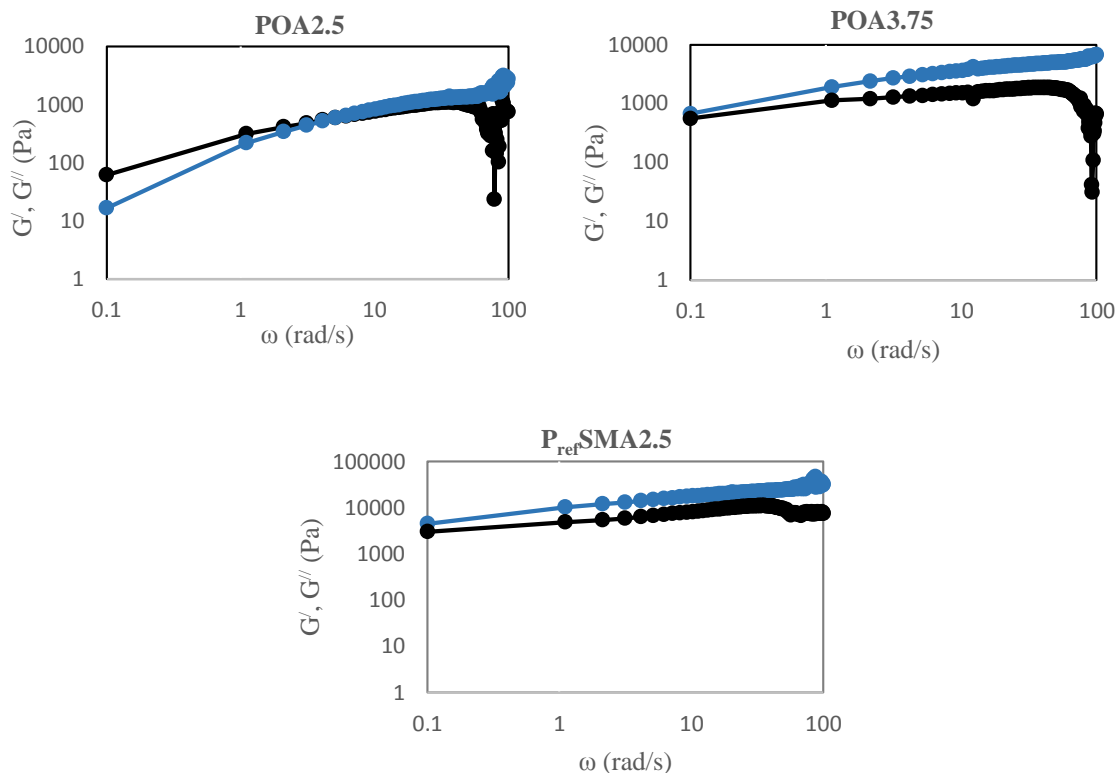


Figure 7.6. Storage modulus G' (—●—) and loss modulus G'' (—●—) as a function of frequency for **POA2.5**, **POA3.75** and **P_{ref}SMA2.5** at 15 wt%.

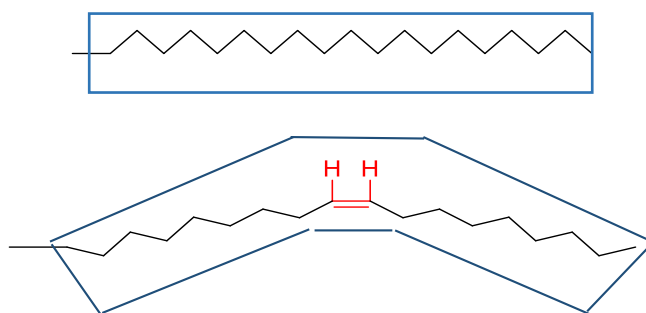


Figure 7.7. Saturated and unsaturated side chain structure.

The comparison between **P_{ref}SMA2.5** and **POA2.5** shows the significant difference of the solution properties of these two copolymers. **P_{ref}SMA2.5** displays a higher storage and loss modulus with solid-like response ($G' > G''$). This can be interpreted by the presence of the cis double bond in the side chain of **POA2.5**. The stearyl methacrylate with a fully saturated alkyl chain can pack tightly against one another. In contrast, the cis double bond of the oleyl

acrylamide side chain is bent, which makes it difficult for the hydrophobic tails to pack tightly. Therefore, **POA2.5** illustrates lower stiffness in comparison to its references copolymer Figure 7.7.

7.2.2.3 Modulus as a function of time

Modulus as a function of time at constant frequency (1Hz) was measured for the copolymers at 10, 12.5 and 15 wt% polymer solutions. The results are shown in Figure 7.8 for 15 wt%. It can be seen, that with increasing content of the hydrophobe both moduli increased and for the solutions obtained from copolymers consisting of 1.25 and 2.5% mol% OA, G' is lower than G'' indicating that the copolymers are more liquid-like. On the other hand, copolymers consisting of 3.75% OA exhibit the opposite behaviour with, G'' lower than G' suggesting that the samples become more elastic. This change in behaviour of the dynamic moduli can be explained by the formation of stronger and more dense hydrophobic associations for **POA3.75**. The results for **POA3.75** at 12.5 wt% shows an elastic response while at 10 wt% the copolymer is more viscous ($G'' > G'$).

If we compare the results with those obtained for the gels obtained from **P_{ref}SMA2.5** with 2.5% of SMA monomer, a drastic difference in the values can be seen. This leads to the conclusion that the presence of the double bond in the side chain does indeed have a significant impact on the resulting solution properties.

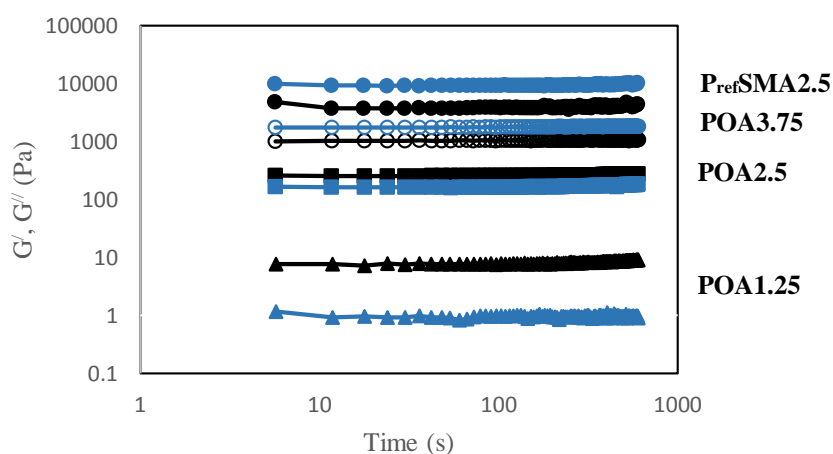


Figure 7.8. G' (blue symbol) and G'' (black symbol) as a function of time reading for **POA1.25**, **POA2.5**, **POA3.75** and **P_{ref}SMA2.5** using solution consisting of 15 wt% of each polymer.

7.2.3 Synthesis of copolymer containing oleyl acrylamide and cationic monomer (PCOA1.25)

A polymeric fatty acid bearing positive charges was synthesized in order to obtain copolymers with unique properties of cationic polymers. The cationic functionalised copolymer was synthesized with a composition of 1.25 mol% OA and 10 mol% MADQUAT. The polymerization was performed as before for 20 hours at 65 °C in toluene/methanol mixture with AIBN as an initiator. The resulting copolymer was obtained by precipitation in diethyl ether and characterized by SEC and ^1H NMR.

Analysis using ^1H NMR confirmed the success of the polymerization. The double bond peak corresponding to the OA could be identified in addition to those characteristic of the remaining functional groups, as is illustrated by the following figure.

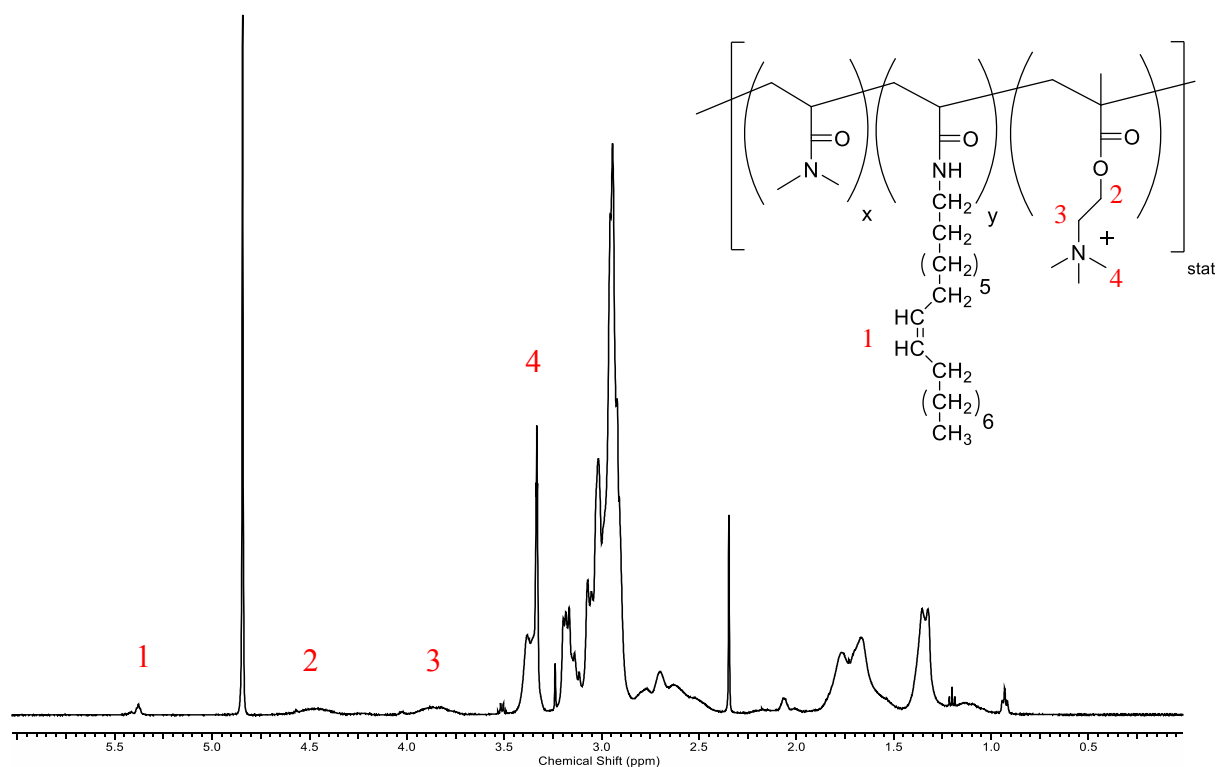


Figure 7.9. ^1H NMR of copolymer containing oleyl acrylamide and cationic monomer (in MeOD).

Table 7.2. Analytical data of the **PCOA1.25** copolymer.

Sample	Copolymer composition (mol%) (DMAM: OA: MADQUAT) ^{a,b}	M _n (g/mol) ^c	Đ ^c	Yield %
PCOA1.25	88.75: 1.3 (1.25): 10.7 (10)	39500	2.45	79%

^{a)} The polymerization was carried out with 0.01 mol/L AIBN; at T= 65 °C for 20 h, ^{b)} copolymer composition was determined by ¹H NMR, in brackets are theoretical values, DMAM (*N,N'*-dimethyl acrylamide), OA (oleyl acrylamide), MADQUAT ((methacryloyloxyethyl trimethyl ammonium chloride), ^{c)} determined by SEC in DMF with 5 g L⁻¹ LiCl, T= 60 °C.

7.2.4 Synthesis of linoleyl methacrylate copolymer (PLM)

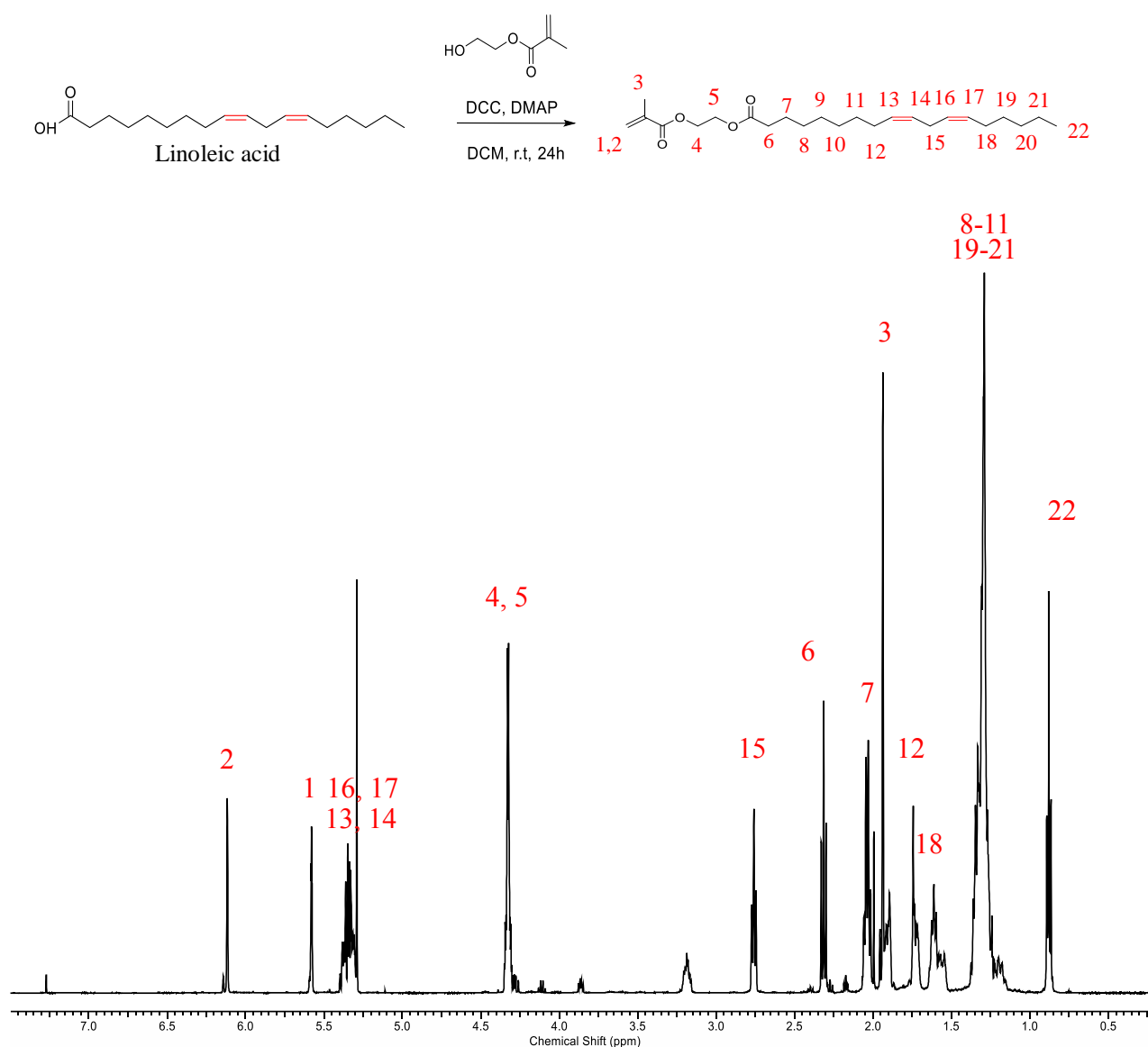


Figure 7.10. ¹H NMR of linoleyl methacrylate (LM) in CDCl₃.

This section elaborates the experimental results obtained for the synthesis of the precursor monomer, linoleyl methacrylate (LM) by esterification of 2-hydroxyethyl methacrylate (HEMA) in the presence of dicyclohexylcarbodiimide (DCC) as coupling agent and 4-dimethylaminopyridine (DMAP) as catalyst at room temperature for 24 h in DCM solvent [249]. As can be seen in ^1H NMR spectrum (Figure 7.10), successful synthesis was achieved with a yield of 60%. The peak corresponding to the double bond appearing between 5.0-5.5 ppm and those from the remaining functional groups can be easily identified and are in agreement with the expected spectrum

DMAM hydrophobically modified polymers using LM as a hydrophobic monomer were prepared by free radical polymerization, initiated by AIBN, proceeded in degassed toluene at 65 °C for 20 hours. The copolymer was obtained by precipitation in diethyl ether. For this purpose, two different copolymer compositions of 1.25 mol% (**PLM1.25**), 2.5 mol% (**PLM2.5**) of LM were synthesized. The copolymer compositions were characterized by ^1H NMR. The molecular weight and dispersity of the copolymers were determined by size exclusion chromatography (SEC) in DMF. The analytical data are listed in Table 7.3.

Analysis using ^1H NMR spectroscopy (Figure 7.11) reveals that the polymerization was successful, the double bond peaks appear between 5.0-5.5 ppm.

Table 7.3. Analytical data of the copolymers **PLM1.25** and **PLM2.5** containing LM.

Samples	Copolymer composition (mol%) (DMAM: LM)^{a,b)}	M_n (g/mol)^{c)}	Đ^{c)}	Yield (%)
PLM1.25	99.1 (98.75): 0.9 (1.25)	28200	2.81	76
PLM2.5	98.2 (97.5): 1.8 (2.5)	33800	3.03	73

^{a)} The polymerizations were carried out with 0.01 mol/L AIBN; at T= 65 °C for 20 h, ^{b)} copolymer composition was determined by ^1H NMR, in brackets: theoretical values, DMAM (*N,N'*-dimethyl acrylamide), LM (oleylacrylamide), ^{c)} determined by SEC in DMF with 5 g L⁻¹ LiCl, T= 60 °C.

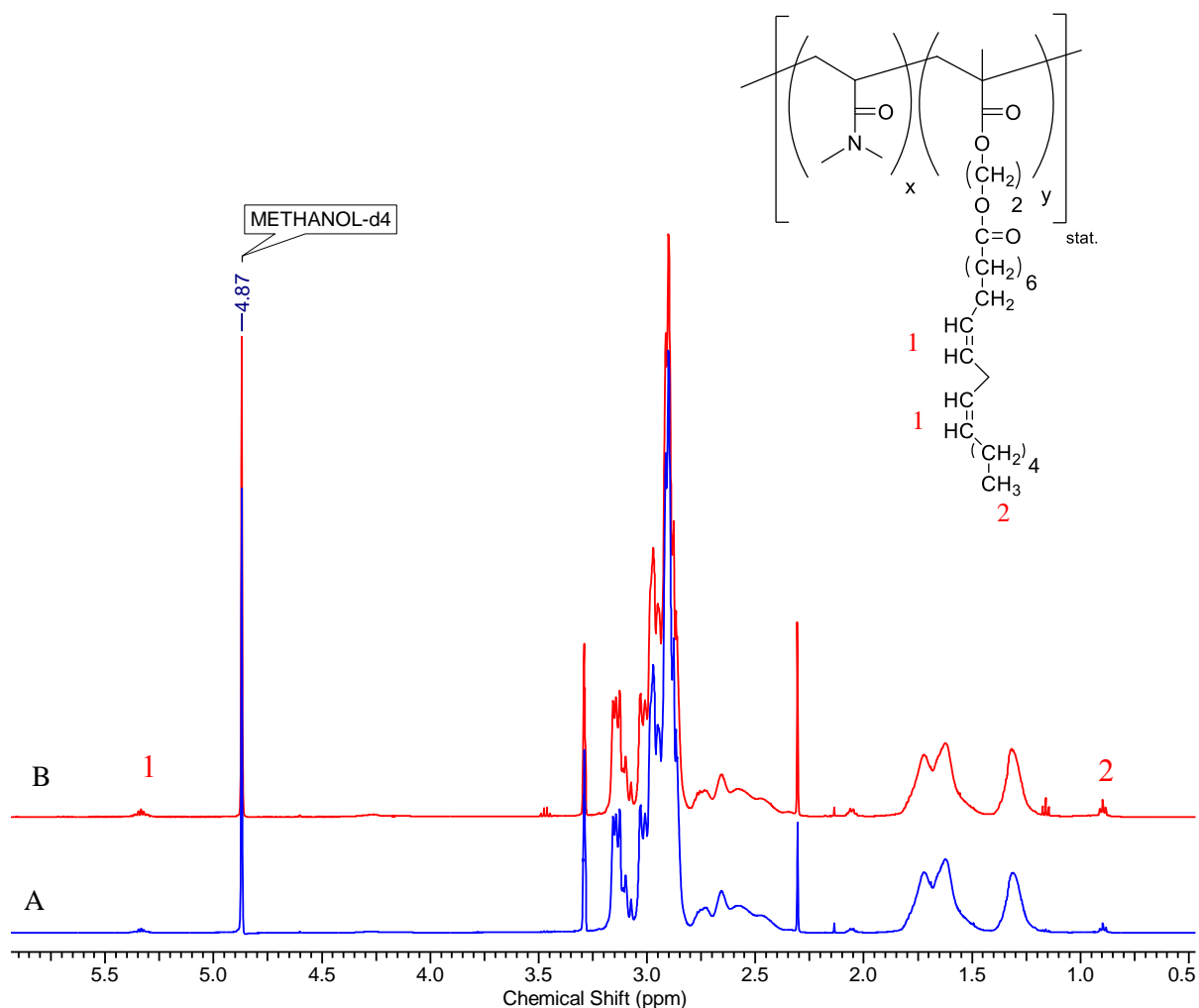


Figure 7. 11. ^1H NMR spectrum of A) **PLM1.25** and B) **PLM2.5** (in MeOD).

7.2.5 Viscosity as a function of shear rate

The effect of polyunsaturated fatty acid structure on the solution viscosity was investigated first. Figure 7.12 compares the steady shear viscosity profile for **PLM1.25** and **PLM2.5** at 10 and 15 wt%. It can be seen that an increase in each polymer concentration leads to higher viscosity. Moreover, at higher LM content (**PLM2.5** mol%) an enhancement in viscosity was observed.

A comparison between **POA** (Figure 7.3) and **PLM** viscosity shows that polymers containing OA are more viscous. Consequently, viscosity values varied clearly depending on the type of unsaturation. Linoleyl methacrylate with more double bonds does not allow to stack closely together, thus interfering with packing in the crystalline state and shows a more fluid-like behavior [255].

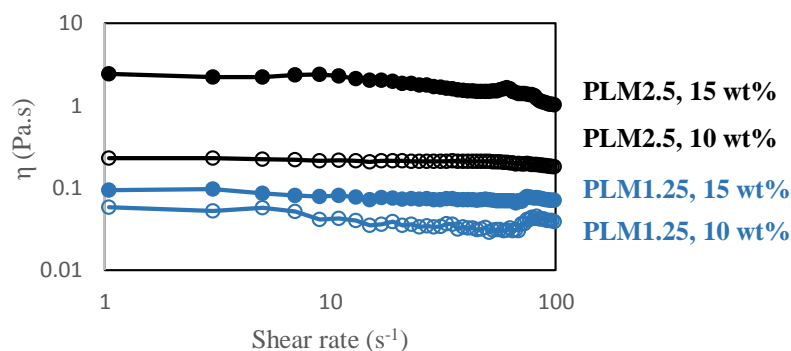


Figure 7.12. The effect of copolymers concentration and LM content on the shear viscosity of **PLM1.25** and **PLM2.5** in buffer solution at 37 °C.

7.2.3 Photo-dimerization of unsaturated double bonds

Since the regulation of cell processes such as differentiation, proliferation and migration is dependent on interactions with the extra cellular matrix, the composition and features of the ECM, for example its elasticity and/or viscoelasticity, play a vital role in controlling the cellular response and behaviour. The same principle applies to hydrogels that are used to imitate the ECM. However, a feature of the native ECM that gives it a marginal advantage compared to a hydrogel is the fact that it is dynamic, meaning the physical properties are tunable during cellular processes and can be adjusted to the cell requirements. Recently, studies have been conducted with the aim of synthesizing hydrogels that can mimic this behaviour of native ECMs, in that the hydrogel can be made to respond to external stimuli such as pH, temperature and addition of ions. One such example is the research conducted by *Tamate group* [253], where UV light irradiation has been employed to modulate the viscoelastic hydrogel properties. This cytocompatible hydrogel consisted of an ABA triblock copolymer where *N*-isopropylacrylamide together with an acrylate monomer bearing a coumarin side chain formed the first block and the polyethylene oxide formed the second block. The hydrogel obtained from this polymer is initially only physically crosslinked under physiologically relevant conditions, but once exposed to UV-light, the coumarin moieties undergo photo-dimerization via [2+2]-cycloaddition which results in the formation of chemical crosslinks.

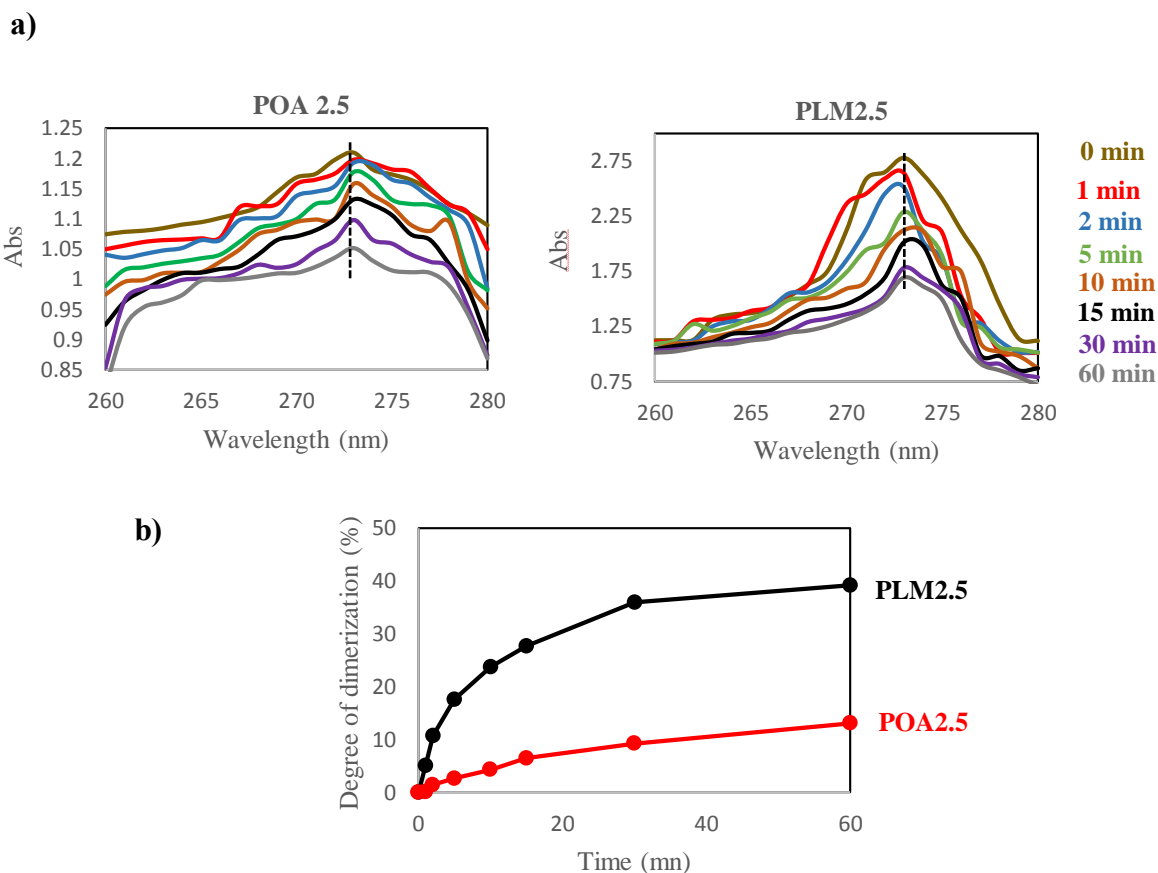


Figure 7. 13. a) UV-vis spectra of **POA2.5** and **PLM2.5** (6 wt%) recorded after UV/vis light irradiation ($\lambda=273$ nm) at 37 °C, b) degree of dimerization for the copolymers was obtained from the change in the absorption peak of OA and LM moieties at 273 nm.

For photo-cross linking, a 6 wt% solution of **POA2.5** and **PLM 2.5** were exposed to $\lambda=273$ nm and the disappearance of the double was monitored by UV spectroscopy bond after photo-dimerization. UV-spectra of both samples were recorded during irradiation for 60 min and are summarized in Figure 7.13a. The absorption peak of OA and LM at ~ 273 nm demonstrate a continuous decrease with increasing irradiation time, suggesting a growing degree of dimerization.

When comparing the degree of dimerization which was calculated from the spectra (Figure 7.13 b) it can be seen that the photoreaction for POA with one unsaturated bond appears to proceed more slowly. The dimerization degree is only $\sim 13\%$, but for **PLM2.5** this value could reach up to $\sim 40\%$ after 1 h irradiation. The results are in a good agreement with studies from *He and Tamate* who exposed copolymers containing coumarin moieties at $\lambda \sim 310$ and 360 nm UV light, respectively, for photo-cross-linking. They observed a continuous decrease in the absorption peak of coumarin at ~ 310 nm with increasing irradiation time. They could reach a degree of dimerization of up to 75 % after ~ 2 h. *Tamate and coworkers* also investigated

the viscoelastic properties of coumarin hydrogels. An increase in storage (G') modulus and decreasing in loss (G'') modulus was observed after UV irradiation. As a result, it is possible to control the viscoelastic properties of polymer containing double bond in side chain utilizing irradiation time.

7.4 Conclusion

Two types of hydrophobically modified polymers based on fatty acid monomers were prepared by free radical polymerization. For this purpose, monounsaturated OA and polyunsaturated LM acrylate monomers were synthesized and then successfully copolymerized with DMAM in three varying concentration 1.25, 2.5 and 3.75 mol% for OA and 1.25 and 2.5 mol% of LM. A comparison of the viscosity of solutions made from copolymers containing OA, LM and SMA side chains showed that the viscosity of the copolymers may be predicted by using polysaturated and monosaturated fatty acid composition. A drastic difference in the values was observed here.

Solutions of these copolymers with unsaturated double bonds can undergo a $[2\pi+2\pi]$ cycloaddition by UV-vis irradiation. Consequently, a decreasing absorbance of **POA2.5** and **PLM2.5** as a function of total applied energy at 273 nm was observed.

7.5 Experimental

7.5.1 Synthesis of Oleylacrylamide

5.48 mL (4.46 g, 16.67 mmol) of oleylamine were reacted with 4.56 mL (3.33 g, 32.9 mmol) of triethylamine in 33 mL of anhydrous dichloromethane under stirring and the reaction mixture cooled to -10°C . Another solution of 1.47 mL (1.65 g, 18.23 mmol, 1 eq) acryloyl chloride in 17 mL of dichloromethane was prepared and added dropwise to the reaction mixture. This was then allowed to stir for 4 hours at 0°C . After removal of excess acryloyl chloride by distillation, the organic layer was extracted with saturated NaHCO_3 (50 ml), demineralized water (50 ml) and brine (25ml) and then dried over NaSO_4 . Removal of excess dichloromethane using rotary evaporation yielded a light yellow solution of oleyl acrylamide (4.71 g, 14.67 mmol, 86 %). The monomer was confirmed by ^1H NMR. ^1H NMR (500 MHz, CDCl_3 , $\delta = 7.27$), 0.8 (t, - CH_3), 1.2 (m, aliphatic $-\text{CH}_2-$), 1.4 (m, $-\underline{\text{CH}_2}-\text{CH}_2-\text{NH}(=\text{O})$), 1.9 (m, $-\underline{\text{CH}_2}-\text{C}=\text{C}-$), 3.3 (m, $-\underline{\text{CH}_2}-\text{NH}(=\text{O})$), 5,3 (m, $-\text{C}=\text{C}-$), 5.6 (dd, $-\underline{\text{NH}}(=\text{O})$), 6 -6.3 (m, $-\text{HC}-\text{CH}_2-$).

7.5.2 Monomer synthesis based on linoleic acid

For synthesis of the fatty acid monomer containing two double bonds three different method were used:

First method: This section elaborates the experimental results obtained for the synthesis of the precursor monomer, linoleyl amine, in order to use the same procedure for oleyl acrylamide synthesized (as describe before). The three-step synthesis was performed using linoleic acid as the initiating reactant, 10 mL (5 g, 17.83 mmol) of linoleic acid were slowly added to 2.44 mL (4 g, 33.6 mmol) of thionylchloride under stirring, maintaining the temperature below 40 °C. This was then allowed to stir for 30 minutes at 50 °C. Removal of excess thionylchloride by distillation followed by distillation of linoleyl chloride (250 °C, vacuum) yielded 1.51 g (5.05 mmol, 30 %) of the desired product as a light yellow liquid (Figure 7.14). ¹H NMR (500 MHz, DMSO, $\delta = 2.5$), 0.89 (t, 3H, -CH₃), 1.3 (m, 14H, aliphatic -CH₂-), 1.6 (m, 2H, -CH₂-CH₂-(C=O)Cl), 2.18 (m, 4H, -CH₂-C=C-), 2.9 (m, 4H, -CH₂-(C=O)Cl and C=C-CH₂-C=C), 5-5.5 (m, 4H, HC=CH).

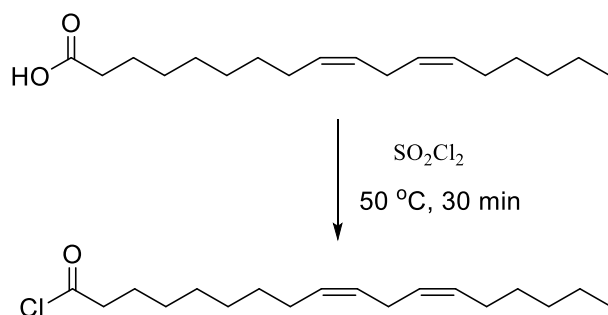


Figure 7.14. Synthesis of linoleyl chloride.

In the following step, 1.51 g (5.05 mmol, 1 eq) of linoleyl chloride were slowly added to 15 mL of an ammonia solution under vigorous stirring. This was then cooled to 5 °C, filtered, washed with cold demineralized water and dried. The product (4 g, 14.31 mmol) was obtained as a yellow-white solid (Figure 7.15). ¹H NMR (500 MHz, DMSO, $\delta = 2.5$), 0.9 (t, 3H, -CH₃), 1.28-1.33 (m, 14H, aliphatic -CH₂-), 1.55 (m, 2H, -CH₂-CH₂-(C=O)NH₂), 2.16 (m, 4H, -CH₂-C=C), 2.8 (m, 2H, C=C-CH₂-C=C), 5-5.5 (m, 4H, HC=CH), 7.05 (s, 2H, NH₂).

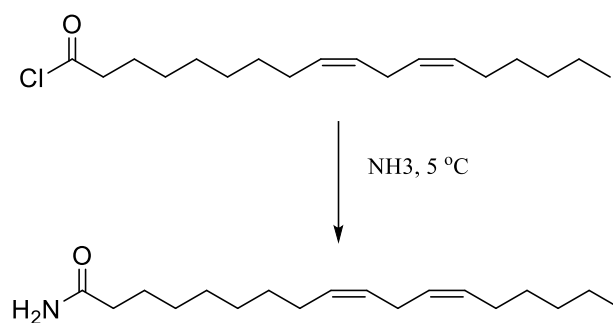


Figure 7.15. Synthesis of linoleyl amide.

The last step, 0.75 g (19.76 mmol) of lithium aluminiumhydride were added to 17 mL of THF under a constant stream of argon. After slow addition of 4 g (14.31 mmol, 1 eq.) of linoleyl amide, the mixture was heated to reflux and then allowed to stir at room temperature overnight. Unfortunately, this procedure resulted in an extremely poor yield of the desired product. ^1H NMR (500 MHz, DMSO, $\delta = 2.5$), 0.9 (t, 3H, $-\text{CH}_3$), 1.28-1.33 (m, 14H, aliphatic $-\text{CH}_2-$), 1.51 (m, 4H, $-\text{CH}_2-\text{CH}_2-\text{NH}_2$), 2.15 (m, 4H, $-\text{CH}_2-\text{C}=\text{C}$), 2.8 (m, 2H, $\text{C}=\text{C}-\text{C}-\text{C}=\text{C}$), 5-5.5 (m, 4H, $\text{HC}=\text{CH}$).

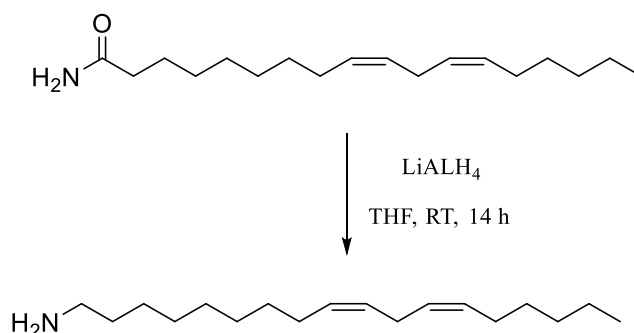


Figure 7.16. Synthesis of linoleyl amine.

Second method [248] for the synthesis of vinyl linoleate: In a two-necked round bottom glass flask involving reflux condenser, linoleic acid (3.5×10^{-3} mol) and a 10eq excess of vinyl acetate (VAc) were mixed under inert atmosphere of argon. The catalysts ($[\text{Ir}(\text{co})\text{Cl}_2$, 0.01eq) with sodium acetate (0.03eq) were added to the mixture, thereafter the reaction was performed under dry argon atmosphere at 100 °C for 20 h. After 20 h, the reaction mixture was extracted with dichloromethane after pouring into water. The organic layer was further dried over anhydrous sodium sulphate followed by removing the solvent in a rotary evaporator. The final

product was purified by silica-gel column chromatography using diethyl ether-dichloromethane (4:1 v/v) in a very low yield of 10%. $^1\text{H NMR}$ (500 MHz, CDCl_3 , $\delta = 7.27$), 0.8 (t, 3H, $-\text{CH}_3$), 1.3 (m, 14H, aliphatic $-\text{CH}_2-$), 1.5 (m, 2H, $-\underline{\text{CH}_2}-\text{CH}_2-\text{C}(=\text{O})$), 1.95 (m, 4H, $-\underline{\text{CH}_2}-\text{C}=\text{C}-$), 2.3 (t, 2H, $-\underline{\text{CH}_2}-\text{C}(=\text{O})$), 2,6 (m, 2H, $-\text{C}=\text{C}-\underline{\text{CH}_2}-\text{C}=\text{C}$), 4.6 and 4.9 (dd, 2H, $-\text{COO}-\text{CH}=\underline{\text{CH}_2}$), 5.2 (m, 4H, $-\text{CH}=\text{CH}-$).

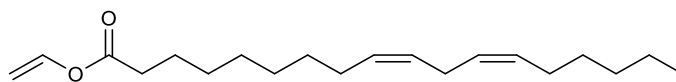


Figure 7.17. Chemical structure of vinyl linoleate.

Third method [249] for the synthesis of the methacrylate linoleic monomer: Linoleic acid (0.104 mol, 2.5 ml) and 4-dimethylamino pyridine (DMAP) (0.0104 mol, 0.108 g) in 7.5 ml dry DCM were placed in 50 ml double neck round bottom flask on ice-water bath. The reaction flask equipped with magnetic bar under dry atmosphere. In another mixture, dicyclohexylcarbodiimide (DCC) was dissolved in the least possible volume of DCM and was then added to the first reaction mixture. Afterwards, 2-hydroxyethyl methacrylate (HEMA) (0.1040 mol, 0.97 g) was added dropwise to the reaction flask. After completing the addition, the solution was stirred in the ice-water bath for 30 min, then it was allowed to stir at room temperature for 24 h. 10 ml distilled water was added to the solution and the organic fraction was washed with saturated NaHCO_3 (20 ml \times 4) and brine solution (15 ml \times 2) and dried over anhydrous Na_2SO_4 before removing the solvent in a rotary evaporator. The residue was purified by silica-gel column chromatography with a 95:5 (v/v) mixture of cyclohexane-EtOAc. This method provided the monomer with two double bonds in the side chain in 60% yield.

7.5.3 Synthesis of POA

40 mg (0.12 mmol) of oleyl acrylamide and 1.03 mL (9.99 mmol) dimethylacrylamide were placed in a round bottomed flask under inert conditions. After addition of 10 mL of toluene under stirring, the reaction mixture was subjected to 7-8 freeze and thaw pump cycles in order to remove any contaminating or terminating species e.g. oxygen or water vapour. The mixture was then reacted in a free radical polymerization reaction using 16.4 mg of AIBN as an initiating species at 65 °C for 20 hours. This yielded a yellow-white copolymer consisting of 1.25% oleyl acrylamide.

The constitution of the polymers was then varied by using two concentrations of the oleyl acrylamide monomer with 2.5 mol% and 3.75 mol%, using 80 mg and 120 mg of the monomer, respectively, without variation of any other quantities. After cooling to room temperature, the copolymers were precipitated in diethyl ether and dried on the vacuum line. $^1\text{H NMR}$ (500 MHz, MeOD, $\delta = 3.31, 4.87$): 0.91 (brs, CH_3 , OA), 1.31 (brs, $-\text{CH}_2-\text{CH}_2-\text{C}=\text{C}$), 1.65, (brs, $-\text{CH}_2-$, backbone, DMAM, OA), 2.04 (brs, $-\text{CH}_2-\text{C}=\text{C}$), 2.68 (brs. $-\text{CH}-$, backbone, DMAM, OA), 2.85 (brs, $-\text{N}-(\text{CH}_3)_2$, DMAM), 5.35 (brs, $-\text{C}=\text{C}-$). SEC in DMF gave the molecular weight of (**POA1.25**, $M_n = 35900$, **POA2.5**, $M_n = 32940$ and **POA3.75**, $M_n = 42800 \text{ g mol}^{-1}$) with dispersities of ($\text{Đ} = 2.77$, $\text{Đ} = 2.81$ and $\text{Đ} = 2.99$ respectively)

7.5.4 Synthesis of copolymer containing oleyl acrylamide and cationic monomer

40 mg (0.12 mmol) of oleyl acrylamide, 1.03 mL (9.99 mmol) dimethylacrylamide and 0.234 g (1.13 mmol) of the cationic monomer [2-(methacryloyloxy) ethyltrimethyl ammoniumchloride] (MADQUAT) were placed in a round bottomed flask under inert condition. After addition of 10 mL of a toluene: methanol mixture (in a 6:4 ratio) under stirring, the reaction mixture was subjected to 7-8 freeze and thaw pump cycles. The mixture was then reacted similarly in a free radical polymerization reaction using 18.6 mg (0.11 mmol) of AIBN as an initiating species at 65°C for 20 hours. This yielded a yellow-white copolymer consisting of 1.25% oleyl acrylamide.

7.5.5 Synthesis of PLM

PLM copolymers were synthesized according to a previously method, as described for POA. Copolymers were prepared by free radical polymerization in toluene in Schlenk-flasks with freeze- pump-thaw cycles to obtain dry atmosphere at room temperature. 1.25 and 2.5 mol% of LM along with DMAM and 0.01 mol/L AIBN were added to flasks to 1 M solution. The reaction carried out at 65°C for 20 h, before the resulting polymers were precipitated in diethyl ether, the solutions were let to cool down and reach the room temperature and dried under vacuum for at least 48 h. $^1\text{H NMR}$ (500 MHz, MeOD, $\delta = 3.31, 4.87$): 0.83 (brs, CH_3 , LM), 1.23 (brs, $-\text{CH}_2-\text{CH}_2-\text{C}=\text{C}$), 1.54 (brs, $-\text{CH}_2-$, backbone, DMAM, LM), 1.97 (brs, $-\text{CH}_2-\text{C}=\text{C}$), 2.58 (brs. $-\text{CH}-$, backbone, DMAM), 2.85 (brs, $-\text{N}-(\text{CH}_3)_2$, DMAM), 5.25 (brs, $-\text{C}=\text{C}-\text{C}=\text{C}$). SEC in DMF gave the molecular weight of (**PLM1.25**, $M_n = 28200$ and **PLM2.5**, $M_n = 33800 \text{ g mol}^{-1}$) with dispersities of ($\text{Đ} = 2.81$ and $\text{Đ} = 3.03$ respectively).

Chapter 8. Characterization techniques

8.1 Nuclear magnetic resonance spectroscopy

Nuclear magnetic resonance (NMR) spectroscopy measurements were done with DRX-500 (500 Hz) on FT-NMR instruments from Bruker at room temperature. The evaluation of the spectra was done utilizing the ACD labs program. The coupling constant (J) studied in Hertz and the chemical shift (δ) in parts per million (ppm). Calibration was performed on the residual protons of the deuterated solvents utilized, here deuterated methanol (MeOD: $\delta = 3.31$ and 4.87), chloroform (CDCl₃: $\delta = 7.27$), water (D₂O: $\delta = 4.75$): Abbreviations for descriptors and multiplicities are: s = singlet, d = doublet, t = triplet, q = quartet, m = multiplet, br = broad.

8.2 Size exclusion chromatography

Size exclusion chromatography (SEC) with PSS GRAM analytical 1000 Å and 30 Å columns equipped with a Knauer RI detectors Smartline 2300 was utilized to measure the molecular weights of the copolymers. The molecular weights of copolymers were studied in DMF with 5 g L⁻¹ LiBr at 60 °C, using PMMA as standards.

8.3 Ubbelohde viscometer

The viscosities of liquid-like solutions were measured by an Ubbelohde capillary viscometer with capillary diameter 0.58 mm which was situated in a thermostat-control water bath at 37°C and were calculated using the equation [8.1]:

$$\eta = A \cdot \rho \cdot t \quad \text{eq. [8.1]}$$

Where A is viscometer constant, ρ is water density and t is the flow time.

8.4 Rheology

Rheological studies were performed at 37°C utilizing Bohlin Gemini rheometer from Malvern. Two types of rheometers were used in order to explain the range of rheological behavior observed. For viscous and high viscous samples, measurements were done using oscillatory rheometry equipped with a cone-plate (150 mm diameter) geometry. For gel-like samples,

measurements were performed on a 1000 mm plate-plate geometry. All samples were heated to 100 °C before rheological measurements.

8.5 Fluorescence spectroscopy

The fluorescence measurements were recorded with a F-2700 fluorescence spectrometer from Hitachi using an excitation wavelength of 334 nm. The spectra intensities were applied at 371 nm (peak 1) and 382 nm (peak 3). Pyrene in methanol (0.1 M) was used as fluorescent dye.

8.6 High-performance liquid chromatography

High-performance liquid chromatography (HPLC) were performed on a Merck Hitachi instrument equipped with L-6200 intelligent pump, 65A variable wavelength UV monitor and a UV detector (L-4000). Acetonitrile/water 50:50 was used as solvent at a flow rate of 1ml/min at room temperature.

8.7 Ultraviolet- visible spectroscopy

UV-vis spectra of the dilute aqueous solutions of **POA2.5** and **PLM2.5** (6 wt%) was measured using an Analytik Jena Specord 210 spectrophotometer.

8.8 Mass Spectrometry

Fourier transformation mass spectrometer (LTQ-Orbitrap) coupled to an Accela HPLC system (including of Accela autosampler, Accela pump and Accela PDA detector). HPLC column was Hypersil Gold, 50 mm*1mm, 1.9 μm (particle size). Both instruments were from Thermo Electron. Mass spectrometer (MS) was recorded on ionization mode ESI (electrospray ionization).with source voltage of 3.8kV. Capillary voltage was 41V at 275 °C and tube lens voltage 140V. The scanned mass range was from 150 to 2000 m/z with resolution set of 60,000.

Chapter 9. Conclusions and Recommendations

The incorporation of a small amount of hydrophobic units into the hydrophilic polymer backbone form a very important class of compounds called hydrophobically modified (HM) polymers with unique rheological properties in aqueous medium. Polymer concentration is one of the most important parameter that determines the rheological properties of such associative polymers. At low concentration (dilute solution) intra-molecular aggregation between hydrophobic groups are predominant which results in polymer coil contraction and viscosity decrease of the solution. Above a certain polymer concentration, the intra-molecular associations convert to inter-molecular associations, resulting in drastic viscosity increases. Therefore, using this conversion the broad variation of polymer solution characteristics can be obtained, from liquid-like at low concentration to high viscous three-dimensional transient network at high concentration. In some cases, this transient networks are strong enough to form hydrogels. The three-dimensional hydrogel structures enable them to absorb large amount of biological fluids or water. Because of soft consistency, porosity and high water content they can mimic natural tissues, more than any other type of synthetic polymeric biomaterials. In this research, free radical polymerization was used to prepare hydrophobically modified polymers with wide range of elastic and viscous moduli.

In the first part of the work, associative copolymers were synthesized as non-ionic reference copolymers. Lauryl methacrylate (LMA) (1.25-10 mol%) or stearyl methacrylate (SMA) (1.25 and 2.5 mol%) were copolymerized with *N,N'*-dimethyl acrylamide (DMAM) to form several copolymers (DMAM-SMA/LMA) (**P_{ref}**). Three different functionalized copolymers were prepared containing additional cationic, zwitterionic and peptide functionalized monomer units.

The cationic copolymers, **P1-series**, were synthesized from DMAM, LMA/SMA and a constant amount of 2-methylamino ethyl acrylate (DMAEA) (10 mol%). The precursor copolymers (DMAM-LMA/SMA-DMAEA) were methylated with methyl iodide to obtain cationic copolymers. The solubility and rheological studies of these copolymers in PBS buffer solution showed that the presence of cationic charge along the polymers side chain has a significant influence on the copolymers properties. It was found that with increasing the hydrophobe content and chain length of the reference copolymers their solubility decreased whereas all cationic copolymers were soluble in PBS buffer solution even up to 40 wt%. The rheological studies showed that the viscosity for polycations is much lower than the viscosity

of their corresponding reference copolymers \mathbf{P}_{ref} while the viscosity increased in both copolymers with increasing copolymer concentration. Additionally, the special concentration corresponding to the onset of semi-dilute unentangled regime for cationic copolymers is higher than their references analogues. The copolymers consist of SMA were found to have increased viscosities in both \mathbf{P}_{ref} and $\mathbf{P1}$ copolymers.

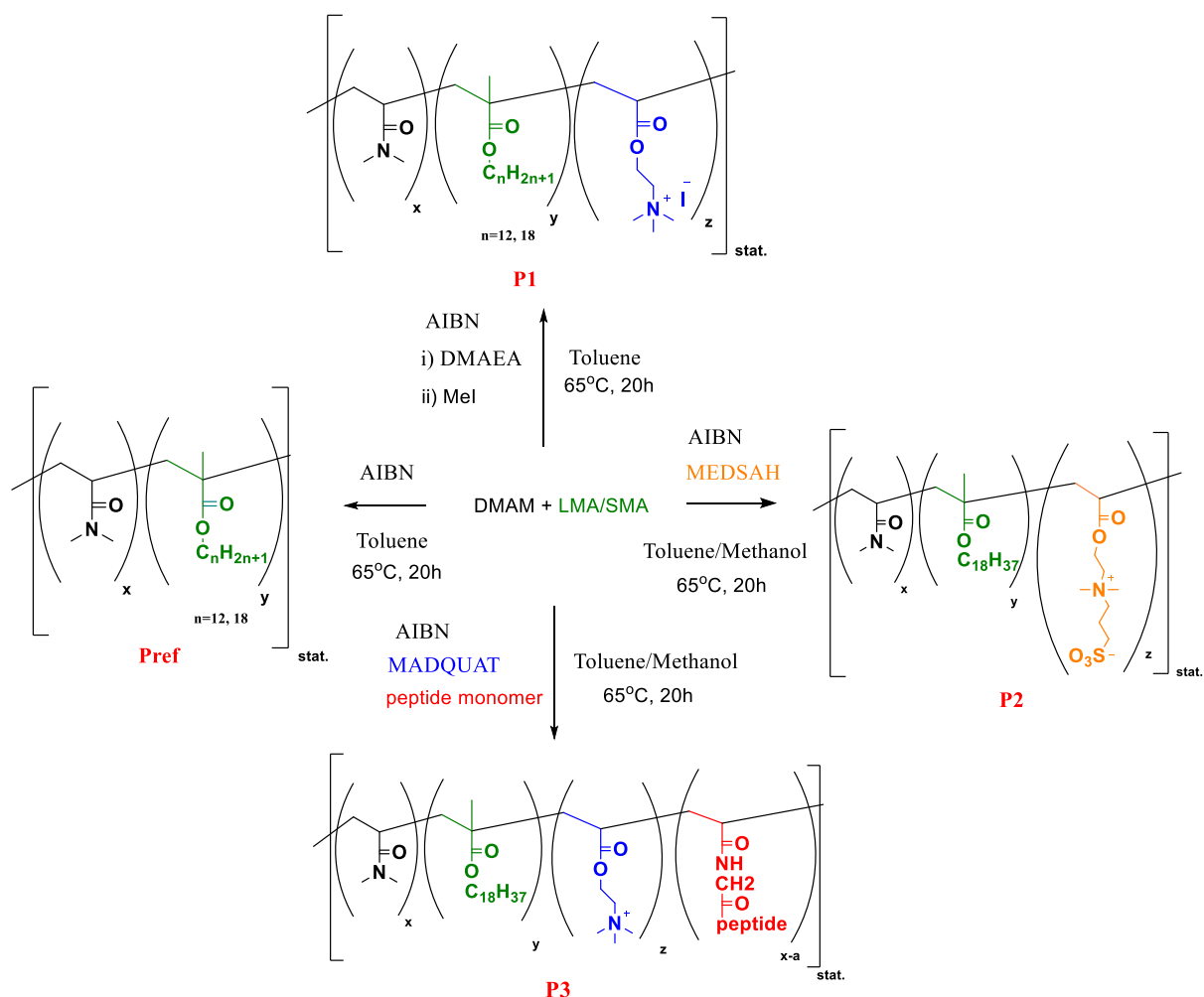


Figure 9.1. Schematic diagram of the preparation of \mathbf{P}_{ref} , $\mathbf{P1}$, $\mathbf{P2}$ and $\mathbf{P3}$.

The zwitterionic copolymer $\mathbf{P2}$ were composed of the zwitterionic monomer MEDSAH (10 mol%), DMAM and 1.25 mol% of SMA. A comparative study between \mathbf{P}_{ref} and $\mathbf{P2}$ proved that the incorporation of 10 mol% zwitterionic monomer leads to a viscosity increase above a critical concentration. This behavior can be explained by the coil expansion due to the repulsion between ionic groups. In addition, the anti-polyelectrolyte behavior and the enhancement of viscosity with addition of NaCl was observed.

To prepare a peptide containing copolymer, a copolymer consisting of DMAM, 1.25 mol% of SMA and peptide monomer (1 mol%) was synthesized. However, the presence of the peptide caused a drastic reduction in solubility. In order to address this limitation the cationic monomer was added to the reaction mixture. Thus, two HM copolymers were prepared containing 10 mol% cationic monomer (MADQUAT), SMA (1.25 mol%), 1 mol% (**P3-1**) and 2 mol% (**P3-2**) peptide monomer. Rheological studies revealed that **P3-2** has higher viscosity compared to **P3-1** and **P_{ref}**, while the viscosity of **P3-1** is lower than **P_{ref}**.

A comparison between the viscosities of all 4 types of copolymers exhibited a remarkable difference between polycations and other copolymers, whereas **P2** was found to have enhanced viscosity. Furthermore, viscoelastic properties were investigated for all samples and the results showed that the elastic (G') modulus and viscous (G'') modulus both increased with increasing the concentration. Moreover, except for **P_{ref}** containing 2.5 mol% SMA above 10 wt% and **P2** at 25 wt% which behave like an elastic gel (G' exceeds G'' over entire frequency measurements) all copolymers presented liquid-like behavior.

In the second part of the research hydrophobically modified polymers based on fatty acids including, monounsaturated oleyl acrylamide (**POA**) and polyunsaturated linoleic methacrylate (**PLM**) using DMAM as a hydrophilic unit were synthesized. Furthermore, the rheological properties were compared with **P_{ref}** in order to understand the influence of the cis-double bond on the solution properties. The results showed that the increase of chain regularities facilitates the intermolecular aggregation behavior and consequently leads to a larger modulus. Therefore, **P_{ref}** has higher modulus compared to **POA** and **PLM**. In addition, in both copolymers **POA** and **PLM**, the control of the mechanical properties was obtained through variation of fatty acid monomer content and number of double bonds. In the case of monomer content, the viscosity increased with increasing the fatty acid monomers content. In the case of the number of double bonds the enhancement of the number of double bond (**PLM**) resulted in softer hydrogel network. Therefore, **PLM** showed lower viscosity compared to **POA**.

These copolymers have the potential to serve as a substrate for stem cell culturing and the results show that the mechanical properties as well as their chemical functionalization can be easily controlled through varying the functional groups, hydrophobe content and chain lengths as well as copolymers concentration. Future experiments will focus on the application of such copolymers to encapsulate stem cells and provide a 3D microenvironment for controlled stem cell culturing.

Chapter 10. References

- [1] González-Díaz, E., Varghese, S. Hydrogels as Extracellular Matrix Analogs. *Gels* 2016, 2, 20.
- [2] Park, S., Park, K. Engineered Polymeric Hydrogels for 3D Tissue Models. *Polymers* 2016, 8, 23.
- [3] Caló, E., Khutoryanskiy, V. V. Biomedical applications of hydrogels: A review of patents and commercial products. *European Polymer Journal* 2015, 65, 252–267.
- [4] Boucard, N., Viton, C., Domard, A. New Aspects of the Formation of Physical Hydrogels of Chitosan in a Hydroalcoholic Medium. *Biomacromolecules* 2005, 6, 3227–3237.
- [5] Tibbitt, M. W., Anseth, K. S. Hydrogels as extracellular matrix mimics for 3D cell culture. *Biotechnology and Bioengineering* 2009, 103, 655–663.
- [6] Sun, M., Chi, G., Li, P., Lv, S., Xu, J., Xu, Z., Xia, Y., Tan, Y., Xu, J., Li, L., Li, Y. Effects of Matrix Stiffness on the Morphology, Adhesion, Proliferation and Osteogenic Differentiation of Mesenchymal Stem Cells. *International Journal of Medical Science* 2018, 15, 257–268.
- [7] Mason, B. N., Califano, J. P., Reinhart-King, C. A. Matrix Stiffness: A Regulator of Cellular Behavior and Tissue Formation. In *Engineering Biomaterials for Regenerative Medicine*; Bhatia, S. K., Ed.; Springer New York: New York, NY, 2012, pp. 19–37.
- [8] Popescu, M.-T., Athanasoulas, I., Tsitsilianis, C., Hadjiantoniou, N. A., Patrickios, C. S. Reversible hydrogels from amphiphilic polyelectrolyte model multiblock copolymers: The importance of macromolecular topology. *Soft Matter* 2010, 6, 5417.
- [9] Smeets, N. M. B., Patenaude, M., Kinio, D., Yavitt, F. M., Bakaic, E., Yang, F.-C., Rheinstädter, M., Hoare, T. Injectable hydrogels with in situ-forming hydrophobic domains: oligo(d l -lactide) modified poly(oligoethylene glycol methacrylate) hydrogels. *Polymer Chemistry* 2014, 5, 6811–6823.
- [10] Kujawa, P., Audibert-Hayet, A., Selb, J., Candau, F. Effect of Ionic Strength on the Rheological Properties of Multisticker Associative Polyelectrolytes. *Macromolecules* 2006, 39, 384–392.
- [11] Dragan, S., Ghimici, L. Viscometric behaviour of some hydrophobically modified cationic polyelectrolytes. *Polymer* 2001, 42, 2887–2891.
- [12] Wagner, M., Pietsch, C., Tauhardt, L., Schallon, A., Schubert, U. S. Characterization of cationic polymers by asymmetric flow field-flow fractionation and multi-angle light scattering—A comparison with traditional techniques. *Journal of chromatography. A* 2014, 1325, 195–203.
- [13] Jones, R. A., Poniris, M. H., Wilson, M. R. pDMAEMA is internalised by endocytosis but does not physically disrupt endosomes. *Journal of controlled release official journal of the Controlled Release Society* 2004, 96, 379–391.
- [14] Elmalem, E., Biedermann, F., Scherer, M. R. J., Koutsioubas, A., Toprakcioglu, C., Biffi, G., Huck, W. T. S. Mechanically strong, fluorescent hydrogels from zwitterionic,

fully π -conjugated polymers. *Chemical communications (Cambridge, England)* 2014, 50, 8930–8933.

[15] Zhang, N., Kohn, D. H. Using polymeric materials to control stem cell behavior for tissue regeneration. *Birth defects research. Part C, Embryo today reviews* 2012, 96, 63–81.

[16] Thompson, C., Mutch, J., Parent, S., Mac-Thiong, J.-M. The changing demographics of traumatic spinal cord injury: An 11-year study of 831 patients. *The journal of spinal cord medicine* 2015, 38, 214–223.

[17] Mashayekhan, S., Hajiabbas, M., Fallah, A. Stem Cells in Tissue Engineering. In *Pluripotent Stem Cells*; Bhartiya, D., Ed.; InTech, 2013.

[18] Chandra, P., Lee, S. J. Synthetic Extracellular Microenvironment for Modulating Stem Cell Behaviors. *Biomarker insights* 2015, 10, 105–116.

[19] Liu, S. Q., Tay, R., Khan, M., Rachel Ee, P. L., Hedrick, J. L., Yang, Y. Y. Synthetic hydrogels for controlled stem cell differentiation. *Soft Matter* 2010, 6, 67–81.

[20] Bindu A, H., B, S. Potency of Various Types of Stem Cells and their Transplantation. *J Stem Cell Research and Therapy* 2011, 01.

[21] Bai, Q., Desprat, R., Klein, B., Lemaitre, J.-M., Vos, J. de. Embryonic Stem Cells or Induced Pluripotent Stem Cells? A DNA Integrity Perspective. *Current Gene Therapy* 2013, 13, 93–98.

[22] Sun, Q., Zhang, Z., Sun, Z. The potential and challenges of using stem cells for cardiovascular repair and regeneration. *Genes & diseases* 2014, 1, 113–119.

[23] Yu, J., Thomson, J. A. Pluripotent stem cell lines. *Genes & development* 2008, 22, 1987–1997.

[24] Bertassoli, B. M., Assis Neto, A. C. d., Oliveira, F. D. d., Arroyo, M. A. M., Ferrão, J. S. P., Silva, J. B. d., Pignatari, G. C., Braga, P. B. Mesenchymal stem cells: emphasis in adipose tissue. *Cell* 2013, 56, 607–617.

[25] Tsou, Y.-H., Khoneisser, J., Huang, P.-C., Xu, X. Hydrogel as a bioactive material to regulate stem cell fate. *Bioactive Materials* 2016, 1, 39–55.

[26] Madl, C. M., Heilshorn, S. C. Engineering Hydrogel Microenvironments to Recapitulate the Stem Cell Niche. *Annual Review of Biomedical Engineering* 2018, 20, 21–47.

[27] Lutolf, M. P. Biomaterials: Spotlight on hydrogels. *Nature materials* 2009, 8, 451–453.

[28] Ullah, F., Othman, M. B. H., Javed, F., Ahmad, Z., Md Akil, H. Classification, processing and application of hydrogels: A review. *Materials science & engineering. C, Materials for biological applications* 2015, 57, 414–433.

[29] Bae, K. H., Wang, L.-S., Kurisawa, M. Injectable biodegradable hydrogels: Progress and challenges. *Journal of Materials Chemistry. B* 2013, 1, 5371.

[30] Ahmed, E. M. Hydrogel: Preparation, characterization, and applications: A review. *Journal of advanced research* 2015, 6, 105–121.

- [31] Ma, S., Wang, S., Li, Q., Leng, Y., Wang, L., Hu, G.-H. A Novel Method for Preparing Poly(vinyl alcohol) Hydrogels: Preparation, Characterization, and Application. *Industrial and Engineering Chemistry Research* 2017, *56*, 7971–7976.
- [32] Hsu, Y.-I., Masutani, K., Yamaoka, T., Kimura, Y. Strengthening of hydrogels made from enantiomeric block copolymers of polylactide (PLA) and poly(ethylene glycol) (PEG) by the chain extending Diels–Alder reaction at the hydrophilic PEG terminals. *Polymer* 2015, *67*, 157–166.
- [33] Zhu, B., Ma, D., Wang, J., Zhang, S. Structure and properties of semi-interpenetrating network hydrogel based on starch. *Carbohydrate polymers* 2015, *133*, 448–455.
- [34] Alvarez-Lorenzo, C., Concheiro, A., Dubovik, A. S., Grinberg, N. V., Burova, T. V., Grinberg, V. Y. Temperature-sensitive chitosan-poly(N-isopropylacrylamide) interpenetrated networks with enhanced loading capacity and controlled release properties. *Journal of controlled release official journal of the Controlled Release Society* 2005, *102*, 629–641.
- [35] Zhang, S., Alvarez, D. J., Sofroniew, M. V., Deming, T. J. Design and synthesis of nonionic copolypeptide hydrogels with reversible thermoresponsive and tunable physical properties. *Biomacromolecules* 2015, *16*, 1331–1340.
- [36] HILLEL, A., SHAH, P., ELISSEEFF, J. Hydrogels in cell encapsulation and tissue engineering. In *Biomedical Polymers*; Elsevier 2007, pp. 57–82.
- [37] Ionov, L. Hydrogel-based actuators: possibilities and limitations. *Materials Today* 2014, *17*, 494–503.
- [38] Kharkar, P. M., Kiick, K. L., Kloxin, A. M. Designing degradable hydrogels for orthogonal control of cell microenvironments. *Chemical Society reviews* 2013, *42*, 7335–7372.
- [39] Chai, Q., Jiao, Y., Yu, X. Hydrogels for Biomedical Applications: Their Characteristics and the Mechanisms behind Them. *Gels* 2017, *3*, 6.
- [40] Zhu, J. Biomimetic Hydrogels as Scaffolds for Tissue Engineering. *Journal of Biochips and Tissue Chips* 2012, *02*.
- [41] Sgambato, A., Cipolla, L., Russo, L. Bioresponsive Hydrogels: Chemical Strategies and Perspectives in Tissue Engineering. *Gels* 2016, *2*, 28.
- [42] Ulijn, R. V., Bibi, N., Jayawarna, V., Thornton, P. D., Todd, S. J., Mart, R. J., Smith, A. M., Gough, J. E. Bioresponsive hydrogels. *Materials Today* 2007, *10*, 40–48.
- [43] Ulijn, R. V. Enzyme-responsive materials: a new class of smart biomaterials. *Journal of Materials Chemistry* 2006, *16*, 2217.
- [44] Draelos, Z., Hornby, S., Walters, R. M., Appa, Y. Hydrophobically modified polymers can minimize skin irritation potential caused by surfactant-based cleansers. *Journal of cosmetic dermatology* 2013, *12*, 314–321.
- [45] Chang, Y., McCormick, C. L. Water-soluble copolymers. 49. Effect of the distribution of the hydrophobic cationic monomer dimethyldodecyl(2-acrylamidoethyl)ammonium bromide on the solution behavior of associating acrylamide copolymers. *Macromolecules* 1993, *26*, 6121–6126.

- [46] Chassenieux, C., Nicolai, T., Benyahia, L. Rheology of associative polymer solutions. *Current Opinion in Colloid & Interface Science* 2011, *16*, 18–26.
- [47] Aricov, L., Băran, A., Simion, E. L., Gîfu, I. C., Anghel, D.-F., Jerca, V. V., Vuluga, D. M. New insights into the self-assembling of some hydrophobically modified polyacrylates in aqueous solution. *Colloid and Polymer Science* 2016, *294*, 667–679.
- [48] Abdala, A. A., Wu, W., Olesen, K. R., Jenkins, R. D., Tonelli, A. E., Khan, S. A. Solution rheology of hydrophobically modified associative polymers: Effects of backbone composition and hydrophobe concentration. *Journal of Rheology* 2004, *48*, 979–994.
- [49] Volpert, E., Selb, J., Candau, F. Influence of the Hydrophobe Structure on Composition, Microstructure, and Rheology in Associating Polyacrylamides Prepared by Micellar Copolymerization. *Macromolecules* 1996, *29*, 1452–1463.
- [50] Rubinstein, M., Semenov, A. N. Dynamics of Entangled Solutions of Associating Polymers. *Macromolecules* 2001, *34*, 1058–1068.
- [51] Annable, T., Buscall, R., Ettelaie, R., Whittlestone, D. The rheology of solutions of associating polymers: Comparison of experimental behavior with transient network theory. *Journal of Rheology* 1993, *37*, 695–726.
- [52] Volpert, E., Selb, J., Candau, F. Associating behaviour of polyacrylamides hydrophobically modified with dihexylacrylamide. *Polymer* 1998, *39*, 1025–1033.
- [53] Hao, J., Weiss, R. A. Viscoelastic and Mechanical Behavior of Hydrophobically Modified Hydrogels. *Macromolecules* 2011, *44*, 9390–9398.
- [54] Philippova, O. Solution Properties of Associating Polymers. In *Macromolecular Self-assembly*; Billon, L., Borisov, O., Eds.; John Wiley & Sons, Inc: Hoboken, New Jersey 2016; Vols. 196, pp. 141–158.
- [55] Liu, R., Pu, W., Jia, H., Shang, X., Pan, Y., Yan, Z. Rheological Properties of Hydrophobically Associative Copolymers Prepared in a Mixed Micellar Method Based on Methacryloxyethyl-dimethyl Cetyl Ammonium Chloride as Surfmer. *International Journal of Polymer Science* 2014, *2014*, 1–14.
- [56] Strauss, U. P., Williams, B. L. The Transition from Typical Polyelectrolyte to Polysoap. III. Light Scattering and Viscosity Studies of Poly-4-Vinylpyridine Derivatives 1. *Journal of Physical Chemistry* 1961, *65*, 1390–1395.
- [57] Varoqui, R., Strauss, U. P. Comparison of electrical transport properties of anionic polyelectrolytes and polysoaps. *Journal of Physical Chemistry* 1968, *72*, 2507–2511.
- [58] McCormick, C. L., Hoyle, C. E., Clark, M. D. Water-soluble copolymers. 35. Photophysical and rheological studies of the copolymer of methacrylic acid with 2-(1-naphthylacetyl)ethyl acrylate. *Macromolecules* 1990, *23*, 3124–3129.
- [59] Winnik, M. A., Bystryak, S. M., Siddiqui, J. Interaction of Pyrene-Labeled Poly(ethylene imine) with Sodium Dodecyl Sulfate in Aqueous Solution. *Macromolecules* 1999, *32*, 624–632.
- [60] Morishima, Y., Kobayashi, T., Furui, T., Nozakura, S. Intramolecular compartmentalization of photoredox centers in functionalized amphiphilic polyelectrolytes: A model for collisionless electron transfer systems. *Macromolecules* 1987, *20*, 1707–1712.

- [61] Taylor, K. C., Nasr-El-Din, H. A. Water-soluble hydrophobically associating polymers for improved oil recovery: A literature review. *Journal of Petroleum Science and Engineering* 1998, 19, 265–280.
- [62] Bastiat, G., Grassl, B., François, J. Micellar copolymerization of associative polymers: study of the effect of acrylamide on sodium dodecyl sulfate-poly(propylene oxide) methacrylate mixed micelles. *Journal of colloid and interface science* 2005, 289, 359–370.
- [63] Regalado, E. J., Selb, J., Candau, F. Viscoelastic Behavior of Semidilute Solutions of Multisticker Polymer Chains. *Macromolecules* 1999, 32, 8580–8588.
- [64] Hill, A., Candau, F., Selb, J. Properties of hydrophobically associating polyacrylamides: Influence of the method of synthesis. *Macromolecules* 1993, 26, 4521–4532.
- [65] Candau, F., Selb, J. Hydrophobically-modified polyacrylamides prepared by micellar polymerization1Part of this paper was presented at the conference on 'Associating Polymer', Fontevraud, France, November 1997.1. *Advances in Colloid and Interface Science* 1999, 79, 149–172.
- [66] Gong, L. X., Zhang, X. F. A new approach to the synthesis of hydrophobically associating polyacrylamide via the inverse miniemulsion polymerization in the presence of template. *Express Polymer Letters* 2009, 3, 778–787.
- [67] Eshuis, A., Leendertse, H. J., Thoenes, D. Surfactant-free emulsion polymerization of styrene using crosslinked seed particles. *Colloid and Polymer Science* 1991, 269, 1086–1089.
- [68] Cram, S. L., Brown, H. R., Spinks, G. M., Hourdet, D., Creton, C. Hydrophobically Modified Dimethylacrylamide Synthesis and Rheological Behavior. *Macromolecules* 2005, 38, 2981–2989.
- [69] Rabiee, A., Ershad-Langroudi, A., Zeynali, M. E. A survey on cationic polyelectrolytes and their applications: acrylamide derivatives. *Reviews in Chemical Engineering* 2015, 31.
- [70] Kwon, H. J. Tissue Engineering of Muscles and Cartilages Using Polyelectrolyte Hydrogels. *Advances in Materials Science and Engineering* 2014, 2014, 1–7.
- [71] Samal, S. K., Dash, M., van Vlierberghe, S., Kaplan, D. L., Chiellini, E., van Blitterswijk, C., Moroni, L., Dubruel, P. Cationic polymers and their therapeutic potential. *Chemical Society Reviews* 2012, 41, 7147.
- [72] Tabujew, I., Peneva, K. CHAPTER 1. Functionalization of Cationic Polymers for Drug Delivery Applications. In *Cationic Polymers in Regenerative Medicine*; Samal, S., Dubruel, P., Eds.; *Royal Society of Chemistry*: Cambridge 2014, pp. 1–29.
- [73] Zwioerek, K., Bourquin, C., Battiany, J., Winter, G., Endres, S., Hartmann, G., Coester, C. Delivery by cationic gelatin nanoparticles strongly increases the immunostimulatory effects of CpG oligonucleotides. *Pharmaceutical research* 2008, 25, 551–562.
- [74] Tseng, C.-L., Chen, K.-H., Su, W.-Y., Lee, Y.-H., Wu, C.-C., Lin, F.-H. Cationic Gelatin Nanoparticles for Drug Delivery to the Ocular Surface: In Vitro and In Vivo Evaluation. *Journal of Nanomaterials* 2013, 2013, 1–11.

- [75] Maeda, H., Greish, K., Fang, J. The EPR Effect and Polymeric Drugs: A Paradigm Shift for Cancer Chemotherapy in the 21st Century. In *Polymer Therapeutics II*; Satchi-Fainaro, R., Duncan, R., Eds.; Springer-Verlag: Berlin/Heidelberg, 2006; Vols. 193, pp. 103–121.
- [76] Chou, M.-J., Yu, H.-Y., Hsia, J.-C., Chen, Y.-H., Hung, T.-T., Chao, H.-M., Chern, E., Huang, Y.-Y. Highly Efficient Intracellular Protein Delivery by Cationic Polyethyleneimine-Modified Gelatin Nanoparticles. *Materials (Basel, Switzerland)* 2018, *11*.
- [77] Cheung, R. C. F., Ng, T. B., Wong, J. H., Chan, W. Y. Chitosan: An Update on Potential Biomedical and Pharmaceutical Applications. *Marine drugs* 2015, *13*, 5156–5186.
- [78] Goy, R. C., Morais, S. T.B., Assis, O. B.G. Evaluation of the antimicrobial activity of chitosan and its quaternized derivative on E. coli and S. aureus growth. *Revista Brasileira de Farmacognosia* 2016, *26*, 122–127.
- [79] Wan, A., Xu, Q., Sun, Y., Li, H. Antioxidant activity of high molecular weight chitosan and N,O-quaternized chitosans. *Journal of agricultural and food chemistry* 2013, *61*, 6921–6928.
- [80] Qi, L., Xu, Z. In vivo antitumor activity of chitosan nanoparticles. *Bioorganic & medicinal chemistry letters* 2006, *16*, 4243–4245.
- [81] Wang, G., Ao, Q., Gong, K., Wang, A., Zheng, L., Gong, Y., Zhang, X. The effect of topology of chitosan biomaterials on the differentiation and proliferation of neural stem cells. *Acta biomaterialia* 2010, *6*, 3630–3639.
- [82] Leipzig, N. D., Shoichet, M. S. The effect of substrate stiffness on adult neural stem cell behavior. *Biomaterials* 2009, *30*, 6867–6878.
- [83] Yang, Z., Mo, L., Duan, H., Li, X. Effects of chitosan/collagen substrates on the behavior of rat neural stem cells. *Science China. Life sciences* 2010, *53*, 215–222.
- [84] Mejia-Ariza, R., Graña-Suárez, L., Verboom, W., Huskens, J. Cyclodextrin-based supramolecular nanoparticles for biomedical applications. *Journal of Materials Chemistry. B* 2017, *5*, 36–52.
- [85] Zhang, J., Ma, P. X. Cyclodextrin-based supramolecular systems for drug delivery: recent progress and future perspective. *Advanced drug delivery reviews* 2013, *65*, 1215–1233.
- [86] Díaz-Moscoso, A., Le Gourriérec, L., Gómez-García, M., Benito, J. M., Balbuena, P., Ortega-Caballero, F., Guilloteau, N., Di Giorgio, C., Vierling, P., Defaye, J., Ortiz Mellet, C., García Fernández, J. M. Polycationic amphiphilic cyclodextrins for gene delivery: synthesis and effect of structural modifications on plasmid DNA complex stability, cytotoxicity, and gene expression. *Chemistry (Weinheim an der Bergstrasse, Germany)* 2009, *15*, 12871–12888.
- [87] Cohen, J. L., Schubert, S., Wich, P. R., Cui, L., Cohen, J. A., Mynar, J. L., Fréchet, J. M. J. Acid-degradable cationic dextran particles for the delivery of siRNA therapeutics. *Bioconjugate chemistry* 2011, *22*, 1056–1065.

- [88] Mai, K., Zhang, S., Liang, B., Gao, C., Du, W., Zhang, L.-M. Water soluble cationic dextran derivatives containing poly(amidoamine) dendrons for efficient gene delivery. *Carbohydrate polymers* 2015, *123*, 237–245.
- [89] Gao, Y., Li, Q., Shi, Y., Cha, R. Preparation and Application of Cationic Modified Cellulose Fibrils as a Papermaking Additive. *International Journal of Polymer Science* 2016, *2016*, 1–8.
- [90] Abbott, A. P., Bell, T. J., Handa, S., Stoddart, B. Cationic functionalisation of cellulose using a choline based ionic liquid analogue. *Green Chemistry* 2006, *8*, 784.
- [91] Littunen, K., Snoei de Castro, J., Samoylenko, A., Xu, Q., Quaggin, S., Vainio, S., Seppälä, J. Synthesis of cationized nanofibrillated cellulose and its antimicrobial properties. *European Polymer Journal* 2016, *75*, 116–124.
- [92] Chaker, A., Boufi, S. Cationic nanofibrillar cellulose with high antibacterial properties. *Carbohydrate polymers* 2015, *131*, 224–232.
- [93] You, J., Cao, J., Zhao, Y., Zhang, L., Zhou, J., Chen, Y. Improved Mechanical Properties and Sustained Release Behavior of Cationic Cellulose Nanocrystals Reinforced Cationic Cellulose Injectable Hydrogels. *Biomacromolecules* 2016, *17*, 2839–2848.
- [94] Jaeger, W., Bohrisch, J., Laschewsky, A. Synthetic polymers with quaternary nitrogen atoms—Synthesis and structure of the most used type of cationic polyelectrolytes. *Progress in Polymer Science* 2010, *35*, 511–577.
- [95] Jiang, X.-l., Chu, Y.-f., Liu, J., Zhang, G.-y., Zhuo, R.-x. Aqueous sec analysis of cationic polymers as gene carriers. *Chinese Journal of Polymer Science* 2011, *29*, 421–426.
- [96] Bonkovoski, L. C., Martins, A. F., Bellettini, I. C., Garcia, F. P., Nakamura, C. V., Rubira, A. F., Muniz, E. C. Polyelectrolyte complexes of poly(2-dimethylamino) ethyl methacrylate/chondroitin sulfate obtained at different pHs: I. Preparation, characterization, cytotoxicity and controlled release of chondroitin sulfate. *International journal of pharmaceutics* 2014, *477*, 197–207.
- [97] Chen, Y., Liu, W. Y., Zeng, G. S. Stimulus-responsive hydrogels reinforced by cellulose nanowhisker for controlled drug release. *RSC Advances* 2016, *6*, 87422–87432.
- [98] Car, A., Baumann, P., Duskey, J. T., Chami, M., Bruns, N., Meier, W. pH-responsive PDMS-b-PDMAEMA micelles for intracellular anticancer drug delivery. *Biomacromolecules* 2014, *15*, 3235–3245.
- [99] Gao, W., Chan, J. M., Farokhzad, O. C. pH-Responsive nanoparticles for drug delivery. *Molecular pharmaceutics* 2010, *7*, 1913–1920.
- [100] Laschewsky, A. Structures and Synthesis of Zwitterionic Polymers. *Polymers* 2014, *6*, 1544–1601.
- [101] Feyerabend, F., Wendel, H.-P., Mihailova, B., Heidrich, S., Agha, N. A., Bismayer, U., Willumeit-Römer, R. Blood compatibility of magnesium and its alloys. *Acta biomaterialia* 2015, *25*, 384–394.

- [102] Sin, M.-C., Chen, S.-H., Chang, Y. Hemocompatibility of zwitterionic interfaces and membranes. *Polymer Journal* 2014, *46*, 436–443.
- [103] Chen, S., Li, L., Zhao, C., Zheng, J. Surface hydration: Principles and applications toward low-fouling/nonfouling biomaterials. *Polymer* 2010, *51*, 5283–5293.
- [104] UTRATA-WESOLEK, A. Antifouling surfaces in medical application. *Polimery* 2013, *58*, 685–695.
- [105] Zhao, W., Ye, Q., Hu, H., Wang, X., Zhou, F. Grafting zwitterionic polymer brushes via electrochemical surface-initiated atomic-transfer radical polymerization for anti-fouling applications. *Journal of Materials Chemistry. B* 2014, *2*, 5352–5357.
- [106] Lin, S., Li, Y., Zhang, L., Chen, S., Hou, L.'a. A Zwitterion-like, Charge-balanced Ultrathin Layers on Polymeric Membranes for Antifouling Property. *Environmental science & technology* 2018.
- [107] Sundhoro, M., Wang, H., Boiko, S. T., Chen, X., Jayawardena, H. S. N., Park, J., Yan, M. Fabrication of carbohydrate microarrays on a poly(2-hydroxyethyl methacrylate)-based photoactive substrate. *Organic & biomolecular chemistry* 2016, *14*, 1124–1130.
- [108] Meyers, S. R., Grinstaff, M. W. Biocompatible and bioactive surface modifications for prolonged in vivo efficacy. *Chemical reviews* 2012, *112*, 1615–1632.
- [109] Li, L., Chen, S., Zheng, J., Ratner, B. D., Jiang, S. Protein adsorption on oligo(ethylene glycol)-terminated alkanethiolate self-assembled monolayers: The molecular basis for nonfouling behavior. *The journal of physical chemistry. B* 2005, *109*, 2934–2941.
- [110] Heuberger, M., Drobek, T., Spencer, N. D. Interaction forces and morphology of a protein-resistant poly(ethylene glycol) layer. *Biophysical journal* 2005, *88*, 495–504.
- [111] Li, B., Ye, Q. Antifouling Surfaces of Self-assembled Thin Layer. In *Antifouling Surfaces and Materials*; Zhou, F., Ed.; Springer Berlin Heidelberg: Berlin, Heidelberg, 2015, pp. 31–54.
- [112] Lokanathan, A. R., Zhang, S., Regina, V. R., Cole, M. A., Ogaki, R., Dong, M., Besenbacher, F., Meyer, R. L., Kingshott, P. Mixed poly (ethylene glycol) and oligo (ethylene glycol) layers on gold as nonfouling surfaces created by backfilling. *Biointerphases* 2011, *6*, 180–188.
- [113] Zhang, W., Martinelli, J., Peters, J. A., van Hengst, J. M. A., Bouwmeester, H., Kramer, E., Bonnet, C. S., Szeremeta, F., Tóth, É., Djanashvili, K. Surface PEG Grafting Density Determines Magnetic Relaxation Properties of Gd-Loaded Porous Nanoparticles for MR Imaging Applications. *ACS applied materials & interfaces* 2017, *9*, 23458–23465.
- [114] Grassl, B., Francois, J., Billon, L. Associating behaviour of polyacrylamide modified with a new hydrophobic zwitterionic monomer. *Polymer International*. 2001, *50*, 1162–1169.
- [115] Dong, Z., Mao, J., Yang, M., Wang, D., Bo, S., Ji, X. Phase behavior of poly(sulfobetaine methacrylate)-grafted silica nanoparticles and their stability in protein solutions. *Langmuir the ACS journal of surfaces and colloids* 2011, *27*, 15282–15291.

- [116] Chang, Y., Chen, S., Zhang, Z., Jiang, S. Highly protein-resistant coatings from well-defined diblock copolymers containing sulfobetaines. *Langmuir the ACS journal of surfaces and colloids* 2006, *22*, 2222–2226.
- [117] Qian, X., Villa-Diaz, L. G., Kumar, R., Lahann, J., Krebsbach, P. H. Enhancement of the propagation of human embryonic stem cells by modifications in the gel architecture of PMEDSAH polymer coatings. *Biomaterials* 2014, *35*, 9581–9590.
- [118] Singh, M., Tarannum, N. Polyzwitterions. In *Engineering of Biomaterials for Drug Delivery Systems*; Elsevier, 2018, pp. 69–101.
- [119] Lewis, A., Tang, Y., Brocchini, S., Choi, J.-W., Godwin, A. Poly(2-methacryloyloxyethyl phosphorylcholine) for protein conjugation. *Bioconjugate chemistry* 2008, *19*, 2144–2155.
- [120] Nakai, K., Nishiuchi, M., Inoue, M., Ishihara, K., Sanada, Y., Sakurai, K., Yusa, S.-i. Preparation and characterization of polyion complex micelles with phosphobetaine shells. *Langmuir the ACS journal of surfaces and colloids* 2013, *29*, 9651–9661.
- [121] Yang, B., Duan, X., Huang, J. Ultrathin, biomimetic, superhydrophilic layers of cross-linked poly(phosphobetaine) on polyethylene by photografting. *Langmuir the ACS journal of surfaces and colloids* 2015, *31*, 1120–1126.
- [122] Zhao, Y., Bai, T., Shao, Q., Jiang, S., Shen, A. Q. Thermoresponsive self-assembled NiPAm-zwitterion copolymers. *Polymer Chemistry* 2015, *6*, 1066–1077.
- [123] Zhang, Z., Chen, S., Jiang, S. Dual-functional biomimetic materials: nonfouling poly(carboxybetaine) with active functional groups for protein immobilization. *Biomacromolecules* 2006, *7*, 3311–3315.
- [124] Wang, F., Li, Y., Shen, Y., Wang, A., Wang, S., Xie, T. The functions and applications of RGD in tumor therapy and tissue engineering. *International journal of molecular sciences* 2013, *14*, 13447–13462.
- [125] Chandrudu, S., Simerska, P., Toth, I. Chemical methods for peptide and protein production. *Molecules (Basel, Switzerland)* 2013, *18*, 4373–4388.
- [126] Chapter 2 Solid-phase peptide synthesis. In *Synthetic Polypeptides as Antigens*; Elsevier, 1988; Vols. 19, pp. 41–94.
- [127] Duro-Castano, A., Conejos-Sánchez, I., Vicent, M. Peptide-Based Polymer Therapeutics. *Polymers* 2014, *6*, 515–551.
- [128] Alemany, A., Florescu, M., Baron, C. S., Peterson-Maduro, J., van Oudenaarden, A. Whole-organism clone tracing using single-cell sequencing. *Nature* 2018.
- [129] Arcangelis, A. de. Integrin and ECM functions: roles in vertebrate development. *Trends in Genetics* 2000, *16*, 389–395.
- [130] Chen, S. S., Fitzgerald, W., Zimmerberg, J., Kleinman, H. K., Margolis, L. Cell-cell and cell-extracellular matrix interactions regulate embryonic stem cell differentiation. *Stem cells (Dayton, Ohio)* 2007, *25*, 553–561.
- [131] Gattazzo, F., Urciuolo, A., Bonaldo, P. Extracellular matrix: a dynamic microenvironment for stem cell niche. *Biochimica et biophysica acta* 2014, *1840*, 2506–2519.

- [132] Marciano, D. K., Denda, S., Reichardt, L. F. Methods for Identifying Novel Integrin Ligands. In *Integrins*; Elsevier, 2007; Vols. 426, pp. 223–237.
- [133] Ross, R. S., Borg, T. K. Integrins and the Myocardium. *Circulation Research* 2001, 88, 1112–1119.
- [134] Srichai, M. B., Zent, R. Integrin Structure and Function. In *Cell-Extracellular Matrix Interactions in Cancer*; Zent, R., Pozzi, A., Eds.; Springer New York: New York, NY, 2010, pp. 19–41.
- [135] Rahmany, M. B., van Dyke, M. Biomimetic approaches to modulate cellular adhesion in biomaterials: A review. *Acta biomaterialia* 2013, 9, 5431–5437.
- [136] Ruoslahti, E. RGD and other recognition sequences for integrins. *Annual review of cell and developmental biology* 1996, 12, 697–715.
- [137] Castelletto, V., Gouveia, R. J., Connon, C. J., Hamley, I. W. Self-assembly and bioactivity of a polymer/peptide conjugate containing the RGD cell adhesion motif and PEG. *European Polymer Journal* 2013, 49, 2961–2967.
- [138] Caliari, S. R., Burdick, J. A. A practical guide to hydrogels for cell culture. *Nature methods* 2016, 13, 405–414.
- [139] Baker, B. M., Chen, C. S. Deconstructing the third dimension: how 3D culture microenvironments alter cellular cues. *Journal of cell science* 2012, 125, 3015–3024.
- [140] Huang, G., Li, F., Zhao, X., Ma, Y., Li, Y., Lin, M., Jin, G., Lu, T. J., Genin, G. M., Xu, F. Functional and Biomimetic Materials for Engineering of the Three-Dimensional Cell Microenvironment. *Chemical reviews* 2017, 117, 12764–12850.
- [141] Abdeen, A. A., Saha, K. Manufacturing Cell Therapies Using Engineered Biomaterials. *Trends in biotechnology* 2017, 35, 971–982.
- [142] Diekjürgen, D., Grainger, D. W. Polysaccharide matrices used in 3D in vitro cell culture systems. *Biomaterials* 2017, 141, 96–115.
- [143] Aizawa, Y., Owen, S. C., Shoichet, M. S. Polymers used to influence cell fate in 3D geometry: New trends. *Progress in Polymer Science* 2012, 37, 645–658.
- [144] Higuchi, A., Suresh Kumar, S., Ling, Q.-D., Alarfaj, A. A., Munusamy, M. A., Murugan, K., Hsu, S.-T., Benelli, G., Umezawa, A. Polymeric design of cell culture materials that guide the differentiation of human pluripotent stem cells. *Progress in Polymer Science* 2017, 65, 83–126.
- [145] Xu, C., Inokuma, M. S., Denham, J., Golds, K., Kundu, P., Gold, J. D., Carpenter, M. K. Feeder-free growth of undifferentiated human embryonic stem cells. *Nature biotechnology* 2001, 19, 971–974.
- [146] Evans, M. J., Kaufman, M. H. Establishment in culture of pluripotential cells from mouse embryos. *Nature* 1981, 292, 154–156.
- [147] Celiz, A. D., Smith, J. G. W., Patel, A. K., Hook, A. L., Rajamohan, D., George, V. T., Flatt, L., Patel, M. J., Epa, V. C., Singh, T., Langer, R., Anderson, D. G., Allen, N. D., Hay, D. C., Winkler, D. A., Barrett, D. A., Davies, M. C., Young, L. E., Denning, C., Alexander, M. R. Discovery of a Novel Polymer for Human Pluripotent Stem Cell

Expansion and Multilineage Differentiation. *Advanced materials (Deerfield Beach, Fla.)* 2015, 27, 4006–4012.

[148] Chun, Y. W., Balikov, D. A., Feaster, T. K., Williams, C. H., Sheng, C. C., Lee, J.-B., Boire, T. C., Neely, M. D., Bellan, L. M., Ess, K. C., Bowman, A. B., Sung, H.-J., Hong, C. C. Combinatorial polymer matrices enhance in vitro maturation of human induced pluripotent stem cell-derived cardiomyocytes. *Biomaterials* 2015, 67, 52–64.

[149] Heras-Bautista, C. O., Katsen-Globa, A., Schloerer, N. E., Dieluweit, S., Abd El Aziz, O. M., Peinkofer, G., Attia, W. A., Khalil, M., Brockmeier, K., Hescheler, J., Pfannkuche, K. The influence of physiological matrix conditions on permanent culture of induced pluripotent stem cell-derived cardiomyocytes. *Biomaterials* 2014, 35, 7374–7385.

[150] Banerjee, A., Arha, M., Choudhary, S., Ashton, R. S., Bhatia, S. R., Schaffer, D. V., Kane, R. S. The influence of hydrogel modulus on the proliferation and differentiation of encapsulated neural stem cells. *Biomaterials* 2009, 30, 4695–4699.

[151] Kong, H. J., Kaigler, D., Kim, K., Mooney, D. J. Controlling rigidity and degradation of alginate hydrogels via molecular weight distribution. *Biomacromolecules* 2004, 5, 1720–1727.

[152] Bencherif, S. A., Srinivasan, A., Horkay, F., Hollinger, J. O., Matyjaszewski, K., Washburn, N. R. Influence of the degree of methacrylation on hyaluronic acid hydrogels properties. *Biomaterials* 2008, 29, 1739–1749.

[153] Federico, S., Nöchel, U., Löwenberg, C., Lendlein, A., Neffe, A. T. Supramolecular hydrogel networks formed by molecular recognition of collagen and a peptide grafted to hyaluronic acid. *Acta biomaterialia* 2016, 38, 1–10.

[154] Yue, K., Trujillo-de Santiago, G., Alvarez, M. M., Tamayol, A., Annabi, N., Khademhosseini, A. Synthesis, properties, and biomedical applications of gelatin methacryloyl (GelMA) hydrogels. *Biomaterials* 2015, 73, 254–271.

[155] Croisier, F., Jérôme, C. Chitosan-based biomaterials for tissue engineering. *European Polymer Journal* 2013, 49, 780–792.

[156] Nilsen-Nygaard, J., Strand, S., Vårum, K., Draget, K., Nordgård, C. Chitosan: Gels and Interfacial Properties. *Polymers* 2015, 7, 552–579.

[157] Zhao, H., Ma, L., Zhou, J., Mao, Z., Gao, C., Shen, J. Fabrication and physical and biological properties of fibrin gel derived from human plasma. *Biomedical materials (Bristol, England)* 2008, 3, 15001.

[158] Li, Y., Meng, H., Liu, Y., Lee, B. P. Fibrin gel as an injectable biodegradable scaffold and cell carrier for tissue engineering. *The Scientific World Journal* 2015, 2015, 685690.

[159] Dai, Y., Liu, G., Ma, L., Wang, D., Gao, C. Cell-free macro-porous fibrin scaffolds for in situ inductive regeneration of full-thickness cartilage defects. *Journal of Materials Chemistry. B* 2016, 4, 4410–4419.

[160] Zhang, Y., Heher, P., Hilborn, J., Redl, H., Ossipov, D. A. Hyaluronic acid-fibrin interpenetrating double network hydrogel prepared in situ by orthogonal disulfide cross-linking reaction for biomedical applications. *Acta biomaterialia* 2016, 38, 23–32.

- [161] Cheng, K., Blusztajn, A., Shen, D., Li, T.-S., Sun, B., Galang, G., Zarembinski, T. I., Prestwich, G. D., Marbán, E., Smith, R. R., Marbán, L. Functional performance of human cardiosphere-derived cells delivered in an in situ polymerizable hyaluronan-gelatin hydrogel. *Biomaterials* 2012, 33, 5317–5324.
- [162] Deng, Y., Ren, J., Chen, G., Li, G., Wu, X., Wang, G., Gu, G., Li, J. Injectable in situ cross-linking chitosan-hyaluronic acid based hydrogels for abdominal tissue regeneration. *Scientific reports* 2017, 7, 2699.
- [163] Khunmanee, S., Jeong, Y., Park, H. Crosslinking method of hyaluronic-based hydrogel for biomedical applications. *Journal of tissue engineering* 2017, 8, 2041731417726464.
- [164] Yu, F., Cao, X., Li, Y., Zeng, L., Yuan, B., Chen, X. An injectable hyaluronic acid/PEG hydrogel for cartilage tissue engineering formed by integrating enzymatic crosslinking and Diels–Alder “click chemistry”. *Polymer Chemistry* 2014, 5, 1082–1090.
- [165] Langer, R., Tirrell, D. A. Designing materials for biology and medicine. *Nature* 2004, 428, 487–492.
- [166] Leach, J. B., Shoichet, M. S. Naturally-derived and bioinspired materials. *Journal of Materials Chemistry. B* 2015, 3, 7814–7817.
- [167] Sallouh, O., Weberskirch, R. Facile formation of hydrogels by using functional precursor polymers and the chemoselective Staudinger coupling. *Polymer* 2016, 86, 189–196.
- [168] Rostovtsev, V. V., Green, L. G., Fokin, V. V., Sharpless, K. B. A Stepwise Huisgen Cycloaddition Process: Copper(I)-Catalyzed Regioselective “Ligation” of Azides and Terminal Alkynes. *Angewandte Chemie (International ed. in English)* 2002, 41, 2596–2599.
- [169] Agard, N. J., Prescher, J. A., Bertozzi, C. R. A strain-promoted 3 + 2 azide-alkyne cycloaddition for covalent modification of biomolecules in living systems. *Journal of the American Chemical Society* 2004, 126, 15046–15047.
- [170] Blackman, M. L., Royzen, M., Fox, J. M. Tetrazine ligation: fast bioconjugation based on inverse-electron-demand Diels-Alder reactivity. *Journal of the American Chemical Society* 2008, 130, 13518–13519.
- [171] Dadová, J., Orság, P., Pohl, R., Brázdová, M., Fojta, M., Hocek, M. Vinylsulfonamide and acrylamide modification of DNA for cross-linking with proteins. *Angewandte Chemie (International ed. in English)* 2013, 52, 10515–10518.
- [172] Nair, D. P., Podgórski, M., Chatani, S., Gong, T., Xi, W., Fenoli, C. R., Bowman, C. N. The Thiol-Michael Addition Click Reaction: A Powerful and Widely Used Tool in Materials Chemistry. *Chemistry of Materials* 2014, 26, 724–744.
- [173] Lutolf, M. P., Hubbell, J. A. Synthetic biomaterials as instructive extracellular microenvironments for morphogenesis in tissue engineering. *Nature biotechnology* 2005, 23, 47–55.
- [174] Underhill, G. H., Chen, A. A., Albrecht, D. R., Bhatia, S. N. Assessment of hepatocellular function within PEG hydrogels. *Biomaterials* 2007, 28, 256–270.

- [175] Jain, E., Hill, L., Canning, E., Sell, S. A., Zustiak, S. P. Control of gelation, degradation and physical properties of polyethylene glycol hydrogels through the chemical and physical identity of the crosslinker. *Journal of Materials Chemistry. B* 2017, 5, 2679–2691.
- [176] Vitz, J., Majdanski, T. C., Meier, A., Lutz, P. J., Schubert, U. S. Polymerization of ethylene oxide under controlled monomer addition via a mass flow controller for tailor made polyethylene oxides. *Polymer Chemistry* 2016, 7, 4063–4071.
- [177] Trappmann, B., Baker, B. M., Polacheck, W. J., Choi, C. K., Burdick, J. A., Chen, C. S. Matrix degradability controls multicellularity of 3D cell migration. *Nature communications* 2017, 8, 371.
- [178] Ruedinger, F., Lavrentieva, A., Blume, C., Pepelanova, I., Scheper, T. Hydrogels for 3D mammalian cell culture: a starting guide for laboratory practice. *Applied microbiology and biotechnology* 2015, 99, 623–636.
- [179] Lutolf, M. P., Lauer-Fields, J. L., Schmoekel, H. G., Metters, A. T., Weber, F. E., Fields, G. B., Hubbell, J. A. Synthetic matrix metalloproteinase-sensitive hydrogels for the conduction of tissue regeneration: engineering cell-invasion characteristics. *Proceedings of the National Academy of Sciences of the United States of America* 2003, 100, 5413–5418.
- [180] Lanzalaco, S., Armelin, E. Poly(N-isopropylacrylamide) and Copolymers: A Review on Recent Progresses in Biomedical Applications. *Gels* 2017, 3, 36.
- [181] Garbern, J. C., Hoffman, A. S., Stayton, P. S. Injectable pH- and temperature-responsive poly(N-isopropylacrylamide-co-propylacrylic acid) copolymers for delivery of angiogenic growth factors. *Biomacromolecules* 2010, 11, 1833–1839.
- [182] Papadakis, C., Tsitsilianis, C. Responsive Hydrogels from Associative Block Copolymers: Physical Gelling through Polyion Complexation. *Gels* 2017, 3, 3.
- [183] Roche, E. T., Hastings, C. L., Lewin, S. A., Shvartsman, D., Brudno, Y., Vasilyev, N. V., O'Brien, F. J., Walsh, C. J., Duffy, G. P., Mooney, D. J. Comparison of biomaterial delivery vehicles for improving acute retention of stem cells in the infarcted heart. *Biomaterials* 2014, 35, 6850–6858.
- [184] Xia, Y., Zhu, K., Lai, H., Lang, M., Xiao, Y., Lian, S., Guo, C., Wang, C. Enhanced infarct myocardium repair mediated by thermosensitive copolymer hydrogel-based stem cell transplantation. *Experimental biology and medicine (Maywood, N.J.)* 2015, 240, 593–600.
- [185] Foster, A. A., Marquardt, L. M., Heilshorn, S. C. The Diverse Roles of Hydrogel Mechanics in Injectable Stem Cell Transplantation. *Current opinion in chemical engineering* 2017, 15, 15–23.
- [186] Choe, G., Park, J., Park, H., Lee, J. Hydrogel Biomaterials for Stem Cell Microencapsulation. *Polymers* 2018, 10, 997.
- [187] Fire, A., Xu, S., Montgomery, M. K., Kostas, S. A., Driver, S. E., Mello, C. C. Potent and specific genetic interference by double-stranded RNA in *Caenorhabditis elegans*. *Nature* 1998, 391, 806–811.

- [188] Akinc, A., Thomas, M., Klivanov, A. M., Langer, R. Exploring polyethylenimine-mediated DNA transfection and the proton sponge hypothesis. *The journal of gene medicine* 2005, 7, 657–663.
- [189] Jiang, X., van der Horst, A., van Steenberg, M. J., Akeroyd, N., van Nostrum, C. F., Schoenmakers, P. J., Hennink, W. E. Molar-mass characterization of cationic polymers for gene delivery by aqueous size-exclusion chromatography. *Pharmaceutical research* 2006, 23, 595–603.
- [190] Zhao, C., Wu, N., Deng, F., Zhang, H., Wang, N., Zhang, W., Chen, X., Wen, S., Zhang, J., Yin, L., Liao, Z., Zhang, Z., Zhang, Q., Yan, Z., Liu, W., Di Wu, Ye, J., Deng, Y., Zhou, G., Luu, H. H., Haydon, R. C., Si, W., He, T.-C. Adenovirus-mediated gene transfer in mesenchymal stem cells can be significantly enhanced by the cationic polymer polybrene. *PloS one* 2014, 9, e92908.
- [191] Liu, Z., Zhang, Z., Zhou, C., Jiao, Y. Hydrophobic modifications of cationic polymers for gene delivery. *Progress in Polymer Science* 2010, 35, 1144–1162.
- [192] Kim, K., Chen, W. C.W., Heo, Y., Wang, Y. Polycations and their biomedical applications. *Progress in Polymer Science* 2016, 60, 18–50.
- [193] Rosa, M. de, Carteni, M., Petillo, O., Calarco, A., Margarucci, S., Rosso, F., Rosa, A. de, Farina, E., Grippo, P., Peluso, G. Cationic polyelectrolyte hydrogel fosters fibroblast spreading, proliferation, and extracellular matrix production: Implications for tissue engineering. *Journal of cellular physiology* 2004, 198, 133–143.
- [194] Luca, I. de, Di Salle, A., Alessio, N., Margarucci, S., Simeone, M., Galderisi, U., Calarco, A., Peluso, G. Positively charged polymers modulate the fate of human mesenchymal stromal cells via ephrinB2/EphB4 signaling. *Stem cell research* 2016, 17, 248–255.
- [195] Jachowicz, J., McMullen, R., Wu, C., Senak, L., Koelmel, D. Effect of hydrophobic modification on the rheological properties of poly(N-vinyl pyrrolidone-co-dimethylaminopropylmethacrylamide). *Journal of Applied Polymer Science* 2007, 105, 190–200.
- [196] Carro, S., Gonzalez-Coronel, V. J., Castillo-Tejas, J., Maldonado-Textle, H., Tepale, N. Rheological Properties in Aqueous Solution for Hydrophobically Modified Polyacrylamides Prepared in Inverse Emulsion Polymerization. *International Journal of Polymer Science* 2017, 2017, 1–13.
- [197] Kujawa, P., Rosiak, J. M., Selb, J., Candau, F. Micellar Synthesis and Properties of Hydrophobically Associating Polyampholytes. *Macromolecular Chemistry and Physics* 2001, 202, 1384–1397.
- [198] Gillet, S., Aguedo, M., Petrut, R., Olive, G., Anastas, P., Blecker, C., Richel, A. Structure impact of two galactomannan fractions on their viscosity properties in dilute solution, unperturbed state and gel state. *International journal of biological macromolecules* 2017, 96, 550–559.
- [199] Sui, K., Gao, S., Wu, W., Xia, Y. Injectable supramolecular hybrid hydrogels formed by MWNT-grafted-poly(ethylene glycol) and α -cyclodextrin. *Journal of Polymer Science. A. Polymer Chemistry*. 2010, 48, 3145–3151.

- [200] Yan, H., Frielinghaus, H., Nykanen, A., Ruokolainen, J., Saiani, A., Miller, A. F. Thermoreversible lysozyme hydrogels: Properties and an insight into the gelation pathway. *Soft Matter* 2008, 4, 1313.
- [201] Leibler, L., Rubinstein, M., Colby, R. H. Dynamics of reversible networks. *Macromolecules* 1991, 24, 4701–4707.
- [202] Hourdet, D., Gadgil, J., Podhajecka, K., Badiger, M. V., Brûlet, A., Wadgaonkar, P. P. Thermoreversible Behavior of Associating Polymer Solutions: Thermo thinning versus Thermo thickening. *Macromolecules* 2005, 38, 8512–8521.
- [203] Kalyanasundaram, K., Thomas, J. K. Environmental effects on vibronic band intensities in pyrene monomer fluorescence and their application in studies of micellar systems. *Journal of the American Chemical Society* 1977, 99, 2039–2044.
- [204] Karpovich, D. S., Blanchard, G. J. Relating the polarity-dependent fluorescence response of pyrene to vibronic coupling. Achieving a fundamental understanding of the py polarity scale. *Journal of Physical Chemistry* 1995, 99, 3951–3958.
- [205] Engelhardt, N., Ernst, A., Kampmann, A.-L., Weberskirch, R. Synthesis and Characterization of Surface Functional Polymer Nanoparticles by a Bottom-Up Approach from Tailor-Made Amphiphilic Block Copolymers. *Macromolecular Chemistry and Physics* 2013, 214, 2783–2791.
- [206] Hiller, W., Engelhardt, N., Kampmann, A.-L., Degen, P., Weberskirch, R. Micellization and Mobility of Amphiphilic Poly(2-oxazoline) Based Block Copolymers Characterized by ¹H NMR Spectroscopy. *Macromolecules* 2015, 48, 4032–4045.
- [207] Truong, N. P., Jia, Z., Burges, M., McMillan, N. A. J., Monteiro, M. J. Self-catalyzed degradation of linear cationic poly(2-dimethylaminoethyl acrylate) in water. *Biomacromolecules* 2011, 12, 1876–1882.
- [208] Grainger, D. W. All charged up about implanted biomaterials. *Nature biotechnology* 2013, 31, 507–509.
- [209] Swartzlander, M. D., Blakney, A. K., Amer, L. D., Hankenson, K. D., Kyriakides, T. R., Bryant, S. J. Immunomodulation by mesenchymal stem cells combats the foreign body response to cell-laden synthetic hydrogels. *Biomaterials* 2015, 41, 79–88.
- [210] Zhang, Z., Chao, T., Liu, L., Cheng, G., Ratner, B. D., Jiang, S. Zwitterionic hydrogels: an in vivo implantation study. *Journal of biomaterials science. Polymer edition* 2009, 20, 1845–1859.
- [211] Mi, L., Jiang, S. Integrated antimicrobial and nonfouling zwitterionic polymers. *Angewandte Chemie (International ed. in English)* 2014, 53, 1746–1754.
- [212] Jiang, S., Cao, Z. Ultralow-fouling, functionalizable, and hydrolyzable zwitterionic materials and their derivatives for biological applications. *Advanced materials (Deerfield Beach, Fla.)* 2010, 22, 920–932.
- [213] Carr, L. R., Zhou, Y., Krause, J. E., Xue, H., Jiang, S. Uniform zwitterionic polymer hydrogels with a nonfouling and functionalizable crosslinker using photopolymerization. *Biomaterials* 2011, 32, 6893–6899.

- [214] Ye, L., Zhang, Y., Wang, Q., Zhou, X., Yang, B., Ji, F., Dong, D., Gao, L., Cui, Y., Yao, F. Physical Cross-Linking Starch-Based Zwitterionic Hydrogel Exhibiting Excellent Biocompatibility, Protein Resistance, and Biodegradability. *ACS applied materials & interfaces* 2016, 8, 15710–15723.
- [215] Jiang, H., Wang, X. B., Li, C. Y., Li, J. S., Xu, F. J., Mao, C., Yang, W. T., Shen, J. Improvement of hemocompatibility of polycaprolactone film surfaces with zwitterionic polymer brushes. *Langmuir the ACS journal of surfaces and colloids* 2011, 27, 11575–11581.
- [216] Liu, P.-S., Chen, Q., Wu, S.-S., Shen, J., Lin, S.-C. Surface modification of cellulose membranes with zwitterionic polymers for resistance to protein adsorption and platelet adhesion. *Journal of Membrane Science* 2010, 350, 387–394.
- [217] Mary, P., Bendejacq, D. D., Labeau, M.-P., Dupuis, P. Reconciling low- and high-salt solution behavior of sulfobetaine polyzwitterions. *The journal of physical chemistry. B* 2007, 111, 7767–7777.
- [218] Zhang, L., Cao, Z., Bai, T., Carr, L., Ella-Menye, J.-R., Irvin, C., Ratner, B. D., Jiang, S. Zwitterionic hydrogels implanted in mice resist the foreign-body reaction. *Nature biotechnology* 2013, 31, 553–556.
- [219] Kudaibergenov, S., Jaeger, W., Laschewsky, A. Polymeric Betaines: Synthesis, Characterization, and Application. In *Supramolecular Polymers Polymeric Betains Oligomers*; Springer Berlin Heidelberg: Berlin, Heidelberg, 2006; Vols. 201, pp. 157–224.
- [220] Ye, T., Song, Y., Zheng, Q. Solubility and solution rheology of acrylamide-sulfobetaine copolymers. *Colloid and Polymer Science* 2014, 292, 2185–2195.
- [221] Villa-Diaz, L. G., Nandivada, H., Ding, J., Nogueira-de-Souza, N. C., Krebsbach, P. H., O'Shea, K. S., Lahann, J., Smith, G. D. Synthetic polymer coatings for long-term growth of human embryonic stem cells. *Nature biotechnology* 2010, 28, 581–583.
- [222] Rodríguez, M., Xue, J., Gouveia, L. M., Müller, A. J., Sáez, A. E., Rigolini, J., Grassl, B. Shear rheology of anionic and zwitterionic modified polyacrylamides. *Colloids and Surfaces A: Physicochemical and Engineering Aspects* 2011, 373, 66–73.
- [223] Fevola, M. J., Bridges, J. K., Kellum, M. G., Hester, R. D., McCormick, C. L. pH-responsive polyzwitterions: A comparative study of acrylamide-based polyampholyte terpolymers and polybetaine copolymers. *Journal of Applied Polymer Science* 2004, 94, 24–39.
- [224] Johnson, K. M., Fevola, M. J., McCormick, C. L. Hydrophobically modified acrylamide-based polybetaines. I. Synthesis, characterization, and stimuli-responsive solution behavior. *Journal of Applied Polymer Science* 2004, 92, 647–657.
- [225] Wang, T., Wang, X., Long, Y., Liu, G., Zhang, G. Ion-specific conformational behavior of polyzwitterionic brushes: exploiting it for protein adsorption/desorption control. *Langmuir the ACS journal of surfaces and colloids* 2013, 29, 6588–6596.
- [226] Grooth, J. de, Dong, M., Vos, W. M. de, Nijmeijer, K. Building polyzwitterion-based multilayers for responsive membranes. *Langmuir the ACS journal of surfaces and colloids* 2014, 30, 5152–5161.

- [227] Zhao, Y.-H., Wee, K.-H., Bai, R. A novel electrolyte-responsive membrane with tunable permeation selectivity for protein purification. *ACS applied materials & interfaces* 2010, 2, 203–211.
- [228] Leng, C., Hung, H.-C., Sun, S., Wang, D., Li, Y., Jiang, S., Chen, Z. Probing the Surface Hydration of Nonfouling Zwitterionic and PEG Materials in Contact with Proteins. *ACS applied materials & interfaces* 2015, 7, 16881–16888.
- [229] Yu, Q., Cho, J., Shivapooja, P., Ista, L. K., López, G. P. Nanopatterned smart polymer surfaces for controlled attachment, killing, and release of bacteria. *ACS applied materials & interfaces* 2013, 5, 9295–9304.
- [230] Wu, B., Zhang, L., Huang, L., Xiao, S., Yang, Y., Zhong, M., Yang, J. Salt-Induced Regenerative Surface for Bacteria Killing and Release. *Langmuir the ACS journal of surfaces and colloids* 2017, 33, 7160–7168.
- [231] He, K., Duan, H., Chen, G. Y., Liu, X., Yang, W., Wang, D. Cleaning of Oil Fouling with Water Enabled by Zwitterionic Polyelectrolyte Coatings: Overcoming the Imperative Challenge of Oil-Water Separation Membranes. *ACS nano* 2015, 9, 9188–9198.
- [232] Zhao, X., Chen, W., Su, Y., Zhu, W., Peng, J., Jiang, Z., Kong, L., Li, Y., Liu, J. Hierarchically engineered membrane surfaces with superior antifouling and self-cleaning properties. *Journal of Membrane Science* 2013, 441, 93–101.
- [233] Chen, M., Briscoe, W. H., Armes, S. P., Klein, J. Lubrication at physiological pressures by polyzwitterionic brushes. *Science (New York, N.Y.)* 2009, 323, 1698–1701.
- [234] Kobayashi, M., Terada, M., Takahara, A. Polyelectrolyte brushes: A novel stable lubrication system in aqueous conditions. *Faraday Discuss.* 2012, 156, 403.
- [235] Peiffer, D. G., Lundberg, R. D. Synthesis and viscometric properties of low charge density ampholytic ionomers. *Polymer* 1985, 26, 1058–1068.
- [236] Che, Y.-J., Tan, Y., Cao, J., Xin, H., Xu, G.-Y. Synthesis and properties of hydrophobically modified acrylamide-based polysulfobetaines. *Polymer Bulletin* 2011, 66, 17–35.
- [237] Chen, H., Wang, Z.-M., Ye, Z.-B., Han, L.-J. The solution behavior of hydrophobically associating zwitterionic polymer in salt water. *Journal of Applied Polymer Science* 2014, 131, 39707.
- [238] Hersel, U., Dahmen, C., Kessler, H. RGD modified polymers: Biomaterials for stimulated cell adhesion and beyond. *Biomaterials* 2003, 24, 4385–4415.
- [239] Mathieu, H. J. Bioengineered material surfaces for medical applications. *Surface and Interface Analysis* 2001, 32, 3–9.
- [240] Joy, A., Cohen, D. M., Luk, A., Anim-Danso, E., Chen, C., Kohn, J. Control of surface chemistry, substrate stiffness, and cell function in a novel terpolymer methacrylate library. *Langmuir the ACS journal of surfaces and colloids* 2011, 27, 1891–1899.
- [241] Tallawi, M., Rosellini, E., Barbani, N., Cascone, M. G., Rai, R., Saint-Pierre, G., Boccaccini, A. R. Strategies for the chemical and biological functionalization of scaffolds for cardiac tissue engineering: a review. *Journal of the Royal Society, Interface* 2015, 12, 20150254.

- [242] Saha, K., Irwin, E. F., Kozhukh, J., Schaffer, D. V., Healy, K. E. Biomimetic interfacial interpenetrating polymer networks control neural stem cell behavior. *Journal of biomedical materials research. Part A* 2007, *81*, 240–249.
- [243] Saha, K., Keung, A. J., Irwin, E. F., Li, Y., Little, L., Schaffer, D. V., Healy, K. E. Substrate modulus directs neural stem cell behavior. *Biophysical journal* 2008, *95*, 4426–4438.
- [244] Missirlis, D., Spatz, J. P. Combined effects of PEG hydrogel elasticity and cell-adhesive coating on fibroblast adhesion and persistent migration. *Biomacromolecules* 2014, *15*, 195–205.
- [245] Sathaye, S., Mbi, A., Sonmez, C., Chen, Y., Blair, D. L., Schneider, J. P., Pochan, D. J. Rheology of peptide- and protein-based physical hydrogels: are everyday measurements just scratching the surface? *Wiley interdisciplinary reviews. Nanomedicine and nanobiotechnology* 2015, *7*, 34–68.
- [246] Mitchell, V. D., Jones, D. J. Advances toward the effective use of block copolymers as organic photovoltaic active layers. *Polymer Chemistry* 2018, *78*, 75.
- [247] Torron, S., Hult, D., Pettersson, T., Johansson, M. Tailoring Soft Polymer Networks Based on Sugars and Fatty Acids toward Pressure Sensitive Adhesive Applications. *ACS Sustainable Chemistry and Engineering* 2017, *5*, 2632–2638.
- [248] Vilela, C., Rua, R., Silvestre, A. J.D., Gandini, A. Polymers and copolymers from fatty acid-based monomers. *Industrial Crops and Products* 2010, *32*, 97–104.
- [249] Maiti, B., De, P. RAFT polymerization of fatty acid containing monomers: Controlled synthesis of polymers from renewable resources. *RSC Advances* 2013, *3*, 24983.
- [250] La Scala, J. J., Sands, J. M., Orlicki, J. A., Robinette, E. J., Palmese, G. R. Fatty acid-based monomers as styrene replacements for liquid molding resins. *Polymer* 2004, *45*, 7729–7737.
- [251] Tarnavchyk, I., Popadyuk, A., Popadyuk, N., Voronov, A. Synthesis and Free Radical Copolymerization of a Vinyl Monomer from Soybean Oil. *ACS Sustainable Chemistry & Engineering* 2015, *3*, 1618–1622.
- [252] Jain, J. P., Sokolsky, M., Kumar, N., Domb, A. J. Fatty Acid Based Biodegradable Polymer. *Polymer Reviews* 2008, *48*, 156–191.
- [253] Tamate, R., Ueki, T., Kitazawa, Y., Kuzunuki, M., Watanabe, M., Akimoto, A. M., Yoshida, R. Photo-Dimerization Induced Dynamic Viscoelastic Changes in ABA Triblock Copolymer-Based Hydrogels for 3D Cell Culture. *Chemistry of Materials* 2016, *28*, 6401–6408.
- [254] Shiono, H., Yoshikawa, M. Polymeric Pseudo-Liquid Membranes from Poly(N-oleyl acrylamide). *Membranes* 2014, *4*, 210–226.
- [255] Kim, J., Kim, D. N., Lee, S. H., Yoo, S.-H., Lee, S. Correlation of fatty acid composition of vegetable oils with rheological behaviour and oil uptake. *Food Chemistry* 2010, *118*, 398–402.

Chapter 11. Appendix

11.1 List of Figures

Figure 2.1. Applications of hydrogels.	7
Figure 2.2. (i) Bioactive hydrogel, (ii) bioresponsive hydrogel in three different types with varying the properties in response to A) small molecules through receptor or ligand interactions, B) enzymes by cleavable linkers, C) small molecules that are changed by immobilized enzymes. The macroscopic transition like swelling or collapse of the hydrogels are illustrated. (adapted from [42])	9
Figure 2.3. Schematic drawing of associating copolymers, a) telechelic and b) multisticker polymers with the hydrophobic units (in green) and the solvophilic blocks (in black). (adapted from [46])	10
Figure 2.4. Schematic illustration of hydrophobically modified polymer solution viscosity as a function of concentration in three different regimes (black line), unmodified polymer (red line).	11
Figure 2.5. Schematic diagrams of storage (G') (blue line) and loss (G'') (black line) modulus as a function of frequency for A) hydrophobically modified polymers, B) unmodified polymers, C) hydrogels, at the same frequency range.	12
Figure 2.6. Scheme of the micellar copolymerization reaction medium. (adapted from [65]).	14
Figure 2.7. DMAM associative copolymer containing DA or ODA.	15
Figure 2.8. Classification of cationic polymers.	16
Figure 2.9. (i) Typical polymerization methods to form polycations, (ii) reactive precursor polymers and their quaternization. (adapted from [94]).	19
Figure 2.10. Possible distribution of ionic moieties within zwitterionic polymers. (adapted from [100]).	21
Figure 2.11. RDG sequence structure.	25
Figure 2.12. Scheme of the solid-phase peptide synthesis (SPPS) developed by <i>Merrifield and coworker</i> . (adapted from [127]).	26
Figure 2.13. Comparison of tissue culture plates and hydrogels for cell culture applications.	28
Figure 2.14. Examples for PEG polymers to form hydrogel with different functionalities and molar masses (commercially available by SigmaAldrich).....	31
Figure 2.15. Design consideration for biomaterials to mimic a 3D cell microenvironment and general cell/matrix requirements for 3D culture systems.....	32
Figure 4.1. Schematic diagram for the synthesis of the precursors and P1 copolymers of different composition.	39

Figure 4.2. ^1H NMR of precursor copolymers with various mole percentage of LMA (d-MeOD).	42
Figure 4.3. ^1H NMR analysis of LMA (mol%) as a function of initial molar percentage of LMA in monomer feed.....	42
Figure 4.4. ^1H NMR of P1LMA1.25 and P1LMA2.5 , the conversion was quantified by comparing peak integrals at 2.2 ppm (methyl groups of the tertiary amine) and 3.3 ppm (methyl groups of the quaternary ammonium group).	43
Figure 4.5. P1SMA1.25 in aqueous PBS buffer solution in concentration range from 15 to 40 wt%.....	45
Figure 4.6. Schematic diagram of the conversion from a dilute to concentrated solution for a hydrophobically modified polymer.	45
Figure 4.7. Zero shear viscosity as a function of shear rate at various concentration (wt%): 25 % (—■—), 22.5 % (—●—), 20% (—▲—), 15% (—◆—), 12.5% (—●—), 10% (—○—), 7.5% (—◇—), 6% (—△—), 5% (—*—) for a) P_{ref}LMA1.25 and P1LMA1.25 b) P_{ref}LMA2.5 and P1LMA2.5 , c) P_{ref}LMA3.75 and P1LMA3.5 , d) P_{ref}SMA1.25 and P1SMA1.25 , demonstrating the effect of hydrophobic content and chain length.....	48
Figure 4.8. Specific zero shear viscosity as a function of concentration, demonstrating the significant effect of charge, hydrophobic content and chain length on solution properties.....	50
Figure 4.9. Zero shear viscosity as a function of concentration for cationic copolymers.....	51
Figure 4.10. Plots of storage modulus G' (—●—) and loss modulus G'' (—●—) against frequency for P1LMA2.5 , P1SMA1.25 , P1SMA2.5 and their references at 20wt%.....	52
Figure 4.11. Elastic moduli G' (blue symbols), the viscous moduli C'' (black symbols) as a function of time at constant frequency (1Hz) for P_{ref}LMA2.5 , P1LMA 1.25 , P_{ref}SMA1.25 , P1SMA1.25 , P_{ref}SMA2.5 and P1SMA2.5 at different concentration.....	55
Figure 4.12. Temperature dependence of the storage G' (—●—) and loss modulus G'' (—●—) between 25 and 80 °C at constant frequency (1 Hz) for P1LMA2.5 , P_{ref}SMA2.5 and P1SMA2.5	57
Figure 4.13. I_1/I_3 intensity ratio as a function of polymer concentration for P1SMA2.5 and P1LMA2.5	58
Figure 5.1. The chemical structure of synthetic polymers for long-term growth of hES. Poly [carboxybetaine methacrylate] (PCBM), poly [poly (ethylene glycol) methyl ether methacrylate] (PPEGM), poly [2-hydroxyethyl methacrylate] (PHEM), poly [3-sulfopropyl methacrylate] (PSPM), poly [[2-(methacryloyloxy) ethyl] trimethylammonium chloride] (PMETA), poly [2-(methacryloyloxy) ethyl dimethyl-(3-sulfopropyl) ammonium hydroxide] (PMEDSAH).	63
Figure 5.2. Structural dependence of salt-responsive polyzwitterionic brushes with an anti-polyelectrolyte effect.....	64
Figure 5.3. Synthetic route of P2 copolymer.	65
Figure 5.4. ^1H NMR spectrum of P2 in D_2O	66

Figure 5 5. Presents a plot of the zero shear viscosity as a function of shear rate at various concentration (wt %): 25 % (—■—), 20 % (—▲—), 15% (—◆—), 12.5% (—●—), 10 % (—○—),7.5% (—◇—) for P2 , P_{ref} SMA1.25 and P1SMA1.25 .	68
Figure 5.6. Zero shear specific viscosity as a function of concentration for P2 , P_{ref}SMA1.25 and P1SMA1.25 in a) semidilute and concentrated regime b) in dilute regime, demonstrating the effect of zwitterion incorporation on the viscosity.	69
Figure 5.7. Elastic moduli G' (—●—), the viscous moduli C'' (—●—) as a function of frequency for P2 and P_{ref} SMA1.25 at a) 20wt% and b) 25 wt%.	71
Figure 5.8. Elastic moduli G' (blue symbols), the viscous moduli C'' (black symbols) as a function of time for P2 , P_{ref}SMA1.25 and P1SMA1.25 , showing the solid-like behavior of P2 at 25 wt%.	72
Figure 5.9. Zero shear viscosity as a function of shear rate for a) P2 in buffer and 2 M solution at 15% (—◆—), 12.5% (—●—), 10 % (—○—), 7.5% (—◇—) (wt%) b) P2 in buffer, 2M and 4M solution at 10wt%.	73
Figure 5.10. Specific viscosity at zero shear rate as a function of concentration for P2 in buffer and 2M solution.	74
Figure 5 11. a) Elastic modulus (blue symbols) and viscous modulus (black symbols) as a function of time for P2 in 2M and 4M NaCl solution at 10, 12.5 and 15wt%, b) elastic modulus as a function of time for P2 in buffer, 2M and 4M solutions.	75
Figure 6.1. The surface properties of biomaterials control the interaction of cells with biomaterials [241].	79
Figure 6.2. The vmIPN structure with monomers used for sequential polymerization [243] .	80
Figure 6.3. Peptide monomer structure.	81
Figure 6.4. Synthesis route of copolymer containing peptide.	81
Figure 6.5. ^1H NMR spectrum of peptide copolymer recorded (in D_2O).	82
Figure 6 6. ^1H NMR spectrum of (A) P3-1 and (B) P3-2 recorded (in D_2O).	84
Figure 6.7. The viscosity as a function of shear rate for P3-1 and P3-2 in 20 (—▲—), 15 (—◆—) and 10 (—○—) wt%.	85
Figure 6.8. The viscosity as a function of shear rate for P1SMA1.25 , P_{ref}SMA1.25 , P2 , P3-1 and P3-2 at 20wt%.	85
Figure 6.9. Elastic modulus (—●—) and viscous modulus (—●—) as a function of frequency for P3-1 and P3-2 at 20wt%.	86
Figure 6.10. Elastic modulus (—●—) and viscous modulus (—●—) as a function of time at 20wt%.	86
Figure 7.1. ^1H NMR spectrum of oelylacrylamide monomer (CDCl_3).	93
Figure 7.2. ^1H NMR spectra of A) POA1.25 , B) POA2.5 and C) POA3.75 (in MeOD).	94

Figure 7.3. Copolymer viscosity as a function of shear rate a) at various concentration of 15 (—■—), 12.5 (—●—) and 10 (—▲—) wt% for POA1.25 and POA2.5 ; b) for POA1.25 , POA2.5 and POA3.75 at 10 wt%.	96
Figure 7.4. Visual inspection for POA1.25 and POA3.75 at 15 wt%.	96
Figure 7.5. POA1.25 and P_{ref}SMA1.25 viscosity at various concentration of 15 (—■—), 12.5 (—●—) and 10 (—▲—) wt% and various shear rates.	97
Figure 7.6. Storage modulus G' (—●—) and loss modulus G'' (—●—) as a function of frequency for POA2.5 , POA3.75 and P_{ref}SMA2.5 at 15 wt%.	98
Figure 7.7. Saturated and unsaturated side chain structure.	98
Figure 7.8. G' (blue symbol) and G'' (black symbol) as a function of time reading for POA1.25 , POA2.5 , POA3.75 and P_{ref}SMA2.5 using solution consisting of 15 wt% of each polymer. .	99
Figure 7.9. ^1H NMR of copolymer containing oleylacrylamide and cationic monomer (in MeOD).	100
Figure 7.10. ^1H NMR of linoleylmethacrylate (LM) in CDCl_3	101
Figure 7.11. ^1H NMR spectrum of A) PLM1.25 and B) PLM2.5 (in MeOD).	103
Figure 7.12. The effect of copolymers concentration and LM content on the shear viscosity of PLM1.25 and PLM2.5 in buffer solution at 37 °C.	104
Figure 7.13. a) UV-vis spectra of POA2.5 and PLM2.5 (6 wt%) recorded after UV-vis light irradiation ($\lambda=273$ nm) at 37 °C, b) degree of dimerization for the copolymers was obtained from the change in the absorption peak of OA and LM moieties at 273 nm.	105
Figure 7.14. Synthesis of linoleyl chloride.	107
Figure 7.15. Synthesis of linoleyl amide.	108
Figure 7.16. Synthesis of linoleyl amine.	108
Figure 7.17. Chemical structure of vinyl linoleate.	109
Figure 9.1. Schematic diagram of the preparation of P_{ref} , P1 , P2 and P3	116
Figure 11.1. ^1H NMR spectrum of peptide monomer.	148
Figure 11.2. Mass spectrometry of peptide monomer	148
Figure 11.3. Elastic moduli G' (—●—) and viscous moduli C'' (—●—) as a function of frequency for P_{ref} and P1 with various hydrophobe content at different concentration.	149

11.2 List of Tables

Table 2.1. Evolution of anti-fouling materials: a) 2-hydroxyethyl methacrylate, b) poly(ethylene glycol), or oligo(ethylene glycol), c) poly(ethylene glycol) methacrylate, d) phosphobetaine methacrylate, e) sulfobetaine methacrylate, f) carboxybetaine methacrylate. (adapted from [102]).	22
Table 2.2. Overview on naturally-derived polymers and their mechanism of gelation and degradation.	30
Table 2.3. Methods of in situ gelation of biomaterials based on their gelation mechanism	33
Table 2.4. Selected examples of injectable gels for human mesenchymal stem cell delivery	34
Table 4.1. Analytical data for the references copolymers.	40
Table 4.2. Analytical data of the cationic copolymers.	41
Table 4.3. Solubility of P_{ref} and P1 copolymers in aqueous buffer solution.	44
Table 4.4. Cross-over frequency, ω_{cross} , for a range of cationic copolymers and their references copolymers with various hydrophobicities and concentrations.	54
Table 5.1. P2 characterization data.	65
Table 6.1. Characterization data of copolymer containing peptide.	82
Table 6.2. Characterization data of P3-1 and P3-2 .	83
Table 7.1. Analytical data of the OA containing copolymers.	94
Table 7.2. Analytical data of PCOA1.25 copolymer.	101
Table 7.3. Characterization data of copolymers containing LM	102

11.3 Nomenclature

11.3.1 Abbreviations

AA	Arachidonic acid
AD	Alzheimer's disease
AIBN	Azobisisobutyronitrile
ATRP	Atom transfer radical polymerization
BOC	t-Butyloxycarbonyl
CBMA	Carboxybetaine methacrylate
CCNCs	Cationic cellulose nanocrystals
CDs	Cyclodextrins
DA	Dodecyl acrylate
DCC	Dicyclohexylcarbodiimide
DCM	Dichloromethane
DiHexAM	N, N-Diehexylacrylamide
DIPEA	N,N'-Diisopropylethylamine
DMAM	N,N'-Dimethyl acrylamide
DMF	Dimethylformamide
DOAB	Dimethyloctane (2-acrylamidopropyl) ammoniumbromide
DOX	Doxorubicin
ECM	Extracellular matrix
EPA	Eicosapentaenoic acid
eφAM	N-4-Ethylphenylacrylamide
ESC	Embryonic stem cells
ESC	Embryonic stem cells
FA	Fatty acids
Fmoc	9-Fluorenylmethyloxycarbonyl
FN	Fibrinogen
FOSA	Perfluorooctane sulfonamide
GPC	Gel-permeation chromatography
GPs	Gelatin nanoparticles

GRP	Gastrin releasing peptide
HA	Hyaluronic acid
HBTU	Hexafluorophosphate benzotriazole tetramethyl uranium
HEK	Human embryonic kidney cells
HEMA	Hydroxyethylmethacrylate
hESCs	Human embryonic stem cells
HM	Hydrophobically modified
HOBT	Hydroxybenzotriazole
HPLC	High-performance liquid chromatography
IBD	Inflammatory bowel disease
IMEP	Inverse miniemulsion polymerization
IPN	Interpenetrating network
IPN	Interpenetrating network
iPSC	Pluripotent stem cells
iPSC	Pluripotent stem cells
LM	Linoleylacrylamide
LMA	Lauryl methacrylate
LMA	Lauryl methacrylate
MADQUAT	Methacryloyloxyethyl trimethyl ammonium chloride
METAC	2-methacryloyloxyethyltrimethyl ammonium chloride
MSCs	Mesenchymal stem cells
MUSFA	Monounsaturated fatty acids
NAFLD	Nonalcoholic fatty liver disease
NMP	N-Methyl-2-pyrrolidone
NMR	Nuclear magnetic resonance
NSC	Neural stem cell
OA	Oleylacrylamide
ODA	Octadecylacrylate
PAA	Polyacrylic acid
PAA	Polyacrylic acid
PBMA	Phosphobetaine methacrylate

PBS	Phosphate-buffered saline
PDMAEMA	Poly [2-(N,N-Dimethylamino) ethyl methacrylate]
PDMS	Poly (dimethylsiloxane)
PEG	Polyethyleneglycol
PEG	Polyethyleneglycol
PEGMA	Poly (ethylene glycol) methacrylate
PEI	Polyethyleneimine
PEs	Polyelectrolytes
PLA	Polylactic acid
PLA	Polylactic acid
PLL	Poly (L-lysine)
PMEDSAH	Poly [2-(methacryloyloxy) ethyl dimethyl-(3-sulfopropyl) ammonium hydroxide]
PNIPA	Poly (N-isopropylacrylamide)
PPO	Poly (propylene oxide)
PUSFA	Polyunsaturated fatty acids
PVA	Polyvinylalcohol
PVA	Polyvinylalcohol
PZs	Polyzwitterions
QC	Quaternized cellulose
RGD	Arginylglycylaspartic acid
SAMs	Self-assembled monolayers
SBMA	Sulfobetaine methacrylate
SCI	Spinal cord injury
SDS	Sodium dodecyl sulfate
SEC	Size-exclusion chromatography
SFA	Saturated fatty acids
SMA	Stearyl methacrylate
SMA	Stearyl methacrylate
SPPS	Solid phase synthesis
SPS	Solution phase synthesis

TFA	Trifluoroacetic acid
USFA	Unsaturated fatty acids
UV-Vis	Ultraviolet-visible spectroscopy
VN	Vitronectin
β -GP	β -Glycerophosphate

11.3.2 Symbols

\bar{D}	Dispersity
M_n	Number-average molecular weight (g mol^{-1})
M_w	Weight-average molecular weight (g mol^{-1})
G'	Elastic modulus (Pa)
G''	Viscous modulus (Pa)
ω_{cross}	Cross-over frequency (rad s^{-1})
η_{sp}	Specific viscosity (Pa.s)
η'	Dynamic viscosity (Pa.s)
η^*	Complex viscosity (Pa.s)

11.4 ^1H NMR and mass spectrometry of peptide monomer

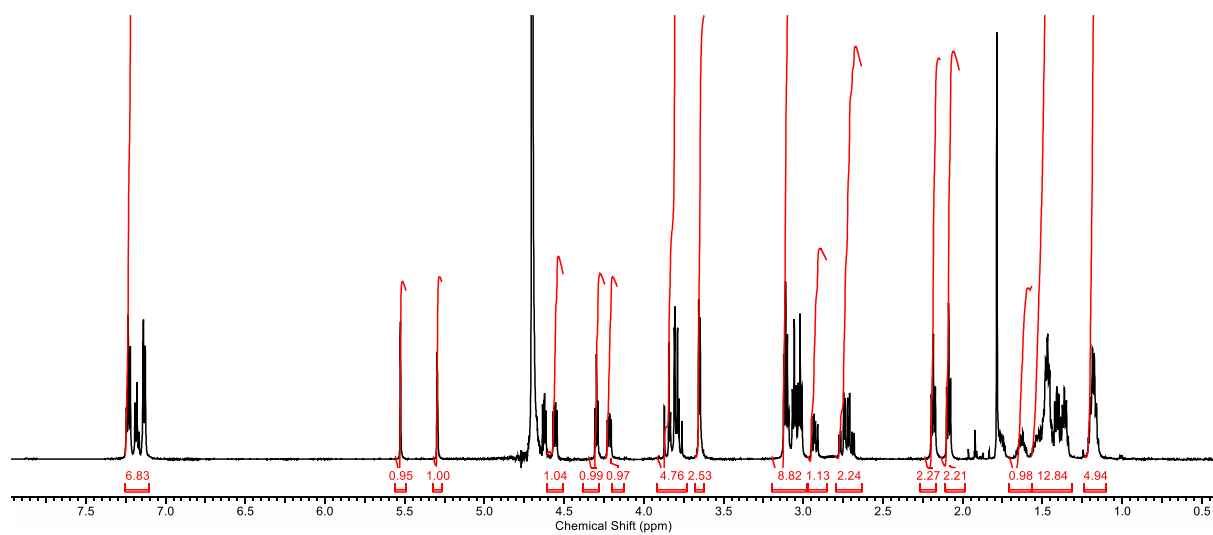


Figure 11.1. ^1H NMR spectrum of peptide monomer.

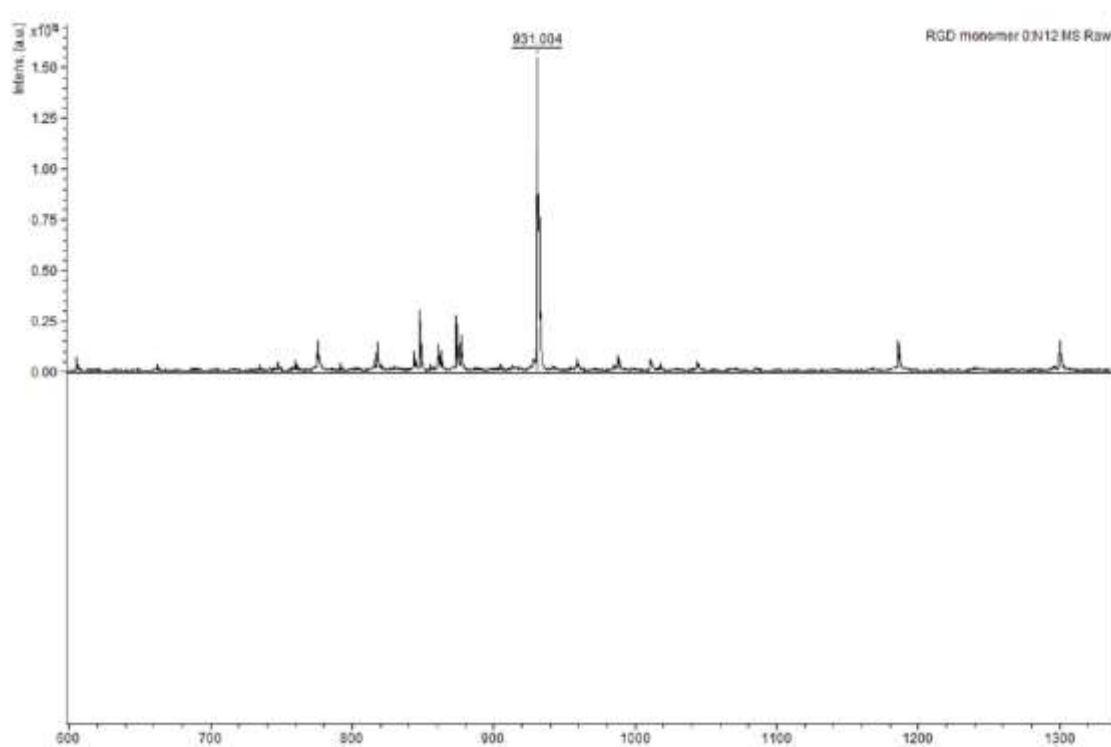


Figure.11.2. Mass spectrometry of peptide monomer.

11.5 Modulus as a function of frequency for P_{ref} and P1 at different concentration

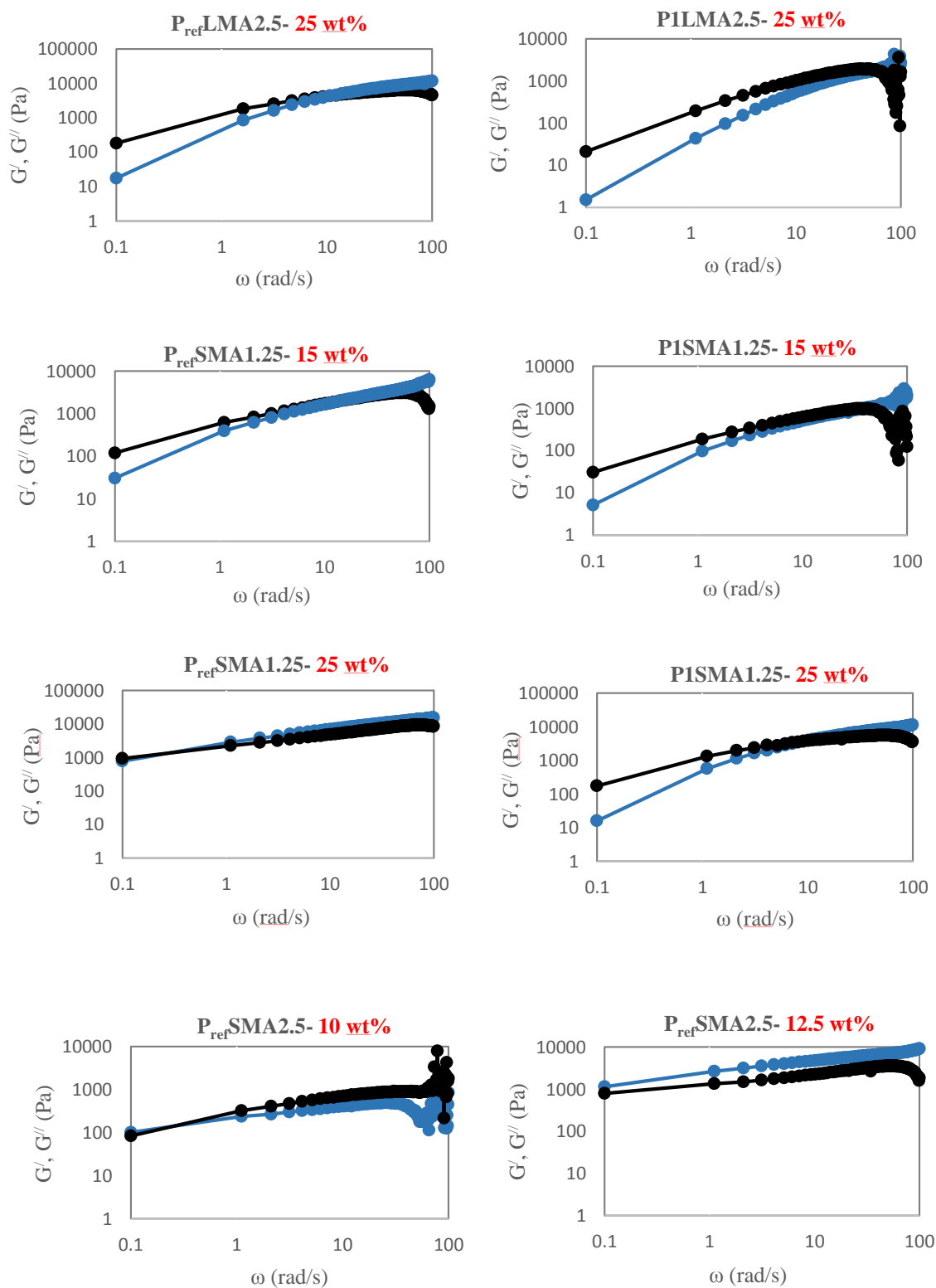


Figure 11.3. Elastic moduli G' (—●—) and viscous moduli G'' (—●—) as a function of frequency for P_{ref} and P1 with various hydrophobe content at different concentration.